

71-16,480

WANG, Paul Por-yuan, 1942-
STATISTICAL MECHANICS OF ONE-DIMENSIONAL
EXCLUDED-VOLUME PROBLEM AND POLYMER CHAIN.

Carnegie-Mellon University, Ph.D., 1971
Physics, solid state

University Microfilms, A XEROX Company , Ann Arbor, Michigan

STATISTICAL MECHANICS OF ONE-DIMENSIONAL
EXCLUDED-VOLUME PROBLEM AND POLYMER CHAIN

A Thesis

Presented to the Department of Physics
of Carnegie-Mellon University in Part-
ial Fulfillment of the Requirements
for the Degree of Doctor of Philosophy

by

Paul Por-yuan Wang

November 12, 1970

Carnegie-Mellon University

CARNEGIE INSTITUTE OF TECHNOLOGY

THESIS

SUBMITTED IN PARTIAL FULFILLMENT OF THE REQUIREMENTS
FOR THE DEGREE OF Doctor of Philosophy

TITLE Statistical Mechanics of One-Dimensional Excluded-Volume

Problem and Polymer Chain

PRESENTED BY Paul Por-Yuan Wang

ACCEPTED BY THE DEPARTMENT OF Physics

James A. Tanger
MAJOR PROFESSOR
Julian Ashkin
DEPARTMENT HEAD

November 12, 1970
DATE
November 12, 1970
DATE

APPROVED BY THE COMMITTEE ON GRADUATE DEGREES

Admonish
CHAIRMAN

Nov 11, 1970
DATE

PLEASE NOTE:

**Some pages have indistinct
print. Filmed as received.**

UNIVERSITY MICROFILMS.

TABLE OF CONTENTS

INTRODUCTION	1
I. DIAGRAMS COUNTING AND EXTRAPOLATION	12
A. Calculations of $c_n(u)$ and $U_n(u)$	15
B. Asymptotic Behaviors of $c_n(u)$ and $U_n(u)$	20
C. Calculations of $\langle r_n^2(u) \rangle$ and $\langle r_n^2'(u) \rangle$	26
D. Probability Distribution of the End Points	31
II. STRONG COUPLING APPROXIMATION	33
A. Calculations of Generating Function	35
B. Calculations of the Total Number of Walks	46
$c_n(u)$	
C. Mean-square Size Calculation	49
D. Probability Distribution $z_n(\ell, u)$	51
E. Calculations of the Total Number of Walks	59
which return to its Starting Point $U_n(u)$	
III. CONTINUOUS MODEL	62
A. Free Green's Function G_0	73
B. Weak Coupling Approximation	77
C. Self-consistent Calculation of $\Sigma(k, \omega)$	86
D. Three Dimensional Problem	90
SUMMARY AND CONCLUSION	100
REFERENCES	106
ACKNOWLEDGMENT	109
APPENDIX	110
TABLES	134
FIGURES	151

LIST OF APPENDICES

- I. Derivation of Flory's Rule by Mean-field Theory
- II. Proof that $\alpha(u=1) = 0$ and $\beta(u=1) = -1/2$
- III. Laplace's Method
- IV. Calculation of $Z_n(\ell, u)$ in the case of very strong coupling
- V. Generating function of summing over the diagrams containing Q_2 , Q_3 , and Q_4
- VI. Punching through analytical continuation

LIST OF TABLES

- I. $U_n(u)$ from $n=2$ to 20
- II. $c_n(u)$ from $n=1$ to 15
- III. Table of $\mu(u)$ for different values of interaction V
- IV. Table of $\mu'(u)$ for different values of interaction V
- V. $r_n^2(u)$ from $n=1$ to 15
- VI. $\langle r_n^2(u) \rangle$ from $n=2$ to 20

FIGURE CAPTIONS

1. Diagram of $U_2(u)$
2. Diagrams of $U_4(u)$
3. Diagrams of $U_6(u)$
4. Diagram of $c_1(u)$
5. Diagrams of $c_2(u)$
6. Diagrams of $c_3(u)$
7. Plot of $\mu(u)$ for different values of V
8. Plot of $\mu'(u)$ for different values of V
9. Plot of $\mu_n(u)$ vs. $1/n$ for different values of V
10. Plot of $\mu_n'^2(u)$ vs. $1/n$ for different values of V
11. Plot of $a_n(u)$ vs. $1/n$ for different values of V
12. Plot of $\beta_n(u)$ vs. $1/n$ for different values of V
13. Above Figure in large
14. Plot of $\gamma_n(u)$ vs. $1/n$ for different values of V
15. Plot of $\gamma_n'(u)$ vs. $1/n$ for different values of V
16. Plot of $P_n(\ell, u)$ for $n=15$
17. Plot of $P_n(\ell, u)$ for $n=14$
18. Contour of eq. (2.4)
19. Diagrams of Ξ
20. Diagrams of Σ
21. Diagrams of Λ
22. Diagrams of Σ in the strong coupling approximation
23. Diagrams of Λ in the strong coupling approximation

24. Diagrams of $\Lambda^*\Sigma$ in the strong coupling approximation
25. Diagrams of Γ in the strong coupling approximation
26. Singularities of the Generating Function $F(z)$
27. Deform the Contour C to C' in eq. (2.4)
28. Plot of $\mu(u)$ for different values of V in the strong coupling approximation
29. Contour and Singularities of eq. (2.71)
30. Deform the Contour C to C' in eq. (2.71) and Indicate the allowed Region of the Saddle Point z_s
31. Plot of $z_n(\ell, u)$ at $n=15$ for different values of V in the strong coupling approximation
32. Plot of $\frac{1}{n} \ln z_n(\ell, u)$ for $u=0.50$
33. Plot of $\frac{1}{n} \ln z_n(\ell, u)$ for $u=0.25$
34. Plot of the Solution of $f'(z_s, y) = 0$ for different values of V
35. Plot of $\mu'(u)$ for different values of V in the strong coupling approximation
36. Polymer Chain in the Space
37. Green's Function Expansion
38. Diagram Expansion of the Self-energy Part
39. Contour of eq. (3.43)
40. Contour of eq. (3.45)
41. Contour of eqs. (3.55), (3.56)
42. Contour of eq. (3.83)
43. Self-energy Part Expansion in the case of neglecting the Vertex Part

44. Second Order Self-energy Part Diagrams
45. Contour of eq. (3.106)
46. Contour of eqs. (3.129) and (3.140)
47. Diagrams of S
48. Diagrams of $S^*\Sigma$
49. Diagrams of θ
50. Diagrams of λ , δ , δ' and $\lambda \Sigma \lambda$
51. Contour of eq. (VI.1)

Paul Por-yuan Wang

Statistical Mechanics of One-dimensional Excluded-volume
Problem and Polymer Chain
Carnegie-Mellon University

ABSTRACT

The one-dimensional excluded-volume problem is studied. Construct a model by considering the ordinary random walk on a finite chain, and assume the existence of a finite strength repulsive interaction for any pair of steps(links) between the same two lattice points. This can be introduced by a weighting factor $u = \exp(-V)$, where V is the strength of the interaction. The total number of walks, $C_n(u)$; the total number of walks returning to the starting point, $U_n(u)$; the mean-square end-to-end distance, $\langle r_n^2(u) \rangle$; and the weighted sum of mean-square deviation of steps(links), $\langle r_n^{2'}(u) \rangle$ are all calculated to the n -th order in one dimension where $n=20$ for calculating $C_n(u)$ and $\langle r_n^2(u) \rangle$; $n=15$ for calculating $U_n(u)$ and $\langle r_n^{2'}(u) \rangle$. In the case of small values of n , use the extrapolation techniques and establish the asymptotic behaviors of these quantities, i.e., $C_n(u) \approx B(u) n^\alpha u^\beta$; $U_n(u) \approx B'(u) n^\beta u^\alpha$; $\langle r_n^2(u) \rangle \approx A(u) n^\gamma$ and $\langle r_n^{2'}(u) \rangle \approx A'(u) n^{\gamma'}$ as $n \rightarrow \infty$. The indices are calculated for different values of V and the results are given as:

$$\alpha(u) = 0 \quad \text{for all } V \geq 0; \quad 0 \leq u \leq 1$$

$$\beta(u) = \begin{cases} -1/2 & \text{for } V=0; \quad u=1 \\ 1 & \text{for } V>0; \quad 0 \leq u < 1 \end{cases}$$

$$\gamma(u) = \gamma'(u) = \begin{cases} 1 & \text{for } V=0; u=1 \\ 2 & \text{for } V>0; 0 \leq u < 1 \end{cases}$$

The probability distribution of the point ℓ on a long chain of n -th order walks, $z_n(\ell, u)$, is also studied. The maximum peak of the distribution shifts to the end of the chain due to the increase of the interaction V .

The generating function method is employed to calculate those quantities $C_n(u)$, $U_n(u)$, $\langle r_n^2(u) \rangle$ and $z_n(\ell, u)$ in the case of strong coupling in which the interaction, V , is large. The asymptotic behaviors as $n \rightarrow \infty$ for the quantities are obtained either by evaluating the residues with respect to the singularities of the generating functions or by applying the saddle-point contour integration. When the results are compared, they turn out to be the same. Last, the Green's function method based on Edwards' suggestion was tried as a solution to this problem. However, the results were not valid.

INTRODUCTION

I. Definition of self-avoiding walk problem and relation to the model of polymer chain

A self-avoiding walk on a lattice is a random walk subject to the condition that no lattice site can be visited more than once in the walk. Self-avoiding walks were first introduced as models of polymer chains which took into account in a realistic manner the 'excluded-volume' effect¹⁻⁶ (the fact that no element of space can be occupied more than once by the polymer chain due to the existence of the repulsive interaction between the molecules). Although the mathematical problem of calculating the properties of self-avoiding walks is formidable, the model is well suited to computer enumerations, and has been the subject of many investigations.

II. Numerical studies and hypotheses

The interesting things are to determine c_n , the total number of self-avoiding walks; U_n , the total number of closed-polygons; and $\langle r_n^2 \rangle$, the mean-square size or end-to-end length of all n step walks with no self-intersection. Fisher and Sykes proposed relations of the form.⁴

$$c_n \approx B n^\alpha \mu^n$$

and

$$U_n \approx B' n^\beta \mu^n \quad \text{as } n \rightarrow \infty \quad (1)$$

where μ is the effective coordination number which depends

on the lattice structure only. Using the extrapolation techniques, one can plot the successive ratios $\frac{c_{n+1}}{c_n}$ and $\frac{U_{n+1}}{U_n}$ vs. n^{-1} . Once the region of asymptotic validity has been attained, one should obtain straight lines whose slopes determine the values of α and β and whose intercepts on the axis $n \rightarrow \infty$ determine μ . Detailed numerical analysis suggests that²⁻⁹

$$\alpha = \begin{cases} 1/3 & \text{for all 2 dimensional lattice} \\ 1/6 & \text{for all 3 dimensional lattice} \end{cases} \quad (2)$$

and

$$\beta = \begin{cases} -3/2 & \text{for all 2 dimensional lattice} \\ -7/4 & \text{for all 3 dimensional lattice} \end{cases} \quad (3)$$

The most important point in the self-avoiding walk problem is the mean-square size $\langle r_n^2 \rangle$. Flory¹⁰ suggested $\langle r_n^2 \rangle$ should vary as

$$\langle r_n^2 \rangle \approx C n^\gamma \quad \text{as } n \rightarrow \infty \quad (4)$$

More generally Flory's argument, which may be recast in the form of a standard mean-field or Van der Waals-like approximation for the long-range part of the interaction, yields

$$\gamma = \frac{6}{d + 2} \quad d=1, 2, 3, 4, \dots \quad (5)$$

By using the ratio test and plotting the successive ratios

$\frac{\langle r_{n+1}^2 \rangle}{\langle r_n^2 \rangle}$ vs. n^{-1} , one should also obtain straight lines whose slope determines the index γ . The numerical values of γ_2 and γ_3 have been estimated to be^{11,12}

$$\gamma = \begin{cases} 1.50 & \text{for all 2 dimensional lattice} \\ 1.18 & \text{for all 3 dimensional lattice} \end{cases} \quad (6)$$

In 1967, Reiss¹³ based on the variation principle and developed a new self-consistent field approach to the excluded-volume problem. The zeroth-order self-consistent field (based on freely orienting chain statistics) is computed and a partial differential equation is developed for the description of the random flight in a field problem emerging from the self-consistent field approach. The appropriate boundary value problem is solved and the mean-square end-to-end distance of the polymer molecule is proportional to $L^{4/3}$ in three dimensions, where L is the length of the chain. This does not satisfy either Domb's computer-generated calculation¹¹ or the analytical approximation of a self-consistent field model by Edwards.^{14,15} Both authors arrived at the prediction that mean-square end-to-end distance for the chain should vary as $L^{6/5}$. More recently des Cloizeaux¹⁶ considered the method by introducing the trial probabilities which are determined by minimization of the free energy; these probabilities define the mean-square size of the chain. The calculation suggests that the mean-square distance is of the

form

$$\langle r_n^2 \rangle \approx A L^{2\vartheta} (\ln L)^\epsilon \quad (7)$$

where	$\vartheta = 1$, $\epsilon = -1$	for $d = 2$
	$\vartheta = 2/3$, $\epsilon = 0$	for $d = 3$
	$\vartheta = 1/2$, $\epsilon = 1/2$	for $d = 4$
	$\vartheta = 1/2$, $\epsilon = 0$	for $d > 4$

In the case of $d=3$, the mean-square size is proportional to $L^{4/3}$. Both Reiss' and des Cloizeaux's results do not agree to Flory's suggestion that $\gamma = 6/5$ in three dimensions.

III. Relation between Self-avoiding walk and Ising problem

Interest has also been centered on the correspondence between the self-avoiding walks and Ising model.^{3,4,8,17-19}

The high temperature expansion of the magnetic susceptibility in zero field can be written as^{3,4,8,17-19}

$$\frac{kT}{m^2} x_0 = \sum_{n=0}^{\infty} d_n w^n \quad (8)$$

Where d_n is the n -th coefficient which is given by the number of configurations of specified types of diagrams which can be constructed from n bonds of the lattice, m is the magnetic moment per spin and $w = \tanh \frac{J}{kT}$ (J is the interaction between two spins). The analogy between Ising configurations

d_n and the self-avoiding walks c_n was discussed by Temperley¹⁸ and Fisher and Sykes⁴. The limit μ of the self-avoiding walks and the Ising critical point w_c differ by 10% in two dimensions and 2.5% in three dimensions. The Ising calculations are much more complicated than those of self-avoiding walks, but the exact analytic solution of the two dimensional problem can be found. We can examine the numerical behavior of the coefficients in series expansions in this case and use them as guides to more complicated problems in which no analytic solution are available. Numerical studies show that the dominant contribution to the magnetic susceptibility series comes from the single chain. If we take only such chains into account, we have a self-avoiding walk approximation in which the behavior of the susceptibility in the critical region is characterized by the function

$$\sum_{n=0} c_n w^n$$

Using the numerical results, the critical point is given by $\mu = w_c^{-1}$ and the behavior in its neighborhood is given by

$$x_o \sim \left(1 - \frac{w}{w_c}\right)^{-(1+\alpha)} \quad (9)$$

Actually,^{3-9,17-19}

$$x_o \sim \left(1 - \frac{w}{w_c}\right)^{-7/4} \quad \text{for all 2 dimensions} \quad (10)$$

$$x_o \sim \left(1 - \frac{w}{w_c}\right)^{-5/4} \quad \text{for all 3 dimensions}$$

The mean-square length of the self-avoiding walk $\langle r_n^2 \rangle$ corresponds to the mean-square correlation length L^2 in Ising model. The diagrams expansion of L^2 are the same as those defined in the susceptibility coefficients d_n , but each diagram is now multiplied by a mean-square length factor. Taking the self-avoiding walk approximation c_n , we find

$$L^2 \sim \left(1 - \frac{w}{w_c}\right)^{-\gamma} \quad (11)$$

$$\text{where } \gamma = \frac{6}{d+2}$$

The correct values are known exactly in two dimensions, and from numerical studies in three dimensions^{11,12}

$$L^2 \sim \left(1 - \frac{w}{w_c}\right)^{-\gamma} \quad \begin{aligned} \gamma &= 2.00 \text{ in 2 dimensions} \\ &\gamma = 1.29 \text{ in 3 dimensions} \end{aligned} \quad (12)$$

IV. One-dimensional Self-avoiding walks

The primary reason for our interest in one-dimensional system is that they afford the simplest example of a non-trivial many body system, and the diagram counting is much easier in one dimension than in the higher dimensions. The hope has been that an understanding of this system will lead to some insight into more realistic two-and three-dimensional systems.

The actual one-dimensional self-avoiding walk can only be a straight line and the walk can never move in two different directions. We may make the one-dimensional problem more interesting and construct a model by considering the ordinary random walk on a finite chain and assume the existence of a finite strength repulsive interaction for any pair of steps (links) between the same two lattice sites. This can be introduced by a weighting factor²⁰ $u = \exp(-V)$, where V is the strength of the interaction.

Now we can calculate the total number of walks $c_n(u)$; the total number of walks returning to the starting point (which is equivalent to closed polygons in two and three dimensions) $U_n(u)$ ⁷; the mean-square end-to-end distance $\langle r_n^2(u) \rangle$; and the weighted sum of mean-square deviation of link (steps) $\langle r_n^{2'}(u) \rangle$ (which is equivalent to $\langle r_n^2(u) \rangle$ while the walk returns to origin), of all order n diagrams in one dimension. Obviously, these quantities are functions of u . In this way, we may have two extreme cases: For $V = 0$, $u = 1$, it reduces to the ordinary random walk problem; for $V \rightarrow \infty$, $u \rightarrow 0$, there is infinite repulsive coupling between the steps (links), and the problem reduces to a complete excluded-volume problem in one dimension.

Then we can write the asymptotic behavior of these quantities same as before, namely

$$c_n(u) \approx B(u) n^{\alpha(u)} \mu(u)^n$$

(13)

$$U_n(u) \approx B'(u) n^{\beta(u)} \mu'(u)^n \quad \text{as } n \rightarrow \infty$$

and

$$\langle r_n^2(u) \rangle \approx A(u) n^{\gamma(u)}$$

(14)

$$\langle r_n^{2'}(u) \rangle \approx A'(u) n^{\gamma'(u)} \quad \text{as } n \rightarrow \infty$$

Both indices and constants are functions of u . In the case of very strong coupling, $V \gg 0$, $u \approx 0$, we can easily see that the total number of walks $c_n(0) = 2$, which yields $\alpha(0) = 0$ and $\mu(0) = 1$; the total number of walks which return to the starting point $U_n(0) = 2ne^{-\frac{n}{2}V}$, has the property $\beta(0) = 1$ and $\mu'(u) = e^{-\frac{n}{2}V}$ and the mean-square end-to-end distance $\langle r_n^2(0) \rangle = n^2$ and $\gamma(0) = 2$.

We may speculate the indices $\alpha(u)$, $\beta(u)$, $\gamma(u)$, and $\gamma'(u)$ are independent of the strength of the interaction V except at $V = 0$. In other words, once there exists a small repulsion V between a pair of steps, then these indices will behave the same as those in the strong coupling approximation (V is large), which are quite different from the case $V = 0$. Therefore, there may exist a discontinuity between $V > 0$ and $V = 0$ ($u=1$ and $0 \leq u < 1$).

V. Description of Methods

In part I of this thesis, we adopt the approach initiated by Fisher and Hiley^{5,6} to count $c_n(u)$, the total number of walks and $\langle r_n^2(u) \rangle$, the mean-square size of walks of order n , up to $n = 15$ and $U_n(u)$, the total number of walks which return to the starting point and the weighted sum of mean-square deviation of links (steps) $\langle r_n^{2'}(u) \rangle$, of all order n diagrams, up to $n = 20$. For small values of n , we can use the extrapolation techniques and establish the asymptotic behaviors of $c_n(u)$, $\langle r_n^2(u) \rangle$, $U_n(u)$, and $\langle r_n^{2'}(u) \rangle$ as $n \rightarrow \infty$, and calculate the indices of $\alpha(u)$, $\beta(u)$, $\gamma(u)$, and $\gamma'(u)$ for different values of u . We also evaluate $z_n(\ell, u)$ the probability distribution of the point ℓ on a long chain of n -th order of walks and examine the shape of the distribution functions and how the maximum peak shifts due to changing the strength of the interaction V .

In the part II of this thesis, we consider a strong coupling approximation and assume the interaction V between the pair of steps is very large, then we can consider those quantities $c_n(u)$, $U_n(u)$, $\langle r_n^2(u) \rangle$, and $z_n(\ell, u)$ to be the expansion coefficients of the generating functions $F(z)$, $G(z)$, $X(z)$ and $F(z, w)$. In the strong coupling limit, we can sum those functions quite easily. Now the singularities of the generating functions play a very important role to calculate those coefficients. We can calculate them simply by evaluating the residue with respect to its singularities or by saddle-point contour integrations and examine quite clearly the asymptotic behaviors for $n \rightarrow \infty$. Comparing the results in

part I, they turn out to be the same.

The last part of this thesis is based on Edward's method.^{14,15} He assumed the interaction of the polymer with itself could be represented by considering the polymer under the influence of a self-consistent field which reduced the problem to an equation like the Hartree equation for an atom. It also can be shown that the probability distribution of a certain configuration of a single chain can be considered as an ordinary diffusion problem in the presence of a potential. In this case, we can use the perturbation method and expand the probability distribution in terms of the free distribution (which is the distribution in the absence of the potential) and potential. It can be represented in a diagrammatic expansion which is similar to the problem of the expansion of the electron Green's function in the problem of electron-phonon interaction. Then the probability distribution of a chain can be calculated by using the field theory method, and the quantities $c(L)$, the total probability of a chain, which is the same as $c_n(u)$ in the discrete case; $U(L)$ the probability of ring closure, which is the same as $U_n(u)$, the walk returns to origin; and the mean-square size $\langle r^2 \rangle$, which is equivalent to $\langle r_n^2(u) \rangle$, can be written as the integrals in the complex plane.

In part I of this thesis, the limiting values $\alpha(u)$, $\beta(u)$ and $\gamma(u)$ can not be seen very clearly in the cases of small v . We hope to calculate the quantities $c(L)$, $U(L)$ and $\langle r^2 \rangle$

and check the indices $\alpha(\lambda)$, $\beta(\lambda)$ and $\gamma(\lambda)$ again by using the perturbation method indicated above. In the case of weak coupling, we may use the first order term in the series expansion. Unfortunately, we can not obtain the physical results.

PART I

DIAGRAMS COUNTING AND EXTRAPOLATION

I. Diagrams Counting and Extrapolation

The lattice model of a one dimensional polymer molecule with excluded-volume can be investigated by exact numerical calculations for short chains of up to 15 steps. A real polymer molecule can not intersect itself; and this restriction introduces long-range correlations between different parts of the chain which invalidate the simple random-walk theory.

First, we are interested in the dependence of the size of the molecule on the number of links (steps) n in the chain. In the absence of the excluded-volume restriction, the chain may be treated as an ordinary random walk;²² and it then follows quite generally that

$$\langle r_n^2 \rangle \approx n \quad \text{as } n \rightarrow \infty \quad (1.1)$$

The excluded-volume restriction destroys the nature of the ordinary random walk; and certainly the mean-square size is increased. The two-and three-dimensional random walks with excluded-volume have been studied by Fisher and Sykes.⁴

Actually, the one-dimensional random walk with the excluded-volume can only be a straight line, and the walk can never move in two different directions (each lattice site can meet only once); so the mean-square distance is just equal to n^2 . We can make the one-dimensional problem more interesting by

replacing the strict excluded-volume condition by a finite-strength repulsive interaction between the molecules. Now we may construct a new model by considering the ordinary random walk on a finite chain. The interaction between the molecules is taken into account by a weighing factor²⁰ $u = \exp(-V)$ for each pair of steps between the same two lattice sites, where V is the strength of the repulsive interaction. If the diagram contains R steps (links) between the same two lattice sites, then it corresponds to the order of u^{p^R} .

Then let $c_n(u)$ be the total number of walks of order n . We define the order n of a walk to be the total number of steps and let $z_n(\vec{l}, u)$ be the corresponding total number of walks starting at 0 (origin) and ending at \vec{l} . Then we can write

$$c_n(u) = \sum_{\vec{l}} z_n(\vec{l}, u) \quad (1.2)$$

Asymptotically, we can write $c_n(u)$ in the form

$$c_n(u) \sim \mu(u)^n \quad \text{as } n \rightarrow \infty \quad (1.3)$$

where $\mu(u)$ is the effective coordination number depending on the strength of the interaction V . Mathematical support for this result has been proved by Hammersley^{23,24} on the existence of the limit

$$\lim_{n \rightarrow \infty} \frac{1}{n} \ln c_n(u) = \ln \mu(u) \quad (1.4)$$

Fisher and Sykes⁴ proposed a relation of the form

$$c_n(u) \approx B(u) n^{\alpha(u)} \mu(u)^n \quad \text{as } n \rightarrow \infty \quad (1.5)$$

The asymptotic behavior of $c_n(u)$, as $n \rightarrow \infty$, does depend on not only $\mu(u)$ but n as well, which gives us more information about $c_n(u)$ as n tends to infinity.

We go on to let $\langle r_n^2(u) \rangle$ be the total mean-square size or mean-square end-to-end length of a walk of order n , we can write this as:^{11,12,25}

$$\langle r_n^2(u) \rangle = \frac{1}{c_n(u)} \sum_{\vec{l}} l^2 z_n(\vec{l}, u) \quad (1.6)$$

Flory¹⁰ suggested $\langle r_n^2(u) \rangle$ should vary as

$$\langle r_n^2(u) \rangle \approx A(u) n^{\gamma(u)} \quad (1.7)$$

where $A(u)$ is an arbitrary constant and a function of u only.

We also study $U_n(u)$, the total number of walks of order which return to origin, up to $n = 20$. (In two-and three-dimensional random walk problems with excluded-volume each of those walks would result in a closed polygon.) Similarly, we can also write

$$U_n(u) \approx B'(u) n^{\beta(u)} \mu'(u)^n \quad \text{as } n \rightarrow \infty \quad (1.8)$$

Now, we are also interested in calculating $\langle r_n^2(u) \rangle$, which is analogous to $\langle r_n^2(u) \rangle$. In this case, where the walk must return to the starting point, we should define $\langle r_n^2(u) \rangle$ to be the weighted sum of mean-square deviations of links (steps) of all order n diagrams. We can also write $\langle r_n^2(u) \rangle$ as follows:

$$\langle r_n^2(u) \rangle \approx A'(u) n^{\gamma'(u)} \quad \text{as } n \rightarrow \infty \quad (1.9)$$

In this part of the thesis, we will discuss the relation (1.5), (1.7), (1.8) and (1.9) in greater detail. Using extrapolation techniques, we establish that the asymptotic behavior is approached by the exact results for small n and different values of the interaction V and determine the indices $\alpha(u)$, $\beta(u)$, $\gamma(u)$ and $\gamma'(u)$ as functions of u.

A. Calculations of $c_n(u)$ and $u_n(u)$

We have introduced the weighting factor $u = \exp(-V)$ for any pair of links (steps) between the same two lattice sites. For instance, we have the following diagrams



which describes a class of walks of order 9 i.e. containing nine steps. Here • represents the starting point and x represents the ending point. There are 3 links between

points a and b, b and c, each produces a u^3 factor. Two links between points d and e, so produces a u factor. Finally, one link occurs between points c and d; it produces a u^0 factor. The total power of u of the above diagrams is equal to $3+3+0+1=7$. Next, we want to count how many different walks from point a can reach point d in 9 steps following the routes (lines) indicated above. It can be seen only two different ways. So the contribution to the above diagrams is $2u^7$.

First, we are going to calculate $U_n(u)$, the total number of n -step walks which return to the starting point. A few lower order diagrams are shown in Fig. 1, 2, 3. Clearly, only even orders of n are allowed in this case; and each single line in Fig. 1, 2, 3 represents a pair of steps. In Fig. 1, either point a or b can be the starting point. We have two different ways for a walk to return to its starting point, namely a-b-a and b-a-b. Also there is one line (actually a pair of steps) between a and b; this will produce a factor u . The value of $U_2(u)$ is therefore $2u$. In calculating $U_4(u)$, we can have two allowed diagrams which are shown in Fig. 2. In Fig. 2 (1), there is one walk with either c or e as a starting point ($c \rightarrow d \rightarrow e \rightarrow d \rightarrow c$ and $e \rightarrow d \rightarrow c \rightarrow d \rightarrow e$) and there are two walks with d as the starting point ($d \rightarrow e \rightarrow d \rightarrow c \rightarrow d$ and $d \rightarrow c \rightarrow d \rightarrow e \rightarrow d$). The total number of walks for this diagram is equal to $4 u^2$ (the factor u^2 is due to having one line in each interval cd and de). In Fig. 2 (2), we have one walk considering either f

and g as a starting point ($f \rightarrow g \rightarrow f \rightarrow g \rightarrow f$ and $g \rightarrow f \rightarrow g \rightarrow f \rightarrow g$), so the total number of walks for this diagram is $2u^6$ (the factor u^6 comes from having two lines between points f and g). We can combine them together, therefore, $U_4(u) = 4u^2 + 2u^6$.

As to higher order walks, first, we can write down all the allowed diagrams of this order. (When $n = 6$, the allowed diagrams are shown in Fig. 3.) Second, choose one special point in each allowed diagram, generally speaking, the ending point (same as starting point) is most convenient. Then we can use the following formula to calculate the contribution corresponding to this diagram:

$$\left[\begin{array}{l} \text{Contribution to } U_n(u) \\ \text{from a given diagram} \end{array} \right] = (\text{number of steps}) \times \frac{\left\{ \begin{array}{l} \text{number of different ways} \\ \text{starting at any special point} \\ \text{and returning to this point} \end{array} \right\}}{\left\{ \begin{array}{l} \text{number of lines connecting} \\ \text{to this point} \end{array} \right\}} \times u^q \quad (1.10)$$

where $q = \text{number of pairs of overlapping links (number of interactions)}$. In Fig. 2 (1), if we look at the point c, the number of different ways of starting at c and returning to the same point is equal to one and the number of lines

connecting to c is also equal to one. From the above equation, we can get the total number of walks of this diagram is equal to

$$4 \times \frac{1}{1} \times u^2 = 4 u^2$$

Similarly in Fig. 2 (2), if we choose the point f, the total number of walks of this diagram is equal to

$$4 \times \frac{1}{2} \times u^6 = 2 u^6$$

Using this method, we can get high order walks up to $n = 20$; and these walks are listed in the Table 1.

Second, we are going to calculate $c_n(u)$, the total number of n-step walks. A few lower diagrams are shown in Fig. 4, 5, 6. From eq. (1.2), we can write $c_n(u)$ in terms of $z_n(\vec{\ell}, u)$, namely

$$c_n(u) = \sum_{\vec{\ell}} z_n(\vec{\ell}, u) \quad (1.2)$$

In one dimension, $\vec{\ell}$ can only be $\pm \ell$. Clearly, we need calculate only for positive ℓ , and then multiply the result by a factor two. It is also easy to see that if n is even, only even ℓ are allowed; and if n is odd, only odd ℓ are allowed. We conclude as follows:

$$\ell = \begin{cases} 0, 2, 4, 6, 8, \dots & n \text{ is even} \\ 1, 3, 5, 7, 9, \dots & n \text{ is odd} \end{cases} \quad (1.11)$$

The diagram of $c_1(u)$ is shown in Fig. 4. The allowed value of ℓ can only be one, i.e. $c_1(u) = 2z_1(1,u) = 2$. The diagrams of $c_2(u)$ are shown in Fig. 5 and the allowed values of ℓ are 0 and 2, $z_2(2,u) = 1$ corresponding to Fig. 5 (1) and $z_2(0,u) = 2u$ corresponding to Fig. 5 (2). So $c_2(u) = z_2(0,u) + 2z_2(2,u) = 2 + 2u$. Similarly, the diagrams of $c_3(u)$ are shown in Fig. 6. The allowed values of ℓ are 1 and 3, $z_3(1,u) = 1$ corresponding to Fig. 6 (1) and $z_3(3,u) = 2u + u^3$ corresponding to Fig. 6 (2,3,4). So $c_3(u) = 2z_3(1,u) + 2z_3(3,u) = 2 + 4u + 2u^3$. We have calculated $c_n(u)$ up to $n = 15$ which are listed in the Table 2.

The summation \sum_{ℓ} in eq. (1.2) is summed over all ℓ ; both positive and negative. We can rewrite eq. (1.2) as follows:

$$c_n(u) = \sum_{\ell=-n}^{\ell=n} z_n(\ell,u) = z_n(0,u) + 2 \sum_{\ell=1}^n z_n(\ell,u) \quad (1.12)$$

$$\text{where } z_n(0,u) = U_n(u) \quad (1.13)$$

If we let $V = 0$, u tends to unity, $c_n(u=1)$ becomes the

ordinary random walk problem. We can show that the total number of walks are equal to

$$c_n(u=1) = 2^n \quad (1.15)$$

It also can be shown that $U_n(u=1)$ has the form

$$U_n(u=1) = \frac{n!}{\left(\frac{n}{2}\right)! \left(\frac{n}{2}\right)!} \quad (1.16)$$

Calculations of $c_n(u)$ and $U_n(u)$ are very complicated up to higher order n and errors are easily made. Fortunately, we can check these results with the help of above two equations.

B. Asymptotic Behaviors of $c_n(u)$ and $U_n(u)$

In this section, we discuss the asymptotic behaviors of $c_n(u)$ and $U_n(u)$, as revealed by the exact values for small n . Basic techniques for the excluded-volume problem had been discussed by Fisher and Hiley,⁵ by Fisher and Sykes⁴ and reviewed by Domb.^{13,17} Equations (1.5) and (1.8) have the forms

$$c_n(u) \approx B(u)n^{\alpha(u)} \mu(u)^n \quad (1.5)$$

$$U_n(u) \approx B'(u)n^{\beta(u)} \mu'(u)^n \quad (1.8)$$

To investigate the behaviors of $c_n(u)$ and $U_n(u)$ it is

natural to consider the successive ratios

$$\mu_n(u) = c_{n+1}(u)/c_n(u) \quad (1.17)$$

$$\mu'_n(u) = U_{n+2}(u)/U_n(u) \quad (1.18)$$

If these ratios approach a limit as $n \rightarrow \infty$ for different values of u , then these limits are equal to the effective coordination numbers $\mu_\infty(u)$ and $\mu'_\infty(u)$.

In practice, it is found that when the ratios $\mu_n(u)$ and $\mu'^2_n(u)$ are plotted against n^{-1} , they lie remarkably close to straight lines of definite slopes and, for n large, these lines intersect the $n \rightarrow \infty$ axis at $\mu_\infty(u)$ and $\mu'^2_\infty(u)$. The linear behaviors of $\mu_n(u)$ and $\mu'^2_n(u)$ with n^{-1} , namely,

$$\mu_n(u) \approx \mu_\infty(u) \left(1 + \frac{a}{n} + O\left(\frac{1}{n^2}\right) \right) \quad (1.19)$$

$$\mu'^2_n(u) \approx \mu'^2_\infty(u) \left(1 + \frac{2\beta}{n} + O\left(\frac{1}{n^2}\right) \right) \quad (1.20)$$

as $n \rightarrow \infty$

It may readily be understood³⁻⁹ by regarding $c_n(u)$ and $U_n(u)$ as the coefficients in the power series expansions of generating functions

$$P(z) = \sum_{n=0}^{\sigma} c_n(u) z^n \quad (1.21)$$

$$Q(z) = \sum_{n=0}^{\infty} U_n(u) z^n \quad (1.22)$$

In virtue of eqs. (1.5) and (1.8), $P(z)$ and $Q(z)$ have their singularities nearest to the origin on the real axis at $z_C = \mu(u)^{-1}$ and $z'_C = \mu'(u)^{-1}$. (We denote $\mu_\infty(u) = \mu(u)$ and $\mu'_\infty(u) = \mu'(u)$ which will be the radius of convergence of the series (1.21) and 1.22). The relations (1.19) and (1.20) imply the dominant behaviors near z_C are

$$P(z) \approx \frac{K}{(1 - \mu(u)z_C)^{1+\alpha}} \quad (1.23)$$

$$Q(z) \approx \frac{K'}{(1 - \mu'(u)z'_C)^{1+\beta}} \quad (1.24)$$

The binomial theorem and Stirling's asymptotic formula yield

$$c_n(u) \approx B(u) n^{\alpha(u)} \mu(u)^n \quad (1.5)$$

$$u_n(u) \approx B'(u) n^{\beta(u)} \mu'(u)^n \quad (1.8)$$

as $n \rightarrow \infty$

where $B(u)$ and $B'(u)$ are constants independent of n . If $P(z)$ and $Q(z)$ have the forms (1.23) and (1.24), then the ratios $\mu_n(u) = c_{n+1}(u)/c_n(u)$ and $\mu_n'^2(u) = u_{n+2}/u_n$ are given by eqs. (1.19) and (1.20), so plots of $\mu_n(u)$ and $\mu_n'^2(u)$ against n^{-1} are

straight lines of slopes α and β which intercept the $n \rightarrow \infty$ axis at $\mu(u)$ and $\mu'^2(u)$. The numerical values of $\mu(u)$ and $\mu'(u)$ are shown in the Table 3 and 4 and the plots of $\mu(u)$ and $\mu'(u)$ vs. V can be seen in Fig. 7 and 8.

Series of coefficients very similar to $c_n(u)$ and $U_n(u)$ arise in many other statistical problems, in particular in the Ising model,^{3,4,17-19} except those coefficients are a pure number not a polynomial of u . If $P(z)$ and $Q(z)$ are not merely a simple binomial expression, then eqs. (1.19) and (1.20) will contain higher power of n^{-1} so that the $\mu_n(u)$ vs. n^{-1} and $\mu_n'^2(u)$ vs. n^{-1} plots will be somewhat curved. Also the points may oscillate slightly about the straight line. In practice it is found that the series $c_n(u)$ and $U_n(u)$ give quite good extrapolation after the fourth or fifth terms. These behaviors are illustrated for different values of interaction in Fig. 9 and Fig. 10.

Next, we want to find out the slope indices α and β in eqs. (1.5) and (1.8). In doing so, we can rewrite the equations (1.19) and (1.20) as

$$\mu_n(u) \approx \mu_\infty(u) \left(1 + \frac{\alpha n}{n}\right) \quad (1.26)$$

$$\mu_n'^2(u) \approx \mu_\infty'^2(u) \left(1 + 2\frac{\beta n}{n}\right) \quad (1.27)$$

as $n \rightarrow \infty$

where $\mu_\infty(u) = \mu(u)$ and $\mu_\infty'(u) = \mu'(u)$.

$$\text{and } \alpha_n \approx \alpha + \frac{\alpha'}{n} + O\left(\frac{1}{n^2}\right) \quad (1.28)$$

$$\beta_n \approx \beta + \frac{\beta'}{n} + O\left(\frac{1}{n^2}\right) \quad (1.29)$$

In the first approximation, as $n \rightarrow \infty$, both α_n and β_n approach the limits α and β . If the values of $\mu(u)$ and $\mu'(u)$ are known, we can get the successive estimations of α_n and β_n by using the following formulas. From eqs. (1.26) and (1.27)

$$\mu_n(u) - \mu_{n+1}(u) \approx \mu(u) \left(\frac{1}{n} - \frac{1}{n+1} \right) \alpha_n(u)$$

then

$$\alpha_n(u) = \frac{\mu_n(u) - \mu_{n+1}(u)}{\mu(u) \left(\frac{1}{n} - \frac{1}{n+1} \right)} \quad (1.30)$$

similarly,

$$\mu_n'^2(u) - \mu_{n+2}'^2(u) \approx 2\mu'(u)^2 \left(\frac{1}{n} - \frac{1}{n+2} \right) \beta_n(u)$$

then

$$\beta_n(u) = \frac{\mu_n'^2(u) - \mu_{n+2}'^2(u)}{2\mu'(u)^2 \left(\frac{1}{n} - \frac{1}{n+2} \right)} \quad (1.31)$$

These imply linearities of α_n and β_n with n^{-1} for large n .

The linear extrapolations will lead to accurate values of α and β . The extrapolations of α_n and β_n vs. n^{-1} for different values of interaction V are plotted in Fig. 11 and Fig. 12.

The results we get, are as follows:

1. Extrapolations of $\beta_n(u)$ vs. n^{-1}
 - a. $V = 0$, $u = 1$, we have the ordinary random walk problem,
 $\beta(u=1) = -1/2$ (See Appendix II).
 - b. Intermediate region $0 < V < 0.25$, the curves bend upward rapidly, and the limiting value β does not equal $-1/2$ any more. We may guess β tends to 1, but we do not have enough walks to see this.
 - c. Strong repulsion, $V > 0.25$, although the extrapolation curves are saw-tooth shapes, we still can see the limiting values of β quite clearly, namely $\beta = 1$ for all $V > 0.25$.
2. Extrapolations of $\alpha_n(u)$ vs. n^{-1}
 - a. $V = 0$, $u = 1$, this is the case of ordinary random walk problem, the index $\alpha(u=1)$ should tend to zero.
 - b. Because we have counted $c_n(u)$ up to $n = 15$, the extrapolations are not so good as that of $U_n(u)$ which we have counted up to $n = 20$. The intermediate region is larger than above, namely, $0 < V < 0.75$. In $0 < V < 0.10$, the curves grow up very rapidly for increasing n . As we increase the interaction V , in the region of $0.10 < V < 0.50$, the curves do not grow up too fast comparing with the cases which are described above. The curves increase and pass through a maximum then drop off. For $0.50 < V < 0.75$, the curves decrease for increasing values of n . We are unable to observe the limiting values of $\alpha_n(u)$ quite easily. But we might guess that those curves

in this region, $0 < V < 0.75$, will also drop to zero which is the same as $V = 0$.

- c. In the cases of strong repulsion, $V > 0.75$, we go on increasing the interaction V . The extrapolation curves are almost straight lines whose intersections on the axis $n \rightarrow \infty$ are all equal to zero.

In the intermediate region, we might guess $\beta(u) \rightarrow 1$ and $\alpha(u) \rightarrow 0$; but we can not count long enough to see these. In summary, our results seem to be consistent with the conjecture:

$$\alpha(u) = 0 \quad \text{for all } V \geq 0; \quad 0 \leq u \leq 1$$

and

$$\beta(u) = \begin{cases} -1/2 & \text{for } V=0, \quad u=1 \\ 1 & \text{for } V>0, \quad 0 \leq u < 1 \end{cases}$$

The indices $\alpha(u)$ and $\beta(u)$ are independent of the strength of the interaction.

c. Calculations of $\langle r_n^2(u) \rangle$ and $\langle r_n^{2'}(u) \rangle$

We then go on to apply the same method to the mean-square size $r_n^2(u)$ which has been defined in eq. (1.6)^{11-12,25}

$$r_n^2(u) = \frac{1}{c_n(u)} \sum_{\ell} \ell^2 z_n(\ell, u) \quad (1.6)$$

The summation over ℓ is only defined for all positive values of ℓ . We also define $r_n^2(u)$ to be the weighted sum of mean-square deviations of links (steps) of all order n diagrams. It can be written as:

$$r_n^2(u) = \frac{1}{U_n(u)} \sum_{\Gamma} \Delta r^2_{n,\Gamma} w_{\Gamma}^n(u) \quad (1.33)$$

where Γ symbolizes the different topological diagrams of order n and $w_{\Gamma}^n(u)$ is the contribution from the diagram Γ . Then

$$U_n(u) = \sum_{\Gamma} w_{\Gamma}^n(u) \quad (1.34)$$

$$\text{and } \langle \Delta r^2 \rangle_{n,\Gamma} = \langle (r - \bar{r})^2 \rangle_{n,\Gamma} = \langle r^2 \rangle_{n,\Gamma} - \langle r \rangle_{n,\Gamma}^2$$

is the mean-square deviation of links of the Γ diagram of order n , the weight factor being the number of links at an arbitrary point r . For example, in Fig. 3 represented $U_6(u)$ we have three different kind of diagrams, then $\Gamma = 1, 2, 3$ and $w_1^6(u) = 6u^3$ (Fig. 3 (1)), $w_2^6(u) = 12u^7$ (Fig. 3 (2)), $w_3^6(u) = 2u^{15}$ (Fig. 3 (3)). In Fig. 3 (1), $\langle r \rangle_{6,1} = 1/3 \times (1 + 2 + 3) = 2$ and $\langle r^2 \rangle_{6,1} = 1/3(1^2 + 2^2 + 3^2) = 14/3$ then $\langle \Delta r^2 \rangle_{6,1} = \langle r^2 \rangle_{6,1} - \langle r \rangle_{6,1}^2 = 2/3$, In Fig. 3 (2), $\langle r \rangle_{6,2} = 1/3 \times (1 + 2 \times 2) = 5/3$ and $\langle r^2 \rangle_{6,2} = 1/3(1^2 + 2 \times 2^2) = 3$ then $\langle \Delta r^2 \rangle_{6,2} = 2/9$. Similarly, in Fig. 3 (3), $\langle r \rangle_{6,3} = 1/3(3 \times 1^2) = 1$ and $\langle r^2 \rangle_{6,3} = 1/3(3 \times 1^2) = 1$ then $\langle \Delta r^2 \rangle_{6,3} = 0$.

From eq. (1.33), combining together we get

$$r_6^2(u) = \frac{1}{U_6(u)} \sum_{\Gamma=1}^3 \Delta r^2_{6,\Gamma} w_{\Gamma}^6(u)$$

$$\langle r_6^2(u) \rangle^{-1} = \frac{1}{U_6(u)} \left[\langle \Delta r_{6,1}^2 W_1^6(u) + \Delta r_{6,2}^2 W_2^6(u) + \Delta r_{6,3}^2 W_3^6(u) \rangle \right]$$

$$= \frac{1}{U_6(u)} (4u^3 + 8/3 u^7)$$

All values of $r_n^2(u)$ and $r_n^{2'}(u)$ are listed in Table 5 and 6.

From eqs. (1.7) and (1.9), we can write:

$$r_n^2(u) \approx A(u) n^{\gamma(u)} \quad (1.7)$$

$$r_n^{2'}(u) \approx A'(u) n^{\gamma'(u)} \quad (1.9)$$

as $n \rightarrow \infty$

where $A(u)$ and $A'(u)$ are constants which are independent of the order of walks n . To analyze the behavior, we consider the ratios

$$v_n(u) = \langle r_{n+1}^2(u) \rangle / \langle r_n^2(u) \rangle \quad (1.35)$$

$$v_n'^2(u) = \langle r_{n+2}^2(u) \rangle / \langle r_n^2(u) \rangle \quad (1.36)$$

In the case of ordinary random walk, the limiting ratios v_∞ and $v_\infty'^2$ exist and we may except this to be true also if we consider the existence of the repulsive interaction between the molecules. We can apply the same ratio test method as in Sec. I. B. From eqs. (1.35) and (1.36), we can get

$$v_n(u) = (1 + \frac{1}{n})^{\gamma(u)} - 1 + \frac{\gamma_n(u)}{n} \quad (1.37)$$

$$v_n^{(2)}(u) = \left(1 + \frac{2}{n}\right) \gamma'(u) \approx 1 + \frac{2\gamma'_n(u)}{n} \quad (1.38)$$

where

$$\gamma_n(u) \approx \gamma + \frac{\delta}{n} + O\left(\frac{1}{n^2}\right) \quad (1.39)$$

$$\gamma_n'(u) \approx \gamma' + \frac{\delta'}{n} + O\left(\frac{1}{n^2}\right) \quad (1.40)$$

Similarly, as $n \rightarrow \infty$, $\gamma_n(u)$ and $\gamma_n'(u)$ approach the values $\gamma(u)$ and $\gamma'(u)$. Then

$$\gamma_n(u) = n(v_n(u) - 1) \quad (1.41)$$

$$\gamma_n'(u) = n/2(v_n^{(2)}(u) - 1) \quad (1.42)$$

These also imply the linear dependence of $\gamma_n(u)$ and $\gamma_n'(u)$ on n^{-1} for large n , and the linear extrapolations will lead to accurate values of $\gamma(u)$ and $\gamma'(u)$. The extrapolations of $\gamma_n(u)$ and $\gamma_n'(u)$ vs. n^{-1} for different values of V are plotted in Fig. 14 and Fig. 15.

We can get the following results: The nature of the extrapolation curves $\gamma_n'(u)$ vs. n^{-1} will be the same as those of $\beta_n(u)$ vs. n^{-1} and $\gamma_n(u)$ vs. n^{-1} also will be the same as those of $\alpha_n(u)$ vs. n^{-1} .

1. Extrapolations of $\gamma_n'(u)$ vs. n^{-1}
 - a. $V = 0, u = 1$, this is the ordinary random walk problem. $\gamma'(u=1)$ is equal to unity as $n \rightarrow \infty$.
 - b. Intermediate region, $0 < V < 0.25$, the tail of the extrapolation curves bend up. Definitely, the limiting values of $\gamma'(u)$ are no longer unity. We might guess $\gamma'(u) \approx 2$. It may be seen quite clearly if we have counted more higher order walks.
 - c. Strong repulsion, $V > 0.25$, as we increase the strength of the interaction V , we can observe all the curves will extrapolate to the value 2 for all $V > 0.25$.
2. Extrapolations of $\gamma_n(u)$ vs. n^{-1}
 - a. $V = 0, u = 1$, this is the case of the ordinary random walk problem, the extrapolation curve is a straight line and the intersection at the axis $n \rightarrow \infty$ is equal to unity.
 - b. Intermediate region, $0 < V < 0.75$
The nature of this region will be the same as that of the extrapolations of $\alpha_n(u)$ vs. n^{-1} . In this region, the curves also bend upward very rapidly. As we increase the interaction V again, the curves will pass through a maximum peak then drop off. We can not observe the limiting value $\gamma(u)$, but we may speculate the curves which will drop to two and it is different from the case of $V = 0$.
 - c. Strong repulsion, $V > 0.75$
We go on increasing the interaction V . The extra-

pulation curves will fall exactly on two whenever $0.75 < V < 1.5$. For $V > 1.5$, the curves almost tend to straight lines whose intersections on the axis are all equal to two.

We may speculate

$$\gamma(u) = \gamma'(u) = \begin{cases} 1 & \text{for } V = 0, u = 1 \\ 2 & \text{for } V > 0; 0 \leq u < 1 \end{cases} \quad (1.43)$$

This is in agreement with Flory's suggestion. The index γ should be equal to 2 in the cases of $V > 0$. $\gamma(u)$ and $\gamma'(u)$ have the same natures as $\alpha(u)$ and $\beta(u)$ indices which are independent of the strength of the interaction V .

D. Probability Distribution of the end-points

From eq. (1.2), we can write $c_n(u)$ as the sum of $z_n(\ell, u)$. Now we want to define a quantity $P_n(\ell, u)$ ²⁶ which will be the probability distribution function of the point ℓ away from the origin after n -step walks.

$$P_n(\ell, u) = \frac{1}{c_n(u)} z_n(\ell, u) \quad (1.44)$$

where $P_n(\ell, u)$ is normalized, i.e.

$$\sum_{\ell} P_n(\ell, u) = 1 \quad (1.45)$$

Substituting eq. (1.12) into eq. (1.44), we will obtain the probability distribution $P_n(\ell, u)$ for all ℓ . Since the distribution function $P_n(\ell, u)$ is symmetric with respect to $\ell = 0$, we only consider the cases for $\ell > 0$.

For $V = 0$; $u = 1$, the probability distribution function $P_n(\ell, u=1)$ will satisfy the simple diffusion equation and is a Gaussian (Appendix I). In the presence of the excluded-volume effect; $V \neq 0$, the distribution function $P_n(\ell, u)$ is no longer expected to be Gaussian. As we increase the strength of the interaction, the peak of the curve moves away from the origin and $P_n(0, u)$ decreases.^{15,26} For very large V ; $u \approx 0$, the walk can only be a straight line and the probability distribution $P_n(\ell, u \approx 0)$ almost looks like a δ -function at $\ell = n$. Then

$$P_n(\ell, u \approx 0) = \begin{cases} 1 & \ell = n \\ 0 & \ell \neq n \end{cases} \quad (1.46)$$

It becomes a complete excluded-volume problem in one dimension. $P_n(\ell, u)$ for $n = 15$ and 14 are plotted in Fig. 16 and Fig. 17 for different values of interaction V .

PART II

STRONG COUPLING APPROXIMATION

II. Strong-coupling approximation

In this part of the thesis we are going to discuss the cases when the repulsive interaction V is very strong, then some of the higher order diagrams can be neglected. The high order diagrams are defined as those which contain many steps between the same two lattice points. In this case, those diagrams will rise to high power of u ($u=\exp(-V)$) which will be a very small quantity (since V is very large), and the contributions from those higher order diagrams can be ignored. Now, we may evaluate the total number of walks; $c_n(u)$, the total number of walks which return to the origin; $U_n(u)$, and the mean-square size; $\langle r_n^2(u) \rangle$ up to higher order of n , say $n \rightarrow \infty$. The asymptotic behaviors of $c_n(u)$, $U_n(u)$ and $\langle r_n^2(u) \rangle$ as $n \rightarrow \infty$ will be easily calculated. We compare the results from eqs. (1.5), (1.7) and (1.8) and also check the values of $v(u)$ and $v'(u)$, the indices of $\alpha(u)$, $\beta(u)$ and $\gamma(u)$ in the cases of strong coupling.

The strong coupling approximation gives quite good asymptotic behaviors for $n \rightarrow \infty$, whereas the counting method is valid for all the interactions but only for finite value of n . This is the most important difference between these two cases. The technical trick to evaluate the quantities $c_n(u)$, $U_n(u)$ and $\langle r_n^2(u) \rangle$ is based on the generating function method which will be described below:

We consider the generating function $F(z)$ which can be written as the sum of an infinite series .

$$F(z) = \sum_{m=0} c_m z^m \quad (2.1)$$

by using the formula

$$\delta_{n,m} = \frac{1}{2\pi i} \oint_C \frac{z^m dz}{z^{n+1}} \quad (2.2)$$

where the contour C is a circle around the origin (Fig. 18), we can evaluate the coefficients c_n very easily by the complex contour integration. From

$$c_n = \sum_m c_m \delta_{n,m} \quad (2.3)$$

and substituting eq. (2.2) into eq. (2.3), we can obtain

$$c_n = \frac{1}{2\pi i} \oint_C \frac{F(z) dz}{z^{n+1}} \quad (2.4)$$

Suppose we can get $F(z)$ by summing all infinite terms from $m = 1$ to $m = \infty$ in eq. (2.1), and using this equation (2.4) we can find out the coefficients c_n .

A. Calculations of generating function²¹

In order to calculate $c_n(u)$, the total number of walks, $\langle r_n^2(u) \rangle$, the mean-square size and $z_n(\ell, u)$, the un-normalized probability distribution at the point ℓ of the n -th order of walks, we consider the generating function $F(z, w)$ which can be defined as

$$F(z, w) = \sum_{m=0}^{\infty} \sum_{\ell'=0}^m z_m(\ell', u) z^m w^{\ell'} \quad (2.5)$$

the factor $z^m w^{\ell'}$ is associated with the diagram which contains m -th order of walk and the length ℓ' (the length ℓ' is defined as the distance between the starting point and the end of a walk). For instance, the diagram appearing in page 15, has a factor of $z^9 w^3$.

By setting $w = 1$, we obtain the generating function of $c_n(u)$. The above equation reduces to

$$F(z) = \sum_{m=0}^{\infty} \sum_{\ell'=0}^m z_m(\ell', u) z^m \quad (2.6)$$

Then

$$F(z) = \sum_{m=0}^{\infty} c_m(u) z^m \quad (2.1)$$

Where

$$c_m(u) = \sum_{\ell'=0}^m z_m(\ell', u) \quad (2.7)$$

Next, we are going to differentiate $F(z,w)$ with respect to w twice and get

$$\sum_{m=0}^{\infty} \sum_{\ell'=0}^m z_m(\ell', u) \ell'^2 z^m w^{\ell'} = w^2 \frac{\partial^2 F}{\partial w^2} + w \frac{\partial F}{\partial w} \quad (2.8)$$

Let $w = 1$ again, we obtain the generating function for the un-normalized mean-square size $\langle r_n^2(u) \rangle_{un.}$. Then

$$x(z) = \sum_{m=0}^{\infty} \langle r_m^2(u) \rangle_{un.} z^m = \left(\frac{\partial^2 F}{\partial w^2} \right)_{w=1} + \left(\frac{\partial F}{\partial w} \right)_{w=1} \quad (2.9)$$

where

$$\langle r_m^2(u) \rangle_{un.} = \sum_{\ell'=0}^m z_m(\ell', u) \ell'^2 \quad (2.10)$$

Now, we can apply the contour integration method in eqs. (2.6) and (2.9). By using the eq. (2.4) and integrating in the complex z -plane, we can obtain the coefficients $c_n(u)$ and $\langle r_n^2(u) \rangle_{un.}$. The quantity $z_n(\ell, u)$ can also be obtained by applying the contour integration twice with respect to the variables z and w , namely

$$z_n(\ell, u) = \frac{1}{2\pi i} \oint_C \frac{dz}{z^{n+1}} \frac{1}{2\pi i} \oint_C \frac{dw}{w^{\ell+1}} F(z, w) \quad (2.11)$$

In order to calculate $F(z, w)$ we consider the positive value

of ℓ only (eqs. (1.11-13)) and multiply the final results by a factor two. Then $F(z,w)$ can be separated into two different types of diagrams:

1. All the diagrams which contain at least one single step.

The general form of this kind of diagram can be represented as follows:



where Σ is called the self-energy part of the diagram and two Σ 's can not contact each other. In other words, two Σ 's must be connected by a free line (at least one single step). The Γ is called the vertex part which is only allowed at the ends of diagrams. Then we can let the sum of these diagrams be

$$F_1(z,w) = \Sigma \Gamma^2 \quad (2.12)$$

where Σ is denoted as the sum of all the diagrams without the vertex part Γ at the ends, which are listed in Fig. 19. The lines between two Σ 's can occur in any steps from 1 to ∞ , since two Σ 's can not contact each other. Each step is denoted by a factor zw (the factor z is due to the order of walks and w is due to the length). Then, the line between two Σ 's has the form of

$$zw + (zw)^2 + (zw)^3 + \dots = \sum_{p=1}^{\infty} (zw)^p = \frac{zw}{1 - zw} \quad (2.13)$$

Now, we can sum up all the diagrams of Σ in Fig. 19, namely,

$$\Sigma = \frac{zw}{1-zw} + \frac{zw}{1-zw} \sum \frac{zw}{1-zw} + \frac{zw}{1-zw} \sum \frac{zw}{1-zw} \sum \frac{zw}{1-zw} + \dots \quad (2.14)$$

$$= \frac{zw}{1-zw} + \frac{zw}{1-zw} \left(\sum + \sum \frac{zw}{1-zw} \sum \dots \right) \frac{zw}{1-zw}$$

$$= \frac{zw}{1-zw} + \frac{zw}{1-zw} \frac{zw}{1-zw - \sum zw}$$

$$= \frac{zw}{1-zw - \sum zw} \quad (2.15)$$

where all the diagrams in Σ are listed in Fig. 20.

From now on, we denote the diagrams  by Q_2 ,  by Q_3 ,  by Q_4etc. Generally, the bubble containing n lines will be denoted by Q_n . Similarly, the diagram  can be denoted as $Q_3 * Q_3$. The asterisk "*" is the "symbolic multiplication" which is quite different from the ordinary algebraic multiplication namely, $Q_3 * Q_3 \neq Q_3 \times Q_3$. We can write all the Σ diagrams in Fig. 20 as

$$\Sigma = \sum_{i=\text{odd}} q_i + \sum_{i,j=\text{odd}} q_i * q_j + \sum_{i,j,k=\text{odd}} q_i * q_j * q_k + \dots \quad (2.16)$$

and, let Λ be the total sum of diagrams which are similar to in Fig. 20 except all the odd-line bubbles are replaced by even-line bubbles. The Λ diagrams are listed in Fig. 21 and also can be written as

$$\Lambda = \sum_{i=\text{even}} q_i + \sum_{i,j=\text{even}} q_i * q_j + \sum_{i,j,k=\text{even}} q_i * q_j * q_k + \dots \quad (2.17)$$

Now, we can define the vertex part

$$\Gamma = \left(1 + \Lambda \right) * \left(1 + \Sigma \right) \quad (2.18)$$

$$1 + \Lambda + \Sigma + \Lambda * \Sigma$$

The multiplication "*" is the same as we defined above, We

can easily observe that all the odd-line bubbles and the single steps are contributed to the "length" of a walk. Then each Q_i , $i = \text{odd}$, will be associated a factor w but Q_i , $i = \text{even}$, does not.

In the strong coupling approximation, u is small ($0 \leq u < 1$), we may sum a few low order diagrams in Σ and Γ . The lowest order diagram in Σ is Q_3 which is equal to wz^3u^3 , the next order term is Q_5 which is equal to wz^5u^{10} .

Of course, Q_5 is much smaller than Q_3 . We may only sum all the diagrams which contain Q_3 (See Fig. 22), then

$$\sum \simeq Q_3 + Q_3 * Q_3 + Q_3 * Q_3 * Q_3 + \dots \quad (2.19)$$

The term $Q_3 * Q_3$ is equal to $2(wz^3u^3)^2$ and $Q_3 * Q_3 * Q_3 = 2^2(wz^3u^3)^3$.

The numerical factors 2 and 2^2 in front of $(wz^3u^3)^2$ and $(wz^3u^3)^3$ are the number of different ways by which the point at the far left can reach the point at the far right in the diagrams of $Q_3 * Q_3$, $Q_3 * Q_3 * Q_3$. Then Σ can be written as follows:

$$\begin{aligned} \sum &\simeq wz^3u^3 (1 + 2wz^3u^3 + 2^2w^2z^6u^6 + \dots) \\ &\simeq \frac{wz^3u^3}{1 - 2wz^3u^3} \end{aligned} \quad (2.20)$$

Similarly, the lowest order diagram Λ is Q_2 which is equal

to $z^2 u$, the next order diagram is Q_4 which is equal to $z^4 u^6$.

In the first order approximation, we neglect the rest of the terms in Λ and only choose the diagrams which contain Q_2 (See Fig. 23), then

$$\Lambda \approx Q_2 + Q_2 * Q_2 + Q_2 * Q_2 * Q_2 + \dots \quad (2.21)$$

In this case, the numerical factor in front of all Q_2 diagrams are equal to unity. We can have $Q_2 * Q_2 = Q_2^2 = (z^2 u)^2$, $Q_2 * Q_2 * Q_2 = Q_2^3 = (z^2 u)^3, \dots$ etc. Then eq. (2.21) gives

$$\Lambda \approx Q_2 (1 + Q_2 + Q_2^2 + \dots) = \frac{Q_2}{1-Q_2} = \frac{z^2 u}{1-z^2 u} \quad (2.22)$$

Next, we are going to evaluate the diagrams of $\Lambda * \Sigma$ in the strong coupling approximation. By using the equations (2.19) and (2.21), we can write $\Lambda * \Sigma$ as the sum of the following series

$$\Lambda * \sum \approx M_1 + M_2 + M_3 + M_4 + \dots \quad (2.23)$$

where

$$M_1 = Q_2 * Q_3 + Q_2 * Q_2 * Q_3 + Q_2 * Q_2 * Q_2 * Q_3 + \dots$$

$$M_2 = Q_2 * Q_3 * Q_3 + Q_2 * Q_2 * Q_3 * Q_3 + \dots$$

$$M_3 = Q_2 * Q_3 * Q_3 * Q_3 + Q_2 * Q_2 * Q_3 * Q_3 * Q_3 + \dots$$
$$(2.24)$$

All the diagrams of $\Lambda^*\Sigma$ are shown in Fig. 24. Now, we must be careful about the numerical factors in front of all diagrams. In general, we consider the diagrams as follows:



It contains $m Q_2$'s and $n Q_3$'s. The point a denoted as the starting point and the point b denoted as the ending point. We are going to count how many different ways from point a can reach point b by following the route which be indicated above. Clearly, the numerical contribution of this diagram is equal to 2^n . Then

$$\begin{aligned} M_1 &= w(z^3 u^3) (2z^2 u + 2(z^2 u)^2 + \dots) \\ &= w(z^3 u^3) (1 + 2z^2 u + 2(z^2 u)^2 + \dots) - wz^3 u^3 \\ &= w(z^3 u^3) \frac{1+z^2 u}{1-z^2 u} - wz^3 u^3 \end{aligned} \quad (2.25)$$

$$\begin{aligned} M_2 &= 2w(z^3 u^3)^2 (2z^2 u + 2(z^2 u)^2 + \dots) \\ &= 2w^2 (z^3 u^3)^2 \frac{1+z^2 u}{1-z^2 u} - 2w^2 (z^3 u^3)^2 \end{aligned} \quad (2.26)$$

$$M_3 = 2^2 w^3 (z^3 u^3)^3 \frac{1+z^2 u}{1-z^2 u} - 2^2 w^3 (z^3 u^3)^3 \quad (2.27)$$

.

.

.

$$M = 2^{n-1} w^n (z^3 u^3)^n \frac{1+z^2 u}{1-z^2 u} - 2^{n-1} w^n (z^3 u^3)^n \quad (2.28)$$

Now, we can obtain $\Lambda * \Sigma$ by summing up all the M 's above

$$\Lambda * \Sigma = -\frac{1+z^2 u}{1-z^2 u} - \frac{w(z^3 u^3)}{1-2w(z^3 u^3)} - \Sigma \quad (2.29)$$

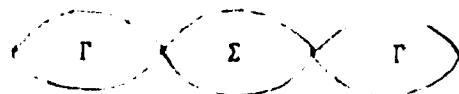
Substituting eqs. (2.20), (2.22) and (2.29) into eq. (2.18), we have the vertex part Γ which yields

$$\begin{aligned} \Gamma &= 1 + \frac{z^2 u}{1-z^2 u} + \frac{1+z^2 u}{1-z^2 u} - \frac{w(z^3 u^3)}{1-2w(z^3 u^3)} \\ &= \frac{1}{1-z^2 u} + \frac{1+z^2 u}{1-z^2 u} - \frac{w(z^3 u^3)}{1-2w(z^3 u^3)} \\ &= \frac{1 - w(z^3 u^3)(1 - z^2 u)}{(1 - z^2 u)(1 - 2w z^3 u^3)} \end{aligned} \quad (2.30)$$

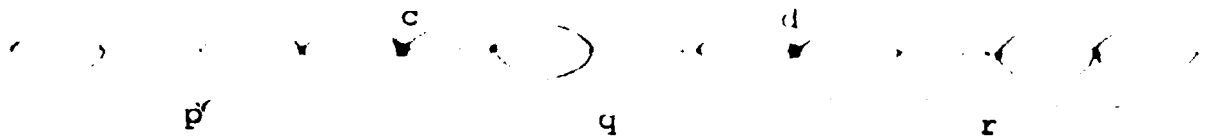
All the Γ -part diagrams in the strong coupling approximation are shown in Fig. 25. Finally, we can obtain F_1 by multiplying Γ^2 and Ξ together, namely,

$$F_1 = \Xi \Gamma^2 = \frac{zw [1-wz^3 u^3 (1-z^2 u)]^2}{(1-z^2 u)^2 (1-2wz^3 u^3) [1-wz(1+2z^2 u^3) + w^2 z^4 u^3]} \quad (2.31)$$

2. All the diagrams which contain NO single step. The general form of this kind of diagrams can be represented as follows:



In the strong coupling approximation, the above diagram simply reduces to



which contains $p Q_2$'s on the left, $r Q_2$'s on the right and $q Q_3$'s in the center (p, q, r are positive integers). We denote the sum of these diagrams by

$$\xi = \sum_{p, q, r} (z^2 u)^{p+r} (w z^3 u^3)^q \nu_{p, q, r} \quad (2.32)$$

The factor $\nu_{p, q, r}$ is the numerical contribution of the diagrams of particular set of indices, p, q , and r . In other words, $\nu_{p, q, r}$ is equal to the number of different ways which the point c can reach the point d by following the route indicated in above diagrams.

We will divide ξ in eq. (2.32) into four different cases:

a. $p \neq 0$ or $r = 0$, then we let the sum be

$$\xi_1 = 2 \sum_{p, q} (z^2 u)^p (w z^3 u^3)^q \nu_{p, q, 0} \quad (2.33)$$

where $p, q \geq 1$, and $r = 0$.

the factor $\nu_{p, q, 0} = 2^q$ (This is the same as the case we discussed before for the diagram $\Lambda * \Sigma$). and the factor 2 is coming from the case of $p = 0$ but $r \neq 0$. Then

$$\begin{aligned} \xi_1 &= 2 \sum_{p=1} (z^2 u)^p \sum_{q=1} (w z^3 u^3)^q \\ &= \frac{2 z^2 u (w z^3 u^3)}{(1 - z^2 u)(1 - w z^3 u^3)} \end{aligned} \quad (2.34)$$

b. $p, q, r \geq 1$. We can obtain

$$\xi_2 = \sum_{p,q,r} (z^2 u)^{p+r} (wz^3 u^3)^q \nu_{p,q,r} \quad (2.35)$$

where the numerical factor $\nu_{p,q,r} = 2^{q+1}$. The sum can be carried out quite easily, then

$$\xi_2 = \left(\frac{z^2 u}{1-z^2 u} \right) \frac{4wz^3 u^3}{1-2wz^3 u^3} \quad (2.36)$$

c. $p = r = 0, q > 0$, we can reduce eq. (2.32) into

$$\xi_3 = \sum_{q=0} (wz^3 u^3)^q \nu_{0,q,0} \quad (2.37)$$

where $\nu_{0,q,0} = 2^{q-1}$ but $\nu_{0,0,0} = 1$

This is the same as the case, we calculate for Σ . Then

$$\begin{aligned} \xi_3 &= \sum_{q=1} (wz^3 u^3)^q 2^{q-1} \\ &= \frac{wz^3 u^3}{1-2wz^3 u^3} \end{aligned} \quad (2.38)$$

d. $p = q = 0$ or $q = r = 0$, the general form of this kind of diagrams can be shown as:



We denote the sum of this type of diagrams be ξ_4 which can be written as

$$\xi_4 = \sum_{p=1} (z^2 u)^p \nu_{p,0,0} \quad (2.39)$$

In this case, all the points in the above diagrams can be the starting point which is the same as the ending point. The numerical factor $v_{p,0,0}=2p$. This is the same as the case, the walk returns to the origin $U_n(u)$, which have discussed in the part I of this thesis. Since we only use one half of the value $U_n(u)$ in calculation of the total number of walk $c_n(u)$, then we should also reduce to half of the value of ξ_4 , namely, $v_{p,0,0}=p$. Then,

$$\xi_4 = \sum_{p=1}^{\infty} p(z^2 u)^p = \frac{z^2 u}{(1-z^2 u)^2} \quad (2.40)$$

Combining all the equations we obtain

$$\begin{aligned} \xi &= \sum_{i=1}^4 \xi_i \\ &= \frac{z^2 u + wz^3 u^3 (1+z^4 u^2)}{(1-z^2 u)^2 (1-2wz^3 u^3)} \end{aligned} \quad (2.41)$$

Now, we can complete the calculation of $F(z,w)$, namely

$$\begin{aligned} F(z,w) &= F_1 + \xi \\ &= \frac{zw [1-wz^3 u^3 (1-z^2 u)]^2}{(1-z^2 u)^2 (1-2wz^3 u^3) [1-wz(1+2z^2 u^3) + w^2 z^4 u^3]} \\ &+ \frac{z^2 u + wz^3 u^3 (1+z^4 u^2)}{(1-z^2 u)^2 (1-2wz^3 u^3)} \end{aligned} \quad (2.42)$$

B. Calculations of the total number of walks $c_n(u)$

We set $w = 1$ in eq. (2.42), the function $F(z,w)$ can be reduced to

$$F(z) = \frac{z [1-z^3 u^3 (1-z^2 u)]^2}{(1-z^2 u)^2 (1-2z^3 u^3)} \frac{[1-z(1+2z^2 u^3) + z^4 u^3]}{(2.43)}$$

$$+ \frac{z^2 u + z^3 u^3 (1+z^4 u^2)}{(1-z^2 u)^2 (1-2z^3 u^3)}$$

$$F(z) = \frac{z [1+z u (1-z) (1+z u^2 + z^5 u^4) + z^6 u^4]}{(1-z^2 u)^2 [1-z(1+2z^2 u^3) + z^4 u^3]} \quad (2.44)$$

which will be the generating function for $c_n(u)$.

The singularities of $F(z)$ are $\theta_{1,2} = \pm u^{-1/2}$ (double poles), and the zeros of the quartic equation $1 - z - 2z^3 u^3 + z^4 u^3 = 0$. The approximate solution of the above equation in the case of very small u , we obtain

$$\begin{aligned} z_1 &\approx \frac{1}{u} + 0.33 + 0.93u + 1.14u^2 + 0.23u^3 + O(u^4) \\ z_2 &\approx 1.00 - 0.05u - 0.22u^2 - 0.07u^3 + O(u^4) \\ z_3 &\approx -\frac{2}{u} + 0.33 - 0.22u - 0.23u^2 - 0.08u^3 \\ &\quad + i(\frac{0.86}{u} - 0.003 + 0.37u - 0.45u^2 + 0.12u^3) \quad (2.45) \\ z_4 &\approx -\frac{2}{u} + 0.33 - 0.22u - 0.23u^2 - 0.08u^3 \\ &\quad - i(\frac{0.86}{u} - 0.003 + 0.37u - 0.45u^2 + 0.12u^3) \end{aligned}$$

These singularities are plotted in Fig. 26.

According to eq. (2.4), we are going to evaluate the integral

$$c_n(u) = \frac{1}{2\pi i} \oint_C -\frac{F(z)}{z^{n+1}} dz \quad (2.4)$$

The coefficient $c_n(u)$ is equal to the residue of $F(z)$ at

$z = 0$, such that

$$c_n(u) = \frac{1}{n!} \left[\frac{d^n}{dz^n} F(z) \right]_{z=0} \quad (2.46)$$

In the case of very large n , say $n \rightarrow \infty$, the residue of $F(z)$ at $z = 0$ becomes a very complicated infinite series which is unable to be summed. Fortunately, we can use the following method which will give a simpler asymptotic expression of $c_n(u)$ for $n \rightarrow \infty$.

Since we know all the singularities of $F(z)$, then we can deform the contour C to C' (Fig. 27). Instead of calculating the residue of $F(z)$ at the origin, all we have to do is to evaluate the residues with respect to those singularities and the problem can be reduced to more compact form.

The poles of z_1 , z_3 , and z_4 are simple poles. The residue at these poles have the same form, namely,

$$R \sim \text{const} \left(\frac{1}{u} \right)^{-(n+1)} \sim A u^{n+1} \quad (2.47)$$

The poles of θ_1 , θ_2 , are double poles, and the residues at these two poles also have the same form

$$\begin{aligned} R' &\sim \text{const} \left(\frac{1}{u}\right)^{-\frac{n+1}{2}} + \text{const}' n \left(\frac{1}{u}\right)^{-\frac{n+2}{2}} \\ &\sim C u^{\frac{n+1}{2}} + C' n u^{\frac{n+2}{2}} \end{aligned} \quad (2.48)$$

where A, C and C' are constants.

If u is small and we are interested in $n \rightarrow \infty$, then both R and R' go to zero very rapidly. The only contribution to $c_n(u)$ comes from the residue at $z = z_2$, then

$$c_n(u) \approx \text{const } z_2^{-(n+1)} = B \left(\frac{1}{z_2}\right)^n \quad (2.49)$$

From eq. (1.5), we assume $c_n(u)$ has the following form

$$c_n(u) \approx B(u) n^{\alpha(u)} \psi(u)^n \quad \text{as } n \rightarrow \infty \quad (1.5)$$

Comparing these two equations, we can easily see that $\alpha(u) = 0$ for all small u and $\psi(u) = z_2^{-1}$. The values of z_2^{-1} for different interaction V are plotted in Fig. 28, which is in agreement with our previous calculation in the Table 3.

C. Mean-square size calculation

In order to calculate the mean-square length

$$\langle r_n^2(u) \rangle_{\text{un-normalized}} = \sum_{\ell} \ell^2 z_n(\ell, u) \quad (2.10)$$

We can obtain the generating function for $\langle r_n^2(u) \rangle_{\text{un.}}$ (eq. (2.9)) by differentiating the function $F(z, w)$ in eq. (2.5) twice with respect to w and setting $w = 1$. Using the same techniques as above, we may get the coefficients $\langle r_n^2(u) \rangle_{\text{un.}}$ by the contour integration, such that

$$\langle r_n^2(u) \rangle_{\text{un.}} = \frac{1}{2\pi i} \int_C \frac{X(z)}{z^{n+1}} dz \quad (2.50)$$

where the contour C is a circle around the origin (Fig. 16).

It is not necessary to calculate all the terms in $X(z)$ explicitly since we know all the singularities of $X(z)$, which will be the same as those of $F(z)$. The most important term of $X(z)$ is the term which contains the cubic power of $(1 - z - 2z^3u^3 + z^4u^3)$ in the denominator. Then,

$$X(z) \sim \frac{X'(z)}{(1 - z - 2z^3u^3 + z^4u^3)^3} \quad (2.51)$$

As $n \rightarrow \infty$, the residue of the pole z_2 should be highly dominant. From eq. (2.50),

$$\langle r_n^2(u) \rangle_{\text{un.}} \sim \text{const } n^2 \left(\frac{1}{z_2} \right)^n \quad \text{as } n \rightarrow \infty \quad (2.52)$$

we can get the normalized $\langle r_n^2(u) \rangle$ by dividing $c_n(u)$ in eq.
(2.49)

$$\langle r_n^2(u) \rangle = \frac{1}{c_n(u)} \langle r_n^2(u) \rangle_{un.} \approx \text{const } n^2 \quad (2.53)$$

This is in agreement to our extrapolation calculation and Flory's suggestion. The index γ should be equal to two in one dimensions in the presence of excluded-volume effect.

D. Probability distribution $z_n(\ell, u)$

The un-normalized probability distribution function $z_n(\ell, u)$ can be obtained by applying the contour integration of $F(z, w)$ twice with respect to the variables z and w , namely,

$$z_n(\ell, u) = \frac{1}{2\pi i} \oint_C \frac{dz}{z^{n+1}} \frac{1}{2\pi i} \oint_C \frac{dw}{w^{\ell+1}} F(z, w) \quad (2.11)$$

The poles in the w -plane are

$$w_1 = \frac{1}{2z^3 u^3} \quad (2.54)$$

and

$$w_{\pm} = \frac{\xi \pm \eta}{2z^3 u^3} \quad (2.55)$$

where $\xi = 1 + 2z^2 u^3$
and $\eta = \sqrt{1 + 4z^4 u^6}$ (2.56)

In order to calculate this integral, we may deform the contour C around the origin to contour C' which will include all the singularities of the integrand except at $w = 0$, and evaluate the residue with respect to the poles w_1 , w_+ and w_- , namely,

$$\begin{aligned} z_n(\ell, u) = & -\frac{1}{2\pi i} \oint_C \frac{dz}{z^{n+1}} \frac{[1 - \frac{1}{2}(\xi + \eta)(1-z^2 u)]^2}{(1-z^2 u)^2 (1-\xi - \eta)^\eta w_+^\ell} \\ & + \frac{1}{2\pi i} \oint_C \frac{dz}{z^{n+1}} \frac{[1 - \frac{1}{2}(\xi - \eta)(1-z^2 u)]^2}{(1-z^2 u)^2 (1-\xi + \eta)^\eta w_-^\ell} \end{aligned} \quad (2.57)$$

The integral has the property that if $\ell = n$, then $z_n(n, u) = 1$. When the interaction V is very large such that the value of u is quite small, w_+ may be expanded as power series of u , i.e.,

$$w_- \approx \frac{1}{z} - zu^3 + \dots \quad (2.58)$$

$$w_+ \approx \frac{1}{z^3 u^3} + \frac{1}{z} + zu^3 + \dots$$

In the cases of strong coupling approximation, the end point ℓ of a n -step walk should be much away from its starting point and has almost the same order of magnitude as n . Suppose we are only interested in the cases $\ell \geq n/3$. Then each walk must contain at least one single step, and the first term in eq. (2.57) can be neglected. Then

$$\begin{aligned} z_n(\ell, u) &= \frac{1}{2\pi i} \oint_C \frac{dz}{z^{n+1}} \frac{[1 - \frac{1}{2}(\xi - \eta)(1-z^2u)]^2}{(1-z^2u)^2 (1-\xi + \eta)^\eta w_-^\ell} \\ &= \frac{1}{2\pi i} \oint_C \frac{dz}{z^{n+1}} \frac{[1 - \frac{1}{2}(\xi - \eta)(1-z^2u)]^2 (\xi + \eta - 1)}{(1-z^2u)^2 \eta w_-^\ell} \end{aligned} \quad (2.59)$$

In these cases, we cannot deform the contour C to C' , and calculate the residues with pole $z^2 = 1/u$. Because the outer-integral doesn't vanish at infinity. Instead of calculating the residues, the saddle-point methods are employed to this integral, which will give us more interesting asymptotic behavior. It is more convenient for us by replacing z^2 by z , then eq. (2.59) reduces to

$$z_n(\ell, u) = \frac{1}{2\pi i} \oint_C dz e^{F(z) + \ln M(z, u)} \quad (2.60)$$

where $F(z) = -m \ln z - \ell \ln(1-zu^3)$ (2.61)

$$m = \frac{1}{2}(n - \ell)$$
 (2.62)

and

$$M(z, u) = \frac{[1 - \frac{1}{2}(\xi - \eta)(1-zu)]^2 (\xi + \eta - 1)}{(1-zu)^2 \eta z}$$
 (2.63)

The saddle point z_s is determined by

$$-\frac{m}{z_s} + \frac{\ell u^3}{1-z_s u^3} + \frac{1}{M(z_s, u)} \left(\frac{\partial M}{\partial z} \right)_{z=z_s} = 0$$
 (2.64)

Now we should make this assumption; in order to calculate the integral in eq. (2.60) asymptotically, we require m and ℓ to be quite large, then the exponent $F(z)$ will change very rapidly for varying z .

Suppose the values of the saddle point z_s is away from the singularities of $M(z, u)$ then the last term in above equation may be neglected. We may obtain the saddle point as

$$z_s = \frac{n - \ell}{(n + \ell) u^3} = \frac{2 m}{(n + \ell) u^3}$$
 (2.65)

Now we are going to determine under what condition that the saddle point z_s always lies inside the pole $z_p = 1/u$, which yields

$$z_s < z_p ; \ell > \bar{\ell} = \frac{1-u^2}{1+u^2} n$$
 (2.66)

In other words, if $\ell > \bar{\ell}$, z_s will lie inside the pole z_p in the z -plane.

It is better to introduce a scaling variable y , such that

$$y = 1 - \frac{\ell}{n} \quad (1 \leq y \leq 0) \quad (2.67)$$

i.e., $\ell = n$, $y = 0$ and $\ell = 0$, $y = 1$. Substituting the value of y into eqs. (2.61) and (2.65), we obtain

$$F(z) = n f(z_s, y) \quad (2.68)$$

where

$$f(z_s, y) = -1/2 y \ln z_s - (1-y) \ln (1 - z_s u^3) \quad (2.69)$$

$$\text{and } z_s = \frac{2y}{(2-y)u^3} \quad (2.70)$$

Then eq. (2.60) can be written as

$$z_n(\ell, u) = \frac{1}{2\pi i} \oint_C dz e^{nz} f(z, y) + \frac{1}{n} \ln M(z, u) \quad (2.71)$$

Next, we want to differentiate $F(z)$ twice with respect to z and substitute the value of z_s . To check at $z = z_s$, $F(z)$ has a maximum or a minimum, which turns out to be

$$F''(z_s) = \frac{m}{z_s^2} + \frac{\ell u^6}{(1-z_s u^3)^2} = \frac{(n+\ell)^3 u^6}{4 \ell (n-\ell)} > 0 \quad (2.72)$$

By substituting eq.(2.67) into above equation, we have $F''(z_s)$ as a function of y , i.e.

$$F''(z_s) = n f''(z_s, y) \quad (2.73)$$

where

$$f''(z_s, y) = \frac{(2-y)^3 u^6}{4y(1-y)} \quad (2.74)$$

We can conclude at $z = z_s$, $F(z)$ has a minimum and assume that the contour of the integration around the origin C (Fig. 29) may be distorted to C' (Fig. 30) so as to pass through this saddle point z_s . The contour now passed through z_s perpendicular to the positive real axis, i.e., $z - z_s$ is pure imaginary and as n gets larger, say $n \rightarrow \infty$, $\exp(n f(z_s, y))$ has an extremely sharp peak at this point. Therefore, if $\ell > \bar{\ell} + \epsilon$ (ϵ is a smaller number compared with ℓ) the saddle point lies inside the pole, the integral in eq. (2.71) yields

$$z_n(\ell, u) \approx M(z_s, u) \frac{e^{nf(z_s, y)}}{[2\pi n f''(z_s, y)]^{1/2}} + O(n^{-1}) \quad (2.75)$$

If $\ell < \bar{\ell} - \epsilon$, the saddle point z_s lies outside the pole, the contour C' will include the pole. Then the integral in eq. (2.71) yields two terms,

$$z_n(\ell, u) \approx M(z_s, u) \frac{e^{nf(z_s, y)}}{[2\pi n f''(z_s, y)]^{1/2}} + R_{\text{pole}} \quad (2.76)$$

first term is identical to eq. (2.75) by integrating through the saddle point z_s , and the second term is due to the residue at the pole $z_p = 1/u$, i.e.,

$$\begin{aligned} R_{\text{pole}} &= - e^{F(z_p)} \frac{(\xi-\eta)(\xi-\eta-1)}{z_p u^\eta} + e^{F(z_p)} \frac{1}{u^2 z_p^\eta} \left\{ \right. \\ &\quad \left. (\xi+\eta-1) \left(\frac{m+1}{z_p} - \frac{\ell u^3}{1-z_p u^3} + \frac{4z_p u^6}{\eta^2} \right) - \left(2u^3 + \frac{4z_p u^6}{\eta} \right) \right\} \end{aligned} \quad (2.77)$$

while $\ell - \bar{\ell}$, we have a 'singularity' in the function $M(z, u)$ (eq. (2.63)) and $z_n(\ell, u)$ in eqs. (2.75) and (2.76) will increase very rapidly. Saddle point approximation may be failed in this case. But we may use the analysis of 'punching through analytical continuation' (see Appendix VI) and calculate the analytical continuation value of the integrand crossing the singularity $z_p = 1/u$. We should expect that $z_n(\ell, u)$ be a smoothly varying function of ℓ .

From eqs. (2.75) and (2.76) and setting $n = 15$, we plot $z_n(\ell, u)$ vs. ℓ for different values of V in Fig. 31 and compared with the exact counting results in Part I. We observe that the distribution are almost the same, which confirm our generating function calculation.

Next, we are interested in the infinite system, as $n \rightarrow \infty$. From eq. (2.75), we take logarithm on both sides,

$$\frac{1}{n} \ln z_n(\ell, u) = f(z_s, y) + \frac{1}{n} \ln M(z_s, u) - \frac{1}{2n} \ln(2\pi n f''(z_s, y)) \quad (2.78)$$

as $n \rightarrow \infty$ therefore

$$\frac{1}{n} \ln z_n(\ell, u) \approx f(z_s, y) \quad \text{for } \ell > \bar{\ell} \quad (2.79)$$

In the case of $\ell < \bar{\ell}$, the exponential function $F(z_p)$ is much larger than $F(z_s)$ for all $z_s > z_p$. The distribution function $z_n(\ell, u)$ is most dominated by the residue term R_{pole} . Taking the logarithm of eq. (2.76) again, we obtain

$$\frac{1}{n} \ln z_n(\ell, u) \approx \frac{1}{n} \ln R_{\text{pole}} = g(z_p, y) \quad \text{for } \ell < \bar{\ell} \quad (2.80)$$

where $g(z_p, y)$ is defined as

$$g(z_p, y) = \frac{y}{2} \ln(u) - (1-y) \ln(1-u^2) \quad (2.81)$$

$$\text{and } F(z_p) = n g(z_p, y) \quad (2.82)$$

For $\ell \rightarrow \bar{\ell}$, we may make $\frac{1}{n} \ln z_n(\ell, u)$ analytical continuation passing through the singular point. It turns out to be both functions $f(z_s, y)$ and $g(z_p, y)$ match quite closely. Now, we may plot $\frac{1}{n} \ln z_n(\ell, u)$ vs. ℓ for different values of u ($u = \exp(-V)$) in Figs.

32 and 33. These curves all have the following properties: if $y \rightarrow 0$, $\ell = n$, $f(z_s, y) \rightarrow 0$, which indicates $z_n(\ell, u) \rightarrow 1$, in this case, the walk can only extend to a straight line; if $y \rightarrow 1$, $\ell = 0$, $g(z_p, y) \rightarrow \frac{1}{2} \ln(u) < 0$, which indicates the probability of finding the end of a walk which returns to its starting point will vanish. This is in agreement to our strong coupling approximation.

Next, we are going to examine the maximum peak of the distribution $\frac{1}{n} \ln z_n(\ell, u)$. From the numerical values of the functions $f(z_s, y)$ and $g(z_p, y)$, such that $f(z_s, y) > g(z_p, y)$ for all y , then the value of ℓ of the maximum peak of the distribution always lies outside $\bar{\ell}$. In other words, the function $f(z_s, y)$ is most important. Differentiating $f(z_s, y)$ with respect to y and setting equal to zero, we can find the maximum of the distri-

bution which is satisfied

$$f'(z_s, y) = 0 \quad (2.83)$$

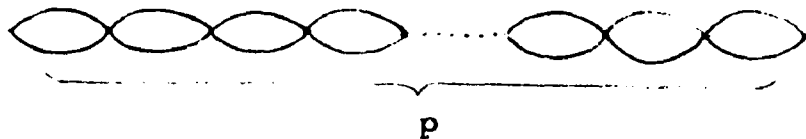
and

$$\frac{3}{2} \ln \frac{1}{u} + \frac{1}{2} \ln y(2-y) = \ln 2(1-y) \quad (2.84)$$

This equation can only be solved graphically. The curves for different values of u are plotted in Fig. 34. We can see quite clearly that the intersection of the two curves which will shift to left and finally goes to zero for the increase of the strength of the repulsion. The maximum peak of the distribution is diffused. In the cases of very strong coupling, u is very small ($u \approx 0$), the solution of eq. (2.84) will almost close to zero; which indicates the end point of a walk, $l = n$, is most probable. They satisfied our previous calculations in the Part I.

E. Calculations of the total number of walks which return to its starting point $U_n(u)$

In the very strong coupling approximation, the walk returns to the origin, $U_n(u)$, can only have the simplest type of diagrams as follows:



We denote the sum of this type of diagrams as $G(z)$ which has the form of

$$G(z) = \sum_{n=2} U_n(u) z^n \quad (2.85)$$

From eq. (2.39), the generating function $G(z)$ can be written as:

$$G(z) = \sum_{p=1} (z^2 u)^p p = \frac{z^2 u}{(1-z^2 u)^2} \quad (2.86)$$

By using eq. (2.4), the coefficient $U_n(u)$ can be written as an integral in the complex z plane, namely

$$U_n(u) = \frac{1}{2\pi i} \oint_C \frac{dz}{z^{n+1}} G(z) \quad (2.87)$$

Similarly, we may deform the contour C to C' (Fig. 25) and evaluate the residue with respect to the singularity $z_p^2 = 1/u$.

In the case of $n \rightarrow \infty$, the residue at z_p has the form of

$$U_n(u) \approx \text{const } n u^{n/2} = B' n u^{n/2} = B' n u^n \quad (2.88)$$

Suppose we include the diagrams which contain both Q_2 and Q_4 , from Appendix V, the generating function of summing those diagrams has the form of

$$G(z) \sim \frac{G'(z)}{(1-z^2 u - 3z^4 u^6 + z^6 u^7)^2} \quad (2.89)$$

It is not necessary to calculate the exact form of the generating function, since the asymptotical behavior is most interesting and the poles of denominator of above equation plays an important role to calculate the coefficient $U_n(u)$. Similarly, we may obtain the coefficient $U_n(u)$ by using the complex integration again, i.e.,

$$U_n(u) \approx \frac{1}{2\pi i} \oint_C \frac{dz}{z^{n+1}} \frac{G'(z)}{(1-z^2 u - 3z^4 u^6 + z^6 u^7)^2} \quad (2.90)$$

In the cases of strong coupling, u is quite small, the equation of $1 - z^2 u - 3z^4 u^6 + z^6 u^7 = 0$ can be only solved numerically. The only physical root is

$$z_p^2 = -\frac{1}{u}(1 + 2u^4) \quad (2.91)$$

Comparing the root of the equation $1 - z^2 u = 0$, the pole is slightly shifted by a factor of $2u^3$ which is expected.

Then the walk returns to the origin may have the form of

$$U_n(u) \approx \text{const } n \left(\frac{u}{1+2u^4} \right)^{n/2} = B' n \mu_2^n \quad \text{as } n \rightarrow \infty \quad (2.92)$$

From eq. (1.8), we assume $U_n(u)$ has the following form:

$$U_n(u) \approx B'(u) n^{\beta(u)} \mu'(u)^n \quad \text{as } n \rightarrow \infty \quad (1.8)$$

Comparing these equations (1.8), (2.88) and (2.92), we can observe that

$\beta(u) = 1$ for all small values of u (large V) and $\mu'_1(u) = u^{1/2}$
 $\mu'_2(u) = \left(\frac{u}{1+2u^4} \right)^{1/2}$. The value of $\mu'_1(u)$ for different interaction V ($u = \exp(-V)$) are plotted in Fig. 35 which is in agreement to our previous extrapolation calculations in Table 4 and Fig. 8.

PART III
CONTINUOUS MODEL

III. Continuous Model 14, 15, 28

Consider a single polymer chain with total length L consisting of n identical molecules. The coordinate of i -th molecule is denoted as \vec{R}_i ($\vec{R}_0 = \vec{R}$ and $\vec{R}_n = \vec{R}'$) and the length between the two nearest molecules is denoted as ΔL ; $L = n\Delta L$ (Fig. 36). A polymer chain without the interaction has the well-known Gaussian distribution.

Let $P_o(\vec{R}_{i+1}, \vec{R}_i | \Delta L)$ be the probability of finding one molecule which is initially located at \vec{R}_i , finally at \vec{R}_{i+1} , in the absence of the interaction between the molecules. It should satisfy the simple diffusion equation and can be written as

$$P_o(\vec{R}_{i+1}, \vec{R}_i | \Delta L) = \frac{1}{(2\pi\Delta L)^{3/2}} \exp(-\frac{1}{2\Delta L} (\vec{R}_{i+1} - \vec{R}_i)^2) \quad (3.1)$$

Then the probability distribution of finding a particular configuration ($\vec{R}, \vec{R}_1, \vec{R}_2, \vec{R}_3, \dots, \vec{R}'$) in the absence of the interaction has the property of a Markov process, that one always can break up the interval (\vec{R}, \vec{R}') ($0, L$) into as many pieces as one like: (\vec{R}, \vec{R}_1) ($0, \Delta L$), (\vec{R}_1, \vec{R}_2) ($L, 2\Delta L$), $\dots, (\vec{R}_{n-1}, \vec{R})$ ($(n-1)\Delta L, L$) and write

$$P_o(\vec{R}, \vec{R}_1, \dots, \vec{R}' | L) = P_o(\vec{R}', \vec{R}_{n-1} | \Delta L) P_o(\vec{R}_{n-1}, \vec{R}_{n-2} | \Delta L) \dots$$

$$\dots P_o(\vec{R}_2, \vec{R}_1 | \Delta L) P_o(\vec{R}_1, \vec{R} | \Delta L) \quad (3.2)$$

In short, we have

$$P_o(\vec{R}, \vec{R}_1, \dots, \vec{R}' | L) = \prod_{i=1}^n P_o(\vec{R}_i, \vec{R}_{i-1} | \Delta L) \quad (3.3)$$

Now, we can define $P_O(\vec{R}, \vec{R}' | L)$ is the probability distribution of a chain which starts at \vec{R} and n-th link will end at \vec{R}' , is given by

$$P_O(\vec{R}, \vec{R}' | L) = \int P_O(\vec{R}, \vec{R}_1, \vec{R}_2, \dots, \vec{R}' | L) \prod_i d\vec{R}_i \quad (3.4)$$

By substituting eq. (3.1) into (3.3), we can get

$$P_O(\vec{R}, \vec{R}_1, \dots, \vec{R}' | L) = \frac{1}{(2\pi\Delta L)^{3/2}} \exp\left(-\frac{1}{2\Delta L} \sum_{i=1}^n (\vec{R}_i - \vec{R}_{i-1})^2\right) \quad (3.5)$$

As $\Delta L \rightarrow 0$, the above equation becomes a path integral,

$$P_O(\text{path } \vec{R} \rightarrow \vec{R}' | L) \longrightarrow N \exp\left(-\frac{1}{2} \int_0^L dL' \left(\frac{\partial \vec{R}}{\partial L'}\right)^2\right) \quad (3.6)$$

which is originally considered by Weiner and N is the normalization constant. Now, we can rewrite the eq. (3.4) in the form of a path integral, namely

$$P_O(\vec{R}, \vec{R}' | L) = N \int_{\vec{R}(0) = \vec{R}}^{\vec{R}(L) = \vec{R}'} d(\text{path } \vec{R}(L')) \exp\left(-\frac{1}{2} \int_0^L dL' \left(\frac{\partial \vec{R}}{\partial L'}\right)^2\right) \quad (3.7)$$

If we let $\vec{R}' = \vec{r}$ and $\vec{R} = 0$, then

$$P_O(\vec{r}, L) = N \int_0^{\vec{r}} d(\text{path } \vec{R}(L')) \exp\left(-\frac{1}{2} \int_0^L dL' \left(\frac{\partial \vec{R}}{\partial L'}\right)^2\right) \quad (3.8)$$

In the presence of the repulsive interaction between the molecules in the polymer chain, the distribution function can not have the simple form as above. Considering $V(\vec{R}_i - \vec{R}_j)$ as the repulsive interaction between i-th and j-th molecules, the probability of finding a particular configuration $(\vec{R}, \vec{R}_1, \vec{R}_2, \vec{R}_3, \dots, \vec{R}')$ is given by

$$P(\vec{R}, \vec{R}_1, \dots, \vec{R}' | L) = \prod_{i=1}^n P_O(\vec{R}_i, \vec{R}_{i-1} | \Delta L) \exp\left(-\sum_{i \neq j} V(\vec{R}_i - \vec{R}_j)\right) \quad (3.9)$$

where $P_O(\vec{R}_i, \vec{R}_{i-1} | \Delta L)$ is defined in eq. (3.1). We can replace

$$-\sum_{i \neq j} V(\vec{R}_i - \vec{R}_j) \quad \text{by} \quad -\frac{1}{2} \int_0^L \int_0^L V[\vec{R}(L') - \vec{R}(L'')] dL' dL''$$

Finally, the probability distribution of a chain that starts at 0 and ends at \vec{r} is given by

$$P(\vec{r}, L) = N \int_0^{\vec{r}} d(\text{path } \vec{R}(L')) \exp\left[-\frac{1}{2} \int_0^L dL' \left(\frac{\partial \vec{R}}{\partial L'}\right)^2 - \frac{1}{2} \int_0^L \int_0^L V[\vec{R}(L') - \vec{R}(L'')] dL' dL''\right] \quad (3.10)$$

At this point a parametric representations can be employed.

It is well-known that

$$\exp\left(-\frac{a^2}{2}\right) = \frac{\int_{-\infty}^{\infty} \exp(iax - x^2/2) dx}{\int_{-\infty}^{\infty} \exp(-x^2/2) dx} \quad (3.11)$$

This can be generalized to

$$\exp\left(-\frac{1}{2} \sum_{i,j} a_i A_{ij} a_j\right) = \frac{\iint_{-\infty}^{\infty} \exp(i \sum_j a_j x_j - \frac{1}{2} \sum_{i,k} x_i A_{ik}^{-1} x_k) \Pi dx}{\iint_{-\infty}^{\infty} \exp(-\frac{1}{2} \sum_{i,k} x_i A_{ik}^{-1} x_k) \Pi dx} \quad (3.12)$$

where A^{-1} is the inverse matrix to A , and hence to the functional form

$$\frac{\exp(-\iint a(\alpha) A(\alpha\beta) a(\beta) d\alpha d\beta)}{\int \dots \int \Pi dx \exp(i a(\alpha) x(\alpha) d\alpha - \frac{1}{2} \iint x(\alpha) A^{-1}(\alpha\beta) x(\beta) d\alpha d\beta} = \int \dots \int \Pi dx \exp(-\frac{1}{2} \iint x(\alpha) A^{-1}(\alpha\beta) x(\beta) d\alpha d\beta) \quad (3.13)$$

where A^{-1} is the inverse operator to A , such that

$$\int A^{-1}(\alpha\beta) A(\beta\gamma) d\beta = \delta(\alpha-\gamma) \quad (3.14)$$

The theorem allows us to write

$$\begin{aligned} & \exp(-\frac{1}{2} \int_0^L \int_0^L V[\vec{R}(L') - \vec{R}(L'')] dL' dL'') \\ &= M \int \delta x \exp \left[i \int_0^L x[\vec{R}(L')] dL' - \frac{1}{2} \iint d\vec{r} d\vec{s} x(\vec{r}) V^{-1}(\vec{r}-\vec{s}) x(\vec{s}) \right] \end{aligned} \quad (3.15)$$

where M is an another normalization constant and

$$\int V^{-1}(rs) V(sr') ds = \delta(r-r') \quad (3.16)$$

and $\int \delta x$ represents the integral over all functions.

It is supposed that $\int x V^{-1} x \delta x$ is positive definite, corresponding to V being repulsive. Finally we can write eq. (3.10) as

$$\begin{aligned} P(\vec{r}, L) &= N \cdot M \int_0^r \exp \left[-\frac{1}{2} \int_0^L dL' \left(\frac{\partial \vec{R}}{\partial L'} \right)^2 - i \int_0^L x[\vec{R}(L')] dL' \right. \\ &\quad \left. - \frac{1}{2} \int x^2(\vec{r}') d\vec{r}' \right] \delta x \delta \vec{R} \end{aligned} \quad (3.17)$$

δ^R is denoted as the integral over all path. The theorem states that the probability $P(r,L)$ is that of diffusion in the presence of a potential $i\chi$, averaged over all potentials with a Gaussian weight. It is a well-known theorem elsewhere in physics, since the evaluation of the function integral over δ^R is equivalent to solving the diffusion equation.

One can obtain the final form

$$P(r,L) = N \cdot M \int \delta(x) G(r,L,(x)) W(x) \\ = \langle G(r,L) \rangle \quad (3.18)$$

where

$$W(x) = \exp(-\frac{1}{2} \int x^2(s) ds) \quad (3.19)$$

and $G(r,L,(x))$ satisfies the following equation

$$\left(\frac{\partial}{\partial L} - \nabla^2 + i\chi \right) G(r,L,(x)) = \delta(r) \delta(L) \quad (3.20)$$

and $N \cdot M$ is defined from

$$\int P(\vec{r},L) d\vec{r} = 1$$

Now we can solve this problem by the standard field theory

methods to study the perturbation expansion series of
 $G(r, L, (x))$ in terms of the complex potential
 $i x$ and the free Green's function $G_0(r, L)$ ($G_0(r, L)$
is defined in eq. (2.30) when $x = 0$). We obtain

$$G = G_0 + G_0(i x) G_0 + G_0(i x) G_0(i x) G_0 + \dots \dots \dots \quad (3.21)$$

Since we want to average G over all the potentials by a Gaussian weight (eq. (3.18) and eq. (3.19)). Then

$$\langle G \rangle = \langle G_0 \rangle + \langle G_0(i x) G_0 \rangle + \langle G_0(i x) G_0(i x) G_0 \rangle + \dots \dots \dots$$

(3.22)

Obviously, only terms of even-order in x remain, namely

$$\langle G \rangle = G_0 - G_0 x G_0 x G_0 + \dots \dots \dots \quad (3.23)$$

Then we can write $\langle G(r, L) \rangle$ in terms of diagrams which are equivalent to the diagrams occurring in the expansion of electron Green's function in the problem of electron-phonon interactions, we replace each phonon line by $\langle x(\vec{r}) x(\vec{r}') \rangle$ (Fig. 37). For the simplest case, we only consider the δ -function interaction between the points \vec{r} and \vec{r}' , namely

$$\langle x(r) x(r') \rangle = \lambda \delta(r-r') \quad (3.24)$$

where λ is the strength of the pairwise interaction between the molecules and the problem can be easily solved.

Now, we are interested in one dimensional problem and study the Fourier transformation of $\langle G(x, L) \rangle$, which can be defined as

$$\langle G(x, L) \rangle = \int_{-i}^{i\infty} \frac{d\omega}{2\pi i} e^{-\omega L} \int_{-\infty}^{\infty} \frac{dk}{2\pi i} e^{ikx} \langle G(k, \omega) \rangle \quad (3.25)$$

In the absence of x , $\langle G(k, \omega) \rangle$ reduces to $G_0(k, \omega)$ which has a simple form

$$G_0(k, \omega) = \frac{1}{k^2 - \omega} \quad (3.26)$$

In the majority of problems of quantum field theory it is as a rule impossible to confine ourselves to the first few terms of the perturbation series. Instead, we have to sum different infinite series of terms. A remarkable property of the diagrams techniques for Green's functions is that we can associate summation of an infinite set of terms of the perturbation series with a special type of graphical summation of diagrams. The diagram representing the sum is composed of elements, each of which is in turn

the result of a summation. Now we shall describe Σ as the self-energy part of a diagram joined with the rest by two Go-lines. A self-energy part will be called irreducible if it cannot split into two parts joined by a single Go-line. It is impossible to sum all the diagrams for the Green's functions in the general case. However, we can carry out a partial summation, in such a way that there only remains a sum over different irreducible self-energy parts.

Let us take any diagram for a G-function. It starts with a Go-line. Then there is an irreducible self-energy part. If we chop off these two elements from the diagram, the remainder will again start with Go and may contain any number of arbitrary self-energy parts. Thus, the remainder is again a complete G-function. This gives us the following equation for G:²⁷

$$G = G_0 + G_0 \Sigma G \quad (3.27)$$

$$\text{or} \quad G^{-1} = G_0^{-1} - \Sigma \quad (3.28)$$

$$\text{where} \quad \Sigma = \Sigma_1 + \Sigma_2 + \Sigma_3 + \dots \quad (3.29)$$

is the sum of different irreducible self-energy parts.

We shall call Σ the total irreducible self-energy part.

We can find Σ by using diagrams that differ from the diagrams for G in that the two end Go-lines are absent.

But in these cases it is impossible to confine ourselves to evaluating the first diagrams and an infinite series has to be summed. It is as a rule more convenient to express Σ in term of another set of diagrams, which will call the vertex part. The Fourier transform of self-energy part Σ in the momentum space (k, ω) can be shown in Fig. 38. The double line is represented the exact G-line and the shadow region is denoted as the vertex part.

Now we can define $c(L)$, the total probability of a polymer chain with length L by integrating $\langle G(x, L) \rangle$ in eq. (3.18) over all x , then

$$c(L) = \int_{-\infty}^{\infty} \langle G(x, L) \rangle dx \quad (3.30)$$

which is equivalent to the total number of walks $c_n(u)$ in the part I and II of this thesis. By substituting eq.(3.25) into (3.30), we have

$$c(L) = \int_{-i\omega}^{i\omega} \frac{d\omega}{2\pi i} e^{-\omega L} \int_{-\infty}^{\infty} \frac{dk}{\pi} \langle G(k, \omega) \rangle \int_{-\infty}^{\infty} e^{ikx} dx \quad (3.31)$$

and the integral

$$\frac{1}{2\pi} \int_{-\infty}^{\infty} e^{ikx} dx = \delta(x) \quad (3.32)$$

Then it can be shown that

$$c(L) = \int_{-i}^{i\infty} \frac{d\omega}{2\pi i} e^{-\omega L} G(0, \omega) \quad (3.33)$$

Similarly, the mean-square length of a long chain can be defined as

$$\langle r^2 \rangle_{\text{un-normalized}} = \int_{-\infty}^{\infty} x^2 \langle G(x, L) \rangle dx \quad (3.34)$$

and

$$\langle r^2 \rangle = \frac{1}{c(L)} \langle r^2 \rangle_{\text{un-normalized}} \quad (3.35)$$

by using eq.(3.25) again, we have

$$\langle r^2 \rangle_{\text{un}} = \int_{-ix}^{ix} \frac{d\omega}{2\pi i} e^{-\omega L} \int_{-\infty}^{\infty} \frac{dk}{2\pi} \int_{-\infty}^{\infty} x^2 dx e^{ikx} \langle G(k, \omega) \rangle \quad (3.36)$$

and the integral

$$\frac{1}{2\pi} \int_{-\infty}^{\infty} x^2 e^{ikx} dx = \left(\frac{1}{i} \frac{d}{dk} \right)^2 \delta(k) \quad (3.37)$$

After integration by part of eq. (2.36), we obtain

$$\langle r^2 \rangle_{\text{un.}} = \int_{-ix}^{ix} \frac{d\omega}{2\pi i} e^{-\omega L} i^2 \left[\frac{d^2}{dk^2} \langle G(k, \omega) \rangle \right]_{k=0} \quad (3.38)$$

The probability distribution of "ring closure" $U(L)$, while the end of a chain coincides with the beginning of

the chain, can be obtained by setting $x=0$ in eq. (3.25), (which is equivalent to $U_n(u)$ in the part I and II of this thesis, the walk returns to the origin after n steps walk). i.e.

$$U(L) = \langle G(0, L) \rangle$$

$$= \int_{-i\infty}^{i\infty} \frac{d\omega}{2\pi i} e^{-\omega L} \int_{-\infty}^{\infty} \frac{dk}{2\pi} \langle G(k, \omega) \rangle \quad (3.39)$$

Now, we can evaluate these quantities $c(L)$, $U(L)$ and $\langle r^2 \rangle$ by, first, computing the self-energy part and using Dyson's equation in eq. (3.28), obtaining the true Green's function $\langle G(k, \omega) \rangle$; secondly, applying eqs. (3.33), (3.38) and (3.39) and integrating in the complex plane.

A. Free Green's function G_0

In the case of $x = 0$, the equation (3.20) reduces to

$$\left(\frac{\partial}{\partial L} - \frac{\partial^2}{\partial x^2} \right) G_0(x, L) = \delta(x) \delta(L) \quad (3.40)$$

and $G_0(k, \omega)$ is the Fourier transform of $G_0(x, L)$, namely,

$$G_0(x, L) = \int_{-i\infty}^{i\infty} \frac{d\omega}{2\pi i} e^{-\omega L} \int_{-\infty}^{\infty} \frac{dk}{2\pi} e^{ikx} G_0(k, \omega) \quad (3.41)$$

where $G_0(k, \omega)$ has the simple form as

$$G_0(k, \omega) = \frac{1}{k^2 - \omega} \quad (3.26)$$

From eq. (3.41), we obtain that

$$G_0(x, L) = \begin{cases} \int_{-i\infty}^{i\infty} \frac{d\omega}{2\pi i} e^{-\omega L} G_0(\omega) & L > 0 \\ 0 & L < 0 \end{cases} \quad (3.42)$$

where

$$G_0(\omega) = \int_{-\infty}^{\infty} \frac{dk}{2\pi} e^{ikx} G_0(k, \omega) \quad (3.43)$$

Since L is always positive, we should expect that $G_0(\omega)$ is analytic in the left half ω -plane, and close the contour in the right half ω -plane in order to evaluate $G_0(x, L)$.

To calculate $G_0(x, \omega)$ in eq. (3.43), we should examine the poles of $G_0(k, \omega)$ carefully. The poles of $G_0(k, \omega)$ are located at $k = \pm\sqrt{\omega}$ in the complex k -plane. In order to get rid of the trouble integrating along the real axis, we can displace the poles: One slightly above the positive real axis and the other slightly below the negative real axis. (See Fig. 39). Then we can get

$$G_0(x, \omega) = \begin{cases} \frac{i}{2\sqrt{\omega}} e^{i\sqrt{\omega}x} & x > 0 \\ \frac{i}{2\sqrt{\omega}} e^{-i\sqrt{\omega}x} & x < 0 \end{cases} \quad (3.44)$$

and

$$G_0(x, L) = \int_{-i\infty}^{i\infty} \frac{d\omega}{2\pi i} \frac{i}{2\sqrt{\omega}} \left(\frac{e^{i\sqrt{\omega}x}}{e^{-i\sqrt{\omega}x}} \right) e^{-\omega L} \quad \begin{matrix} x > 0 \\ x < 0 \end{matrix} \quad (3.45)$$

Now, we have a branch point at $\omega=0$, because $G_0(x, \omega)$ is analytic in the left half ω -plane, we should put the branch cut in the right half ω -plane. In this case, eq. (3.45) can be calculated by deforming the contour (Fig. 40) around the branch cut. We will obtain the same result for both cases; $x > 0$ and $x < 0$ both yield

$$G_0(x, L) = \frac{1}{(4\pi L)^{1/2}} e^{-\frac{x^2}{4L}} \quad (3.46)$$

The total probability of a chain, $c(L)$, can be obtained by using either eq. (3.33) directly or integrating $G_0(x, L)$ for all L .

$$c(L) = \int_{-i\infty}^{i\infty} \frac{d\omega}{2\pi i} \frac{-1}{\omega} e^{-\omega L}$$

or

$$c(L) = \frac{1}{(4\pi L)^{1/2}} \int_{-\infty}^{\infty} e^{-\frac{x^2}{4L}} dx = 1 \quad (3.47)$$

It should be expected, since $G_o(x, L)$ is normalized. Similarly, the mean-square length can also be obtained by using either eq. (3.38) directly or eq. (3.34) from the result of $G_o(x, L)$ in eq. (3.46).

$$\langle r^2 \rangle = \int_{-i\infty}^{i\infty} \frac{d\omega}{2\pi i} \frac{2}{\omega^2} e^{-\omega L}$$

or

$$\langle r^2 \rangle = \frac{1}{(4\pi L)^{1/2}} \int_{-\infty}^{\infty} x^2 dx e^{-\frac{x^2}{4L}} = 2L \quad (3.48)$$

This is expected, since the molecules can move in two different directions; left and right, in one dimension.

The probability distribution of "ring closure" can be obtained by setting $x=0$ in eq. (3.46), i.e.

$$G_o(0, L) = \frac{1}{(4\pi L)^{1/2}} \quad (3.49)$$

or by using eqs. (3.39) and (3.41) and integrating in the complex plane, namely

$$\begin{aligned}
 G_O(0, L) &= \int_{-i\infty}^{i\infty} \frac{d\omega}{2\pi i} e^{-\omega L} \int_{-\infty}^{\infty} \frac{dk}{2\pi} \frac{1}{k^2 - \omega} \\
 &= \int_{-i\infty}^{i\infty} \frac{d\omega}{4\pi} \frac{1}{\sqrt{\omega}} e^{-\omega L} \sim L^{-1/2} \tag{3.50}
 \end{aligned}$$

Comparing the results in eqs. (1.4), (1.7) and 1.8) we may conclude that

$$\begin{aligned}
 \alpha &= 0 \\
 \beta &= -1/2 \\
 \gamma &= 1 \tag{3.51}
 \end{aligned}$$

in the absence of the repulsive coupling between the molecules in one dimension and it confirms our previous calculations.

B. Weak Coupling Approximation

In this case, we assume the strength of the repulsive interaction λ is very small. Then we can only use the first order term in Σ in the self-energy part (Fig. 38), which yields

$$\Sigma(k, \omega) \approx \Sigma_1(\omega) \quad (3.52)$$

where

$$\Sigma_1(\omega) = -\lambda \sum_k G_O(k, \omega) = -\frac{\lambda}{2\pi} \int_{-\infty}^{\infty} \frac{dk}{k^2 - \omega} = -\frac{\lambda i}{2\sqrt{\omega}} \quad (3.53)$$

We should indicate here the imaginary part of $\sqrt{\omega}$ be positive. From Dyson's equation in (3.28), we may write

$$\langle G(k, \omega) \rangle^{-1} = G_O(k, \omega)^{-1} - \Sigma_1 = k^2 - \omega + \frac{\lambda i}{2\sqrt{\omega}} \quad (3.54)$$

By using the eqs. (3.33), (3.38), and (3.39), we get

$$c(L) = - \int_{-i\infty}^{i\infty} \frac{d\omega}{2\pi i} e^{-\omega L} \frac{1}{\omega - \frac{\lambda i}{2\sqrt{\omega}}} \quad (3.55)$$

and

$$\langle r^2 \rangle_{un} = - \int_{-i\infty}^{i\infty} \frac{d\omega}{2\pi i} \frac{2 e^{-\omega L}}{\left(\omega - \frac{\lambda i}{2\sqrt{\omega}} \right)^2} \quad (3.56)$$

and

$$U(L) = \int_{-i\infty}^{i\infty} \frac{d\omega}{2\pi i} e^{-\omega L} \int_{-\infty}^{\infty} \frac{dk}{2\pi} \frac{1}{k^2 - \omega - \Sigma_1(\omega)} \quad (3.57)$$

$$= \int_{-i\infty}^{i\infty} \frac{d\omega}{4\pi} \frac{e^{-\omega L}}{\left(\omega - \frac{\lambda i}{2\sqrt{\omega}}\right)^{1/2}} \quad (3.58)$$

Next, we are going to discuss the singularities in the integrands of above equations, and consider

$$f(\omega) = \frac{1}{\omega - \frac{\lambda i}{2\sqrt{\omega}}} \quad (3.59)$$

At $\omega=0$ is the branch point and the poles can be determined by

$$\omega^{3/2} = \frac{\lambda}{2}i = \frac{\lambda}{2} e^{i\pi/2} \quad (3.60)$$

It can be shown that

$$\omega_m = \left(\frac{\lambda}{2}\right)^{2/3} e^{i\left(\frac{\pi}{3} + \frac{4m\pi}{3}\right)} \quad m = 0, 1, 2 \quad (3.61)$$

Then, the poles are located at

$$\begin{aligned} \omega_1 &= \omega_0 e^{i\pi/3} \\ \omega_2 &= \omega_0 e^{i5\pi/3} \\ \omega_3 &= \omega_0 e^{i\pi} + i2\pi \end{aligned} \quad (3.62)$$

where

$$\omega_0 = \left(-\frac{\lambda}{2}\right)^{2/3}$$

As L is positive, we should require the integrands in eqs. (3.55), (3.56), and (3.58) to be analytic in the left half ω -plane. (If $L < 0$, we will expect the results to be zero and close the contour in the left half ω -plane). In this case, the branch cut should be placed in the right half ω -plane in order to satisfy the causality conditions. Because of the existence of the branch cut, the complex plane is divided into two Riemann Sheets; first sheet ($n=0$), $0 \leq \text{Arg } \omega < 2\pi$ and second sheet ($n=1$), $2\pi \leq \text{Arg } \omega < 4\pi$. Obviously, the pole ω_3 , will lie on the second sheet and the poles ω_1 and ω_2 lie on the first sheet. Since we should require the imaginary part of $\sqrt{\omega}$ to be positive (eq. (3.49)), then only the first sheet is allowed, and the pole ω_3 can not satisfy the condition that

$$\text{Im } \sqrt{\omega} > 0$$

Therefore, we may choose the sheet ($n=0$) be the physical sheet and perform the integration only on this sheet. The pole ω_3 lies on an un-physical sheet ($n=1$).

The integral (3.55) can be done by deforming the contour (Fig. 41) and the results can be written in two terms;

one is due to the residues at the poles ω_1 and ω_2 , and the other is due to the contribution by integrating along the branch cut. Then

$$C(L) = I_1 (\text{due to poles}) + I_2 (\text{due to branch cut}) \quad (3.63)$$

$$\begin{aligned} I_1 &= -\frac{1}{2\pi i} \oint_C \frac{d\omega e^{-\omega L}}{\omega - \frac{\lambda i}{2\sqrt{\omega}}} = -\frac{1}{2\pi i} \oint_C \frac{d\omega e^{-\omega L}(\omega^2 + \frac{\lambda i}{2}\sqrt{\omega})}{\omega^3 + \frac{\lambda^2}{4}} \\ &= -\frac{1}{2\pi i} \oint_C \frac{d\omega e^{-\omega L}(\omega^2 + \frac{\lambda i}{2}\sqrt{\omega})}{(\omega - \omega_1)(\omega - \omega_2)(\omega - \omega_3)} \end{aligned} \quad (3.64)$$

The contour C is indicated in Fig. 41 and the poles are shown in eq. (3.62). The integral can be carried out quite easily, the result is

$$I_1 = \frac{\omega_1^2 + \frac{\lambda i}{2}\sqrt{\omega_1}}{(\omega_1 - \omega_2)(\omega_1 - \omega_3)} e^{-\omega_1 L} + \frac{\omega_2^2 + \frac{\lambda i}{2}\sqrt{\omega_2}}{(\omega_2 - \omega_1)(\omega_2 - \omega_3)} e^{-\omega_2 L} \quad (3.65)$$

Now, we should be careful which sign we are using in order to calculate $\sqrt{\omega_1}$ and $\sqrt{\omega_2}$. From eq. (3.62), we have already discussed the poles in detail, the poles ω_1 and ω_2 lie on a physical sheet which corresponds to $n=0$. In this case, we obtain

$$\sqrt{\omega_1} = \omega_0^{1/2} e^{i\pi/6} \quad (3.66)$$

$$\sqrt{\omega_2} = \omega_0^{1/2} e^{i5\pi/6}$$

and the integral I_1 has the form of

$$I_1 = -\frac{2}{3} e^{-\frac{1}{2}\omega_0 L} \cos \frac{\sqrt{3}}{2}\omega_0 L \quad (3.67)$$

To calculate I_2 , the Laplace's method can be employed (See Appendix III), and the function $f(\omega)$ in eq.(3.59) can be separated into two parts:

$$\begin{aligned} f(\omega) &= f_1(\omega) + f_2(\omega) \\ &= \frac{\omega^2}{\omega^3 + \frac{\lambda^2}{4}} + \frac{\frac{\lambda i}{2}\omega^{1/2}}{\omega^3 + \frac{\lambda^2}{4}} \end{aligned} \quad (3.68)$$

where $f_1(\omega)$ is continuous by crossing the branch cut and $f_2(\omega)$ is discontinuous by crossing the branch cut.

Obviously, only the function $f_2(\omega)$ contributes to the integral I_2 . Near $\omega=0$, we can expand $f_2(\omega)$ into power series of ω , which yields

$$f_2(\omega) \approx \frac{\lambda i}{2} \omega^{1/2} \sum_{p=0}^{\infty} a_p \omega^p \quad (3.69)$$

From Appendix III, $\nu=1/2$, we can establish the asymptotic behavior of I_2 when L is large.

$$I_2 \approx A_1 (\omega_0 L)^{-3/2} + A_2 (\omega_0 L)^{-9/2} + \dots \quad (3.70)$$

where A_1 and A_2 are constants and ω_0 has been defined in eq. (3.62). Combining eqs. (3.67) and (3.70), we obtain

$$c(L) \approx \frac{2}{3} e^{-\frac{1}{2}\omega_0 L} \cos \frac{\sqrt{3}}{2}\omega_0 L + A_1 (\omega_0 L)^{-3/2} + A_2 (\omega_0 L)^{-9/2} + \dots \quad (3.71)$$

Similarly, from eq.(3.56), we have

$$\langle r^2 \rangle_{un.} = J_1 (\text{due to poles}) + J_2 (\text{due to branch cut}) \quad (3.72)$$

and define

$$g(\omega) = f(\omega)^2 = \frac{1}{\left(\omega - \frac{\lambda i}{2\sqrt{\omega}}\right)^2} \quad (3.73)$$

which has two double poles at ω_2 and ω_3 . Then

$$\begin{aligned} J_1 &= -\frac{1}{2\pi i} \oint_C \frac{d\omega e^{-\omega L}}{\left(\omega - \frac{\lambda i}{2\sqrt{\omega}}\right)^2} = -\frac{1}{2\pi i} \oint_C \frac{d\omega \omega e^{-\omega L}}{\left(\omega^{3/2} - i\omega_0^{3/2}\right)^2} \\ &= -\frac{1}{2\pi i} \oint_C \frac{\omega^4 - \omega_0^3 \omega + 2i\omega_0^{3/2} \omega^{5/2}}{\left(\omega^3 + \frac{\lambda^2}{4}\right)^2} e^{-\omega L} d\omega \end{aligned} \quad (3.74)$$

The contour C is indicated in Fig. 38. After lengthy algebraic calculation, we obtain the result when L is large, i.e.

$$J_1 \approx \frac{8}{9} L e^{-\frac{1}{2}} \omega_0^L \sin\left(\frac{\sqrt{3}}{2}\omega_0 L - \frac{\pi}{3}\right) \quad (3.75)$$

In order to calculate the integral J_2 , we can use the same method as before and decompose $g(\omega)$ into two terms $g_1(\omega)$ and $g_2(\omega)$. The former is continuous across the cut, and the latter is not.

$$\begin{aligned} g(\omega) &= g_1(\omega) + g_2(\omega) \\ &= \frac{\omega^4 + \frac{\lambda^2}{4}\omega}{\left(\omega^3 + \frac{\lambda^2}{4}\right)^2} + \frac{i\lambda\omega^{5/2}}{\left(\omega^3 + \frac{\lambda^2}{4}\right)^2} \end{aligned} \quad (3.76)$$

Near $\omega \approx 0$, we can expand $g_2(\omega)$ as

$$g_2(\omega) \simeq i \lambda \omega^{5/2} \sum_p b_p \omega^p \quad (3.77)$$

From Appendix III, $\nu=5/2$, we also have the asymptotic behavior of J_2 when L is large.

$$J_2 \simeq B_1 (\omega_0 L)^{-7/2} + B_2 (\omega_0 L)^{-13/2} + \dots \quad (3.78)$$

where B_1 and B_2 are constants.

Combining eqs. (3.75) and (3.78), we can obtain

$$\langle r^2 \rangle_{un} \simeq \frac{8}{9} L e^{-\frac{1}{2}\omega_0 L} \sin\left(\frac{\sqrt{3}}{2}\omega_0 L - \frac{\pi}{3}\right) + B_1 (\omega_0 L)^{-7/2} + B_2 (\omega_0 L)^{-13/2} + \dots \quad (3.79)$$

Now, we are interested in the case, while L is large, say $L \rightarrow \infty$, then the exponential term in both eqs. (3.71) and (3.79) are much smaller compared with the terms which have the form like L^{-p} . In other words, the most important contributions are due to the branch cut, but not the poles. Then

$$c(L) \simeq \text{const } (\omega_0 L)^{-3/2} \quad \text{as } L \rightarrow \infty \quad (3.80)$$

and

$$\langle r^2 \rangle_{un.} \simeq \text{const } (\omega_0 L)^{-7/2} \quad \text{as } L \rightarrow \infty \quad (3.81)$$

The normalized mean-square size is given by

$$\langle r^2 \rangle = \frac{1}{c(L)} \langle r^2 \rangle_{un.} \approx \text{const } (\omega_0 L)^{-2} \text{ as } L \rightarrow \infty \quad (3.82)$$

The probability of "ring closure" $U(L)$ in eq. (3.58) can also be obtained by the same argument as before. In this case, all the poles in eq. (3.62) become the branch points. Since we require $\text{Im}\sqrt{\omega} > 0$, then the branch point ω_3 does not lie on the same sheet as the sheet of ω_1 and ω_2 . Perform the integration on the physical sheet (the contour is indicated in Fig. 42) and obtain the result by applying the Laplace's method again as $L \rightarrow \infty$, namely,

$$U(L) = \int_{-i\infty}^{i\infty} d\omega h(\omega) e^{-\omega L} \quad (3.83)$$

where

$$h(\omega) = \frac{1}{4\pi} \frac{1}{\left(\omega - \frac{\lambda i}{2\sqrt{\omega}} \right)^{1/2}} \quad (3.84)$$

It is easy to see that the most dominant contribution to this integral is the one by integrating around the branch point at $\omega=0$. Near, $\omega \approx 0$, $h(\omega)$ can be expanded as

$$h(\omega) \approx \frac{1}{4\pi} \sqrt{\frac{2}{\lambda i^3}} \omega^{1/4} \sum_p c_p \omega^p \quad (3.85)$$

From Appendix III, $\nu = 1/4$, we can obtain the asymptotic behavior of $U(L)$ while $L \rightarrow \infty$, i.e.

$$U(L) \simeq \text{const } (\omega_0 L)^{-5/4} \quad \text{as } L \rightarrow \infty \quad (3.86)$$

In this section, we concentrate on the cases of weak coupling between the molecules, so only the first order term in $\Sigma(k, \omega)$ has been used. In the part I of this thesis, the extrapolations of $\alpha_n(u)$, $\beta_n(u)$ and $\gamma_n(u)$ vs. n^{-1} are not quite clearly in the cases of V is small. We hope the perturbation method will give us more information when the coupling strength is weak. But, unfortunately, this method gives

$$\begin{aligned} \alpha(\lambda) &= -3/2 \\ \beta(\lambda) &= -5/4 \\ \gamma(\lambda) &= -2 \end{aligned} \quad (3.87)$$

which are unexpected. Maybe we only used the first order term in $\Sigma(k, \omega)$ and it is necessary to go on to the higher orders.

C. Self-consistent Calculation of $\Sigma(k, \omega)$.

In the last section, we only used the first order term in $\Sigma(k, \omega)$ and neglected those of higher order terms.

Now, we try to sum more diagrams in $\Sigma(k, \omega)$. If we neglect the vertex part in $\Sigma(k, \omega)$, which will be a function of ω only and can be written as the sum of infinite terms which are shown in Fig. 43, then the self-energy part $\Sigma(\omega)$ can be solved self-consistently, we obtain

$$\Sigma(\omega) = -\lambda \sum_k \langle G(k, \omega) \rangle \quad (3.88)$$

In this equation, $\langle G(k, \omega) \rangle$ is the true Green's function which is quite different from the case in eq. (3.53).

Then

$$\Sigma(\omega) = -\frac{\lambda}{2\pi} \int_{-\infty}^{\infty} \frac{dk}{k^2 - \omega - \Sigma(\omega)} \quad (3.89)$$

$$= -\frac{\lambda i}{2(\omega + \Sigma)^{1/2}} \quad (3.90)$$

Now, we can determine Σ by solving the cubic algebraic equation

$$\Sigma^3 + \omega \Sigma^2 + \lambda^2/4 = 0 \quad (3.91)$$

This equation can only be solved approximately in two extreme cases:

1. When the coupling strength λ , is small, we can neglect the higher order terms in λ . The only physical answer is

$$\Sigma(\omega) = -\frac{\lambda i}{2\omega} 1/2 \quad (3.92)$$

This is the same as weak coupling case which we have discussed before.

2. The coupling strength λ , is large, we may expand the solution in the power of λ^{-1} and get

$$\Sigma(\omega) \approx -\left(\frac{\lambda}{2}\right)^{2/3} - \frac{\omega}{3} = -\omega_0 - \frac{\omega}{3} \quad (3.93)$$

From Dyson's equation, we get

$$\begin{aligned} \langle G(k, \omega) \rangle^{-1} &= k^2 - \omega - \Sigma(\omega) \\ &= k^2 - \frac{2}{3}\omega + \omega_0 \end{aligned} \quad (3.94)$$

By using eqs. (3.33), (3.38) and (3.39), we can obtain $c(L)$, $\langle r^2 \rangle$ and $U(L)$ quite easily, namely

$$c(L) \approx \text{const } e^{-\frac{3}{2}\omega_0 L} \quad (3.95)$$

$$\langle r^2 \rangle \approx \frac{1}{c(L)} \int_{-i\infty}^{i\infty} \frac{d\omega}{2\pi i} \frac{-2e^{-\omega L}}{\left(\frac{2}{3}\omega - \omega_0\right)^2} = 2L \quad (3.96)$$

The mean-square size has the same result as the free particle case ($\chi = 0$), and

$$U(L) = \int_{-i\infty}^{i\infty} \frac{d\omega}{2\pi i} e^{-\omega L} \int_{-\infty}^{\infty} \frac{dk}{2\pi} \frac{1}{k^2 - \omega - \Sigma(\omega)} \quad (3.39)$$

$$U(L) = \int_{-i\infty}^{i\infty} \frac{d\omega}{2\pi i} e^{-\omega L} \frac{i}{2(\omega + \Sigma(\omega))^{1/2}} \quad (3.97)$$

By substituting the value of Σ , obtain

$$U(L) = \frac{i}{2} \int_{-i\infty}^{i\infty} \frac{d\omega}{2\pi i} e^{-\omega L} \frac{1}{\left(\frac{2}{3}\omega - \omega_0\right)^{1/2}} \quad (3.98)$$

$$\approx \text{const } L^{-1/2} e^{-\frac{3}{2}\omega_0 L} \quad (3.99)$$

This approach gives the results that

$$\begin{aligned} \alpha(\lambda) &= 0 \\ \beta(\lambda) &= -1/2 \\ \gamma(\lambda) &= 1 \end{aligned} \quad (3.100)$$

which are identical to the case that the polymer chain is in the absence of the repulsive interaction and the results are still unexpected. Maybe the vertex diagrams in the self-energy part Σ are important. Suppose we calculate the second order diagram Σ_2 (vertex) and $\Sigma_2(\omega)$ (Fig. 44) in the self-energy part Σ , i.e.

$$\begin{aligned} \Sigma_2(\text{vertex}) &= \lambda^2 \sum_{q_1, q_2} \frac{1}{(k-q_1)^2 - \omega} \frac{1}{(k-q_1-q_2)^2 - \omega} \frac{1}{(k-q_2)^2 - \omega} \\ &= -\frac{3\lambda^2}{4\omega} \frac{1}{k^2 - 9\omega} \end{aligned} \quad (3.101)$$

and

$$\begin{aligned} \Sigma_2(\omega) &= \lambda^2 \sum_{q_1, q_2} \frac{1}{((k-q_1)^2 - \omega)^2} \frac{1}{(k-q_1-q_2)^2 - \omega} \\ &= \frac{\lambda^2}{8\omega^2} \end{aligned} \quad (3.102)$$

From Dyson's equation (3.28), the true Green's function can be written as

$$\begin{aligned} \langle G(k, \omega) \rangle^{-1} &= k^2 - \omega - (\Sigma_1(\omega) + \Sigma_2(\omega) + \Sigma_2(\text{vertex})) \\ &\approx k^2 - \omega + \frac{\lambda i}{2\sqrt{\omega}} - \frac{\lambda^2}{8\omega^2} + \frac{3\lambda^2}{4\omega} \frac{1}{k^2 - 9\omega} \end{aligned} \quad (3.103)$$

since the vertex part diagram $\Sigma_2(\text{vertex})$ is a function of both variables k and ω . The analyticity of the function $\langle G(k, \omega) \rangle$ in the complex plane is much more complicated and we are unable to discuss the singularities of this function. Maybe the Green's function expansion failed in this kind of problem.

D. Three Dimensional Problem

Flory suggested that γ should be equal to $6/5$ in the three dimensional cases. We are going to apply the same method and examine the behaviors of $c(L)$, $\langle r^2 \rangle$ and $U(L)$ in three dimensions. By using the same approximation in the last section and neglecting the vertex part in the self-energy diagrams, we can also write

$$\Sigma(\omega) \approx -\lambda \sum_{\mathbf{k}} G(\mathbf{k}, \omega) \quad (3.88)$$

and the summation in \mathbf{k} can be replaced by

$$\sum_{\mathbf{k}} \rightarrow \frac{1}{(2\pi)^3} \int d^3 \bar{\mathbf{k}} \quad (3.104)$$

Then

$$\begin{aligned} \Sigma(\omega) &= -\frac{\lambda}{(2\pi)^3} \int \frac{d^3 \bar{\mathbf{k}}}{\mathbf{k}^2 - \omega - \Sigma(\omega)} \\ &= -\frac{4\pi\lambda}{(2\pi)^3} \int_0^\infty \frac{k^2 dk}{k^2 - \omega - \Sigma(\omega)} \end{aligned} \quad (3.105)$$

The integral diverges at large k , we cannot integrate over whole k -space. The cut-off k_0 is necessary to replace the upper limit ∞ and the result will be in a finite form. Then

$$\oint_C \frac{k^2 dk}{k^2 - \omega - \Sigma(\omega)} = i\pi(\omega + \Sigma)^{1/2} \quad (3.106)$$

The contour of integration C is indicated in Fig. 45. From eq. (3.106), we can write

$$\int_C \frac{k^2 dk}{k^2 - \omega - \Sigma(\omega)} = 2 \int_0^\infty \frac{k^2 dk}{k^2 - \omega - \Sigma(\omega)} - k_o \quad (3.107)$$

The self-energy part $\Sigma(\omega)$ can be written as

$$\Sigma(\omega) \approx -\frac{\lambda}{4\pi^2} (k_o + i\pi (\omega + \Sigma)^{1/2}) \quad (3.108)$$

Solving the quadratic equation, yields

$$\Sigma(\omega) = -\frac{\lambda}{4\pi^2} (k_o + \frac{\lambda}{8}) \pm \frac{i\lambda}{4\pi^2} \sqrt{\frac{\lambda k_o}{4} + \frac{\lambda^2}{64} - \omega\pi^2} \quad (3.109)$$

Eq. (3.108) can be reduced to

$$\omega + \Sigma(\omega) = -\frac{16\pi^2}{\lambda^2} \left(\Sigma + \frac{\lambda k_o}{4\pi^2} \right)^2 \quad (3.110)$$

By substituting the value of Σ in eq. (3.109), finally we have

$$\omega + \Sigma(\omega) = \omega - \frac{\lambda}{4\pi^2} (k_o + \frac{\lambda}{8}) \pm i \frac{\lambda}{4\pi} \sqrt{\omega - \frac{\lambda}{4\pi^2} (k_o + \frac{\lambda}{16})} \quad (3.111)$$

Since k_o is a very large quantity and λ is not too large and can always be negligible compared with k_o . Then

$$\frac{\lambda}{4\pi^2} (k_o + \frac{\lambda}{8}) \approx \frac{\lambda k_o}{4\pi^2} = \Delta > 0 \quad (3.112)$$

Then eq. (3.111) has the form

$$\omega + \Sigma(\omega) \simeq \omega - \Delta \pm i \frac{\lambda}{4\pi} (\omega - \Delta)^{1/2} \quad (3.113)$$

From Dyson's equation in (3.28), we can obtain

$$\begin{aligned} \langle G(k, \omega) \rangle^{-1} &= k^2 - (\omega + \Sigma(\omega)) \\ &= k^2 - (\omega - \Delta) \pm i \frac{\lambda}{4\pi} (\omega - \Delta)^{1/2} \end{aligned} \quad (3.114)$$

The Fourier transform of Green's function $\langle G(r, L) \rangle$ in three dimension can be written as

$$G(r, L) = \int_{-i\infty}^{i\infty} \frac{d\omega}{2\pi i} e^{-\omega L} \int \frac{d^3 \vec{k}}{(2\pi)^3} e^{i\vec{k} \cdot \vec{r}} \langle G(k, \omega) \rangle \quad (3.115)$$

and the total probability of a chain with length L can be defined as

$$c(L) = \int d^3 \vec{r} \langle G(r, L) \rangle \quad (3.116)$$

By substituting $\langle G(r, L) \rangle$ into this equation, we obtain

$$c(L) = \int_{-i\infty}^{i\infty} \frac{d\omega}{2\pi i} e^{-\omega L} \int \frac{d^3 \vec{k}}{(2\pi)^3} \langle G(k, \omega) \rangle \int d^3 \vec{r} e^{i\vec{k} \cdot \vec{r}} \quad (3.117)$$

and the integral

$$\int d^3 \vec{r} e^{i\vec{k} \cdot \vec{r}} = \delta(\vec{k}) (2\pi)^3 \quad (3.118)$$

Then, it can be easily shown that

$$c(L) = \int_{-i\infty}^{i\infty} \frac{d\omega}{2\pi i} e^{-\omega L} \langle G(0, \omega) \rangle \quad (3.119)$$

which is identical to eq. (3.33)

Similarly, the mean-square length of a chain in three dimension can be defined as

$$\langle \mathbf{r}^2 \rangle_{\text{un.}} = \int \mathbf{r}^2 \langle G(\mathbf{r}, L) \rangle d^3 \mathbf{r} \quad (3.120)$$

and

$$\langle \mathbf{r}^2 \rangle = \frac{1}{c(L)} \langle \mathbf{r}^2 \rangle_{\text{un.}} \quad (3.121)$$

By using eq. (3.115), we have

$$\langle \mathbf{r}^2 \rangle_{\text{un.}} = \int_{-i\infty}^{i\infty} \frac{d\omega}{2\pi i} e^{-\omega L} \int \frac{d^3 \mathbf{k}}{(2\pi)^3} \langle G(\mathbf{k}, \omega) \rangle \int d^3 \mathbf{r} \mathbf{r}^2 e^{i\mathbf{k} \cdot \mathbf{r}} \quad (3.122)$$

and the last integral becomes

$$\int d^3 \mathbf{r} \mathbf{r}^2 e^{i\mathbf{k} \cdot \mathbf{r}} = -\frac{2\pi}{ik} \int_{-\infty}^{\infty} r^3 dr e^{ikr} = \frac{(2\pi)^2}{ik} \left(\frac{d}{dr} \right)^3 \delta(k) \quad (3.123)$$

Then

$$\langle \mathbf{r}^2 \rangle_{\text{un.}} = \int_{-i\infty}^{i\infty} \frac{d\omega}{2\pi i} e^{-\omega L} \int_0^{\infty} \frac{4\pi k^2 dk}{(2\pi)^3} \frac{(2\pi)^2}{k} \frac{d^3}{dk^3} \delta(k) \langle G(\mathbf{k}, \omega) \rangle \quad (3.124)$$

After lengthy calculation, $\langle \mathbf{r}^2 \rangle_{\text{un.}}$ -normalized reduces to a simple form

$$\langle \mathbf{r}^2 \rangle_{\text{un.}} = -3 \int_{-i\infty}^{i\infty} \frac{d\omega}{2\pi i} e^{-\omega L} \left[\frac{d^2}{dk^2} \langle G(\mathbf{k}, \omega) \rangle \right]_{k=0} \quad (3.125)$$

This equation is quite identical to eq. (3.38) except a factor of 3. The probability of "ring closure" $U(L)$ can be also obtained by setting $r=0$ in eq. (3.115), i.e.

$$U(L) = \int_{-i\infty}^{i\infty} \frac{d\omega}{2\pi i} e^{-\omega L} \int \frac{d^3 k}{(2\pi)^3} \langle G(k, \omega) \rangle \quad (3.126)$$

From eq. (3.88), we can write $U(L)$ in term of the self-energy part Σ , i.e.

$$U(L) = -\frac{1}{\lambda} \int_{-i\infty}^{i\infty} \frac{d\omega}{2\pi i} e^{-\omega L} \Sigma(\omega) \quad (3.127)$$

and it can also be written as:

$$U(L) = \frac{1}{\lambda 2\pi i} \int_0^\infty d\omega e^{-\omega L} \text{Im } \Sigma(\omega) \quad (3.128)$$

Now, substituting the Green's function $\langle G(k, \omega) \rangle$ (3.114) into (3.119), we obtain

$$c(L) = - \int_{-i\infty}^{i\infty} \frac{d\omega}{2\pi i} \frac{e^{-\omega L}}{\omega - \Delta \pm i\frac{\lambda}{4\pi}(\omega - \Delta)}^{1/2} \quad (3.129)$$

First, we choose the positive square root in this equation, and let $\omega' = \omega - \Delta$, then

$$c(L) = -e^{-\Delta L} \int_{-\Delta-i\infty}^{-\Delta+i\infty} \frac{d\omega'}{2\pi i} \frac{e^{-\omega' L}}{\omega' + \frac{i\lambda}{4\pi}\sqrt{\omega'}} \quad (3.130)$$

Now, we want to discuss the singularities of this integral, at $\omega'=0$, is the branch point and the branch cut should be placed in the right half ω' -plane in order to satisfy the causality condition, and the pole is given by

$$\omega'^{1/2} + \frac{i\lambda}{4\pi} = 0 \quad (3.131)$$

and

$$\omega' = -\frac{\lambda^2}{16\pi^2} = \frac{\lambda^2}{16\pi^2} e^{i\pi} \quad (3.132)$$

We must examine this pole very carefully. By taking the square root on both sides, we obtain

$$\omega'^{1/2} = \frac{\lambda}{4\pi} e^{i\pi/2} + i n\pi = \pm \frac{\lambda i}{4\pi} \quad n=0,1 \quad (3.133)$$

This indicated that there are existing two Riemann Sheets in the complex ω' -plane: $n=0$, corresponding to $\omega'^{1/2} = \frac{\lambda i}{4\pi}$, and $n=1$, corresponding to $\omega'^{1/2} = -\frac{\lambda i}{4\pi}$. From eqs.(3.130) and (3.131), the pole of the integrand function in $c(L)$ lies on the sheet $n=1$, therefore the integrand is analytic in the entire left half ω' -plane of the sheet $n=0$. On this sheet, it is convenient for us to reduce the integral $c(L)$ to

$$c(L) = -e^{-\Delta L} \int_{-i\infty}^{i\infty} \frac{d\omega'}{2\pi i} \frac{e^{-\omega'L}}{\omega' + \frac{\lambda i}{4\pi} \sqrt{\omega'}} \quad (3.134)$$

In this case, we may perform the integration on the physical sheet $n=0$, and the contribution to this integral will be due to the branch cut only (Fig. 46). Similarly, we also can choose minus sign in eq. (3.129), therefore the pole does lie on the sheet $n=0$, and the integration will perform in the physical sheet $n=1$.

The integral of (3.134) can be carried out by separating the integrand into two parts; one is continuous across the branch cut, and the other is not. Therefore,

$$c(L) = -e^{-\Delta L} \int_{-i\infty}^{i\infty} \frac{d\omega'}{2\pi i} u(\omega') e^{-\omega' L} \quad (3.135)$$

where

$$\begin{aligned} u(\omega') &= u_1(\omega') + u_2(\omega') \\ &= \frac{\omega'}{\omega'^2 + a\omega'} + \frac{i a^{1/2}}{\omega'^{1/2}(a + \omega')} \end{aligned} \quad (3.136)$$

and

$$a = \frac{\lambda^2}{16\pi^2} \quad (3.137)$$

Near $\omega' \approx 0$, we can expand $u_2(\omega')$ as

$$u_2(\omega') \approx -i a^{1/2} \omega'^{-1/2} \sum_p d_p \omega'^p \quad (3.138)$$

Since the integration of (3.134) around the branch point vanishes and u_1 is an analytic function, the result of this integral can be obtained from Laplace method again. From Appendix III $v = -1/2$, we have the asymptotic behavior while L is large.

$$c(L) \approx D_1(aL)^{-1/2} e^{-\Delta L} + D_2(aL)^{-3/2} e^{-\Delta L} + \dots \quad (3.139)$$

where D_1 and D_2 are constants.

Next, from eqs. (3.114) and (3.125) we can calculate the mean-square length of a long chain in three dimension, namely

$$\langle r^2 \rangle_{un.} = 6 \int_{-i\infty}^{i\infty} \frac{d\omega}{2\pi i} e^{-\omega L} \frac{1}{(\omega - \Delta + \frac{i\lambda}{4\pi}(\omega - \Delta)^{1/2})^2} \quad (3.140)$$

By using the same argument as eq.(3.130) and setting $\omega' = \omega - \Delta$, we can perform the integral on the physical sheet. Then the integral can be reduced to

$$\langle r^2 \rangle_{un.} = 6 e^{-\Delta L} \int_{-i\infty}^{i\infty} \frac{d\omega'}{2\pi i} \frac{e^{-\omega' L}}{(\omega' + \frac{i\lambda}{4\pi} \omega'^{1/2})^2} \quad (3.141)$$

Similarly, we can separate the integrand into two parts; one is an analytic function by crossing the branch cut, and the other is not. Suppose we let

$$v(\omega') = \frac{1}{(\omega' + \frac{i\lambda}{4\pi} \omega'^{1/2})^2} \quad (3.142)$$

$$= v_1(\omega') + v_2(\omega') \\ = \frac{\omega'^2 - a\omega'}{(\omega'^2 + a\omega'^2)^2} - \frac{2ia\omega'^{1/2}}{\omega'^{1/2}(a + \omega')^2} \quad (3.143)$$

Near $\omega' \approx 0$, we can expand v_2 as

$$v_2(\omega') \approx -2ia\omega'^{1/2} \sum_p e_p \omega'^p \quad (3.144)$$

Now the integration of (3.141) around the branch point is equal to

$$\lim_{\epsilon \rightarrow 0} \frac{1}{2\pi i} \int_0^{2\pi} \frac{\epsilon e^{i\theta} i d\theta e^{-\epsilon e^{i\theta} L}}{(\epsilon e^{i\theta} + \frac{i\lambda}{4\pi} \epsilon^{1/2} e^{i\theta/2})^2} = -\left(\frac{4\pi}{\lambda}\right)^2 = -\frac{1}{a} \quad (3.145)$$

and the result of this integral (3.141) can be obtained from Laplace method, which yields

$$\langle r^2 \rangle_{un} \approx C_1 (aL)^{-1/2} e^{-\Delta L} + C_2 (aL)^{-3/2} e^{-\Delta L} + \frac{C_0}{a} e^{-\Delta L} + \dots \quad (3.146)$$

Dividing eq. (3.146) by eq. (3.139), we obtain the normalized mean-square length

$$r^2 = \frac{\frac{C_0}{a} e^{-\Delta L} + C_1 (aL)^{-1/2} e^{-\Delta L} + \dots}{D_1 (aL)^{-1/2} e^{-\Delta L}} \approx \text{const } L^0 + \text{const } L^{1/2} + \dots \quad \text{as } L \rightarrow \infty \quad (3.147)$$

Finally, we get the result that the index $\gamma = 1/2$, which does not agree with Flory's assumption that γ should be equal to $\frac{6}{5}$ in three dimensions.

We go on to calculate $U(L)$ in eq. (3.138), the self-energy part Σ has the form of

$$\Sigma(\omega) = -\Delta \pm \frac{i\lambda}{4\pi} (\omega - \Delta)^{1/2} \quad (3.148)$$

Then

$$U(L) = \frac{1}{4\pi^2} \int_0^\infty d\omega e^{-\omega L} (\omega - \Delta)^{1/2} = \frac{1}{4\pi^2} e^{-\Delta L} \int_\Delta^\infty d\omega' e^{-\omega' L} \omega'^{1/2} \quad (3.149)$$

$$\approx \text{const } L^{-3/2} e^{-\Delta L} \quad (3.150)$$

From eqs. (3.139), (3.147) and (3.150), we obtain

$$\alpha(\lambda) = -1/2$$

$$\beta(\lambda) = -3/2 \quad (3.151)$$

$$\gamma(\lambda) = 1/2$$

which still does not agree to the actual values that

$$\alpha = 1/6$$

$$\beta = -7/4 \quad (3.152)$$

$$\gamma = 6/5$$

SUMMARY AND CONCLUSION

The extrapolations of $\beta_n(u)$ and $\gamma'_n(u)$ vs. n^{-1} give quite good results in the cases of $V > 0.25$. But in the intermediate region $0 < V < 0.25$, the curves bend up very rapidly, the limiting values can not be easily seen, since we do not have enough walks to see these. We might guess these curves will also fall into the same limits as the strong repulsion cases and speculate

$$\beta(u) = \begin{cases} -1/2 & \text{for } V=0, u=1 \\ 1 & \text{for } V>0, 0 \leq u < 1 \end{cases}$$

and

$$\gamma'(u) = \begin{cases} 1 & \text{for } V=0, u=1 \\ 2 & \text{for } V>0, 0 \leq u < 1 \end{cases}$$

The extrapolations of $\alpha_n(u)$ and $\gamma_n(u)$ vs. n^{-1} give us almost the same figures as above, nevertheless, the intermediate region increases up to $0 < V < 0.75$. Inasmuch as $V > 0.75$, $\alpha_n(u)$ will fall exactly into zero and $\gamma_n(u)$ will be equal to two as $n \rightarrow \infty$. So we may also speculate these curves in the intermediate region will also have the same limiting values as those in the cases of $V > 0.75$. In summary, the results seem to be consistent with the conjecture and we may conclude

$$\alpha(u) = 0 \quad \text{for all } V \geq 0, 0 \leq u \leq 1$$

and

$$\gamma(u) = \begin{cases} 1 & \text{for } V=0, u=1 \\ 2 & \text{for } V>0, 0 \leq u < 1 \end{cases}$$

In the absence of the repulsion, the probability distribution of the point ℓ on a long chain after n -step walk, has a well-known Gaussian distribution. Because of the existence of this repulsive interaction for each pair of steps between the same two lattice points, the distribution functions $Z_n(\ell, u)$ are no longer Gaussians. The peak of the distribution will move away from the origin and shift to the end of the chain as we increase the strength of the interaction V . In the extreme case, V is very large, the distribution function $Z_n(\ell, u)$ looks almost like a δ -function at $\ell=n$. This is the completed excluded-volume problem in one dimension.

The generating function method checks quite well in the cases of strong coupling approximation. In this case, we can sum over infinite diagrams and consider $c_n(u), U_n(u)$ and $\langle r_n^2(u) \rangle$ as the coefficients of the generating functions $F(z), G(z)$ and $X(z)$. Then the following method can be employed to evaluate these coefficients. Consider the function $F(z)$ as the sum of an infinite series c_m ; namely,

$$F(z) = \sum_{m=0} c_m z^m$$

and the coefficients c_n can be easily obtained by evaluating the integral

$$c_n = \frac{1}{2\pi i} \oint_C \frac{F(z) dz}{z^{n+1}}$$

the contour C is a circle around the origin. This method gives us quite good asymptotic behavior as $n \rightarrow \infty$ and the coefficients $c_n(u)$, $U_n(u)$ and $\langle r_n^2(u) \rangle$ are in agreement to our previous calculation.

The probability distribution function $z_n(\ell, u)$ may be studied by using the generating function method. After lengthy calculations, we plot $z_n(\ell, u)$ vs. ℓ for different values of interaction, which quite agrees to the previous extrapolation results. We also plot $\frac{1}{n} \ln z_n(\ell, u)$ vs. ℓ for different values of u (u is small; v is large) and check quite clearly that the peak of the distribution functions moves away from the origin as v increases.

The extrapolations of $\alpha_n(u)$ and $\gamma_n(u)$ vs. n^{-1} can not give us the asymptotic limits quite clearly in the region of $0 < v < 0.75$. Then the Green's function method is introduced. From Edward's assumption, the probability distribution of a polymer chain, $\langle G(x, L) \rangle$ could be considered as an ordinary diffusion problem in the presence of a complex potential. Now, we can expand the distribution $\langle G(x, L) \rangle$ in terms of the free distribution, $G_0(x, L)$ (in the absence of the potential) and the complex potential. Field theory and diagram expansion are used. We hope the perturbation method will give us more insight in the case of small v and examine the indices $\alpha(u)$, $\beta(u)$ and $\gamma(u)$ in this region ($0 < v < 0.75$).

In the weak coupling approximation, we calculate Σ_1 the first order term in the self-energy part and obtain the distribution function in momentum space, $G(k, \omega)$, by using Dyson's equation, i.e.

$$G(k, \omega)^{-1} = G_0(k, \omega)^{-1} - \Sigma_1$$

Then, the total probability $c(L)$, probability of 'ring closure' $U(L)$ and the mean-square size $\langle r^2 \rangle$ of a long chain with length L can be evaluated by the complex integration, namely,

$$c(L) = - \int_{-i\infty}^{i\infty} \frac{d\omega}{2\pi i} \frac{e^{-\omega L}}{\omega - \frac{\lambda i}{2\sqrt{\omega}}}$$

$$U(L) = \int_{-i\infty}^{i\infty} \frac{d\omega}{2\pi i} \frac{e^{-\omega L}}{\left(\omega - \frac{i\lambda}{2\sqrt{\omega}}\right)^{1/2}}$$

and

$$r^2 = -\frac{1}{c(L)} \int_{-i\infty}^{i\infty} \frac{d\omega}{2\pi i} \frac{2 e^{-\omega L}}{\left(\omega - \frac{i\lambda}{2\sqrt{\omega}}\right)^2}$$

The contributions of these integrals have two parts; one is due to the poles and the other is due to integrating along the

branch cut. In the case of large L , say $L \rightarrow \infty$, the most dominant term comes from the cut only. The results behave quite unexpectedly, namely

$$c(L) \approx L^{-3/2}, \quad U(L) \approx L^{-5/4}$$

and

$$\langle r^2 \rangle \approx L^{-2}$$

The trouble may be the fact that we have only used the first order diagram in Σ . So perhaps it is necessary to go on to the higher order diagrams. Instead of taking the fomidable task of including all the higher order terms, we go on to neglect the vertex part in Σ and solve it self-consistently. We get a cubic algebraic equation in Σ , which can be only solved approximately: if the coupling strength is small, we may expect getting the same result as above by using the first order term in Σ and if the coupling strength is large, we can obtain the total probability, 'ring closure' probability and mean-square size which have the form of

$$c(L) \approx e^{-aL}, \quad U(L) \approx L^{-1/2} e^{-aL}$$

and

$$\langle r^2 \rangle \approx L$$

where a is a constant. It turns out to be the same results as free

molecule case (in the absence of the coupling interaction).

Next, we go on applying the same method in three dimensions by neglecting the vertex part in Σ and solving Σ self-consistently, and still can not obtain the physical answers.

These results do not agree to Flory's suggestion and our previous calculations. We may expect the vertex part is to be of importance, and consider the first order vertex diagrams in Σ , which is a function of both variables k and ω . The analiticity of $\langle G(k, \omega) \rangle$ is very complicated and we are unable to solve it. Perhaps, the Green's function methods may not apply to this problem.

REFERENCES

1. For previous reviews on this topic see eg.
F.T. Wall and L.A. Hiller, Ann. Rev. Phys. Chem. 5, 267 (1954);
J.J. Hermans, 8, 179 (1957); E.F. Cassassa, 11, 477 (1960).
2. F.T. Wall, L.A. Hiller and D.J. Wheeler, J. Chem. Phys. 22, 1036 (1954); F.T. Wall, L.A. Hiller and W.F. Atchison, J. Chem. Phys. 23, 913 (1955); 26, 1742 (1957); F.T. Wall, R.J. Rubin and L.M. Isaacson, J. Chem. Phys. 27, 186 (1957); F.T. Wall and J.J. Erpenbeck, J. Chem. Phys. 30, 637 (1959); P.J. Gans, J. Chem. Phys. 42, 4159 (1965). The last paper provides a good reference list to the rest of the literature.
3. C. Domb, Advances in Physics, 9, 149, 245 (1960).
4. M.E. Fisher and F.F. Sykes, Phys. Rev. 114, 45 (1959).
5. M.E. Fisher and B. J. Hiley, J. Chem. Phys. 34, 1253 (1961).
6. B.J. Hiley and M.F. Sykes, J. Chem. Phys. 34, 1531 (1961); M.F. Sykes, J. Chem. Phys. 39, 410 (1963); G.S. Rushbrooke and J. Eve, J. Chem. Phys. 31, 1333 (1959); M.E. Fisher, J. Chem. Phys. 44, 616 (1966); 45, 1469 (1966).
7. M.F. Sykes, J. Math. Phys. 2, 52 (1961); C. Domb and M.F. Sykes, J. Math. Phys. 2, 63 (1961).
8. The best review articles of Critical Phenomena are:
M.E. Fisher, 'The Nature of Critical Points', Lecture in Theoretical Physics, Vol. VIIC 1965, University of Colorado Press and M.E. Fisher 'The Theory of Equilibrium Critical Phenomena' Report in Progress Physics, 30, 615 (1967).
9. J.L. Martin, M.F. Sykes and H.T. Hioe, J. Chem. Phys. 46, 3478 (1967).

10. P.J. Flory, Principle of Polymer Chemistry, (Cornell University Press, Ithaca, New York, 1953), Chapter 14; J. Chem. Phys. 17, 303 (1949); P.J. Flory and S. Fisk, J. Chem. Phys. 44, 2243 (1966).
11. J.L. Martin, Proc. Camb. Phil. Soc. 58, 92 (1962); C. Domb, J. Chem. Phys. 38, 2957 (1963).
12. S. Windwer, J. Chem. Phys. 43, 115 (1965); R.J. Fleming, Proc. Phys. Soc. 90, 1003 (1967).
13. H. Reiss, J. Chem. Phys. 47, 186 (1967); see also H. Yamakawa, 'On the Asymptotic Solution of the Excluded Volume Problem in a Linear Polymer Chain' (to be published).
14. S.F. Edwards, Proc. Phys. Soc. 85, 613 (1965); 88, 265 (1966).
15. S.F. Edwards, 'The Statistical Mechanics of a Single Polymer Chain', Critical Phenomena, Eds. M.S. Green and J.V. Sengers, (National Bureau of Standard, Washington, D.C. 1965) Misc. Publ. 273, p.225.
16. J. des Cloizeaux (to be published).
17. C. Domb, J. Royal Stat. Soc. London, B26, 373 (1964); 'Critical Properties of Lattice Model', Critical Phenomena, Eds. M.S. Green and J.V. Sengers, (National Bureau of Standard, Washington, D.C. 1965) Misc. Publ. 273, p.29.
18. M.E. Fisher, J. Math. Phys. 5, 944 (1964); H.N.V. Temperly, Phys. Rev. 103, 1 (1956).
19. M.F. Sykes, J.W. Essam, B.R. Heap and B.J. Hiley, J. Math. Phys. Rev. 17, 1557 (1966).
20. W.J.C. Orr, Trans. Faraday Soc. 43, 12 (1947).

21. C. Domb, Proc. Camb. Phil. Soc. 50, 586 (1954); E.W. Montroll and G.H. Weiss, J. Math. Phys. 6, 167 (1965).
22. E.W. Montroll, J. Chem. Phys. 18, 734 (1950).
23. J.M. Hammersley, Proc. Camb. Phil. Soc. 53, 642 (1957); Phys. Rev. 118, 656 (1960).
24. H. Kesten, J. Math. Phys. 4, 960 (1963); 5, 1128 (1964).
25. M.E. Fisher and R.J. Burford, Phys. Rev. 156, 583 (1967).
26. C. Domb, J. Gills and G. Williams, Proc. Phys. Soc. 85, 625 (1965).
27. A.A. Abrikosov, L.P. Gor'kov and I.Y. Dzyaloshinskii, Quantum Field Theoretical Methods in Statistical Physics, Pergamon Press, 1965, Chapter 2.
28. P.G. DeGennes, Biopolymers, 6, 715 (1968).

ACKNOWLEDGMENT

The author would like to express his deepest appreciation to his advisor Professor James S. Langer, for his guidance, encouragement, and inspiration, and for the interest which he showed throughout the course of this work.

He also likes to thank Professor Robert B. Griffith and Professor John F. Nagle for some helpful discussion and information, and International Business Machines Corporation for use of its facilities during part of this work.

Finally he is indebted to his wife, Susan, for her patience and encouragement and bringing this thesis into the final form.

APPENDIX

Appendix I Derivation of Flory's rule by Mean-field Theory.

The probability distribution of a single polymer chain of length L without the repulsive interaction between the molecules satisfies the simple diffustion equation

$$\left(\frac{\partial}{\partial L} - a^2 \nabla^2 \right) G_o(r, L) = \delta(r) \delta(L) \quad (I.1)$$

where a is the diffusion coefficient. The solution of this equation has the form of

$$G_o(r, L) = \frac{1}{(4\pi L)^{1/2}} \exp\left(-\frac{r^2}{4aL}\right) \quad (I.2)$$

and

$$\int G_o(r, L) d^3\vec{r} = 1 \quad (I.3)$$

Then the mean-square length $\langle r^2 \rangle$ can be defined as

$$\langle r^2 \rangle = \int r^2 G_o(r, L) d^3\vec{r} \quad (I.4)$$

and it turns out to be

$$\langle r^2 \rangle = r \quad (I.5)$$

Suppose we consider existing the repulsive interaction between

the molecules in the chain and the total energy of the chain has the form of

$$E \sim \iint d^3\vec{r} d^3\vec{r}' v(\vec{r}-\vec{r}') \rho(\vec{r}) \rho(\vec{r}') \quad (I.6)$$

where $\rho(\vec{r})$ and $\rho(\vec{r}')$ are the densities of molecules at \vec{r} and \vec{r}' , and $v(\vec{r}-\vec{r}')$ is the pairwise repulsive interaction between these two points. To simplify the problem, the interaction v can be considered only a short-range δ -function, and can be written as

$$v(\vec{r}-\vec{r}') = v_0 \delta(\vec{r}-\vec{r}') \quad (I.7)$$

where v_0 is the strength of the interaction. We also can consider the densities $\rho(\vec{r})$ of the chain are uniform over whole space, then

$$\rho(\vec{r}) = \rho(\vec{r}') = \bar{\rho} = \frac{L}{\Omega} = \frac{L}{r^d} \quad (I.8)$$

where L is the length of the chain, d is the dimensionality and Ω is the volume of a sphere with radius r in d dimension. Now, the total energy E in eq. (I.6) can be reduced to a simple form

$$E \sim v_0 \bar{\rho}^2 \Omega = v_0 \frac{L^2}{\Omega} = v_0 \frac{L^2}{r^d} \quad (I.9)$$

In the presence of the interaction between molecules, the probability distribution $G(r, L)$ can be written as follows:

$$G(r, L) \sim \sum \exp(-\beta E) \exp\left(-\frac{r^2}{aL}\right) \quad (I.10)$$

sum over all configuration inside the sphere with the radius in d-dimension

where $\beta = \frac{1}{kT}$ and the summation is summing over all the configurations inside the sphere with radius r in the d-dimensional space.

To evaluate the asymptotic behavior of this equation, all we have to do is to find out the largest term in G and this can be done by minimizing the exponential term

$$-\beta E - \frac{r^2}{aL} \quad (I.11)$$

in the summation with respect to r , i.e.

$$L^2 r^{-d-1} \sim L^{-1} r \quad (I.12)$$

Now, we assume the mean-square length $\langle r^2 \rangle$ has the form of

$$\langle r^2 \rangle \approx \text{const } L^\gamma \quad (I.13)$$

Comparing eq. (I.12), finally we obtain Flory's rule, such that

$$\gamma = \frac{6}{d+2} \quad d=1, 2, 3, \dots \quad (I.14)$$

Appendix II. Prove that $\alpha(u=1)=0$ and $\beta(u=1)=-1/2$

We are going to check the indice $\alpha(u)$ and $\beta(u)$ in the case of $v=0$, $u=1$. From eqs. (1.12) and 1.13), the total number of n -th order walk, $c_n(u=1)$, and the n -th order walk which returns to its starting point, $U_n(u=1)$, can be written as

$$c_n(u=1) = 2^n \quad (1.12)$$

$$U_n(u=1) = \frac{n!}{(n/2)! (n/2)!} \quad (1.13)$$

By using the ratio test, we consider the successive ratios of $c_n(u=1)$ and $U_n(u=1)$, which yields

$$\mu_n(u=1) = \frac{c_{n+1}(u=1)}{c_n(u=1)} = 2 \quad \text{for all } n \quad (II.1)$$

and

$$\mu_n^2(u=1) = \frac{U_{n+2}(u=1)}{U_n(u=1)} = \frac{4(n+1)}{n+2} \quad (II.2)$$

From eqs. (1.27) and (1.28), we have

$$\alpha_n(u=1) = \frac{\mu_n(u=1) - \mu_{n+1}(u=1)}{\mu_\infty(u=1) \left(\frac{1}{n} - \frac{1}{n+1} \right)} = 0 \quad (II.3)$$

for all n

and

$$\alpha_n(u=1) = \frac{\mu_n'^2(u=1) - \mu_{n+2}'^2(u=1)}{2\mu_\infty'^2(u=1) \left(\frac{1}{n} - \frac{1}{n+2} \right)} = -\frac{n}{2(n+4)} \quad (\text{II.4})$$

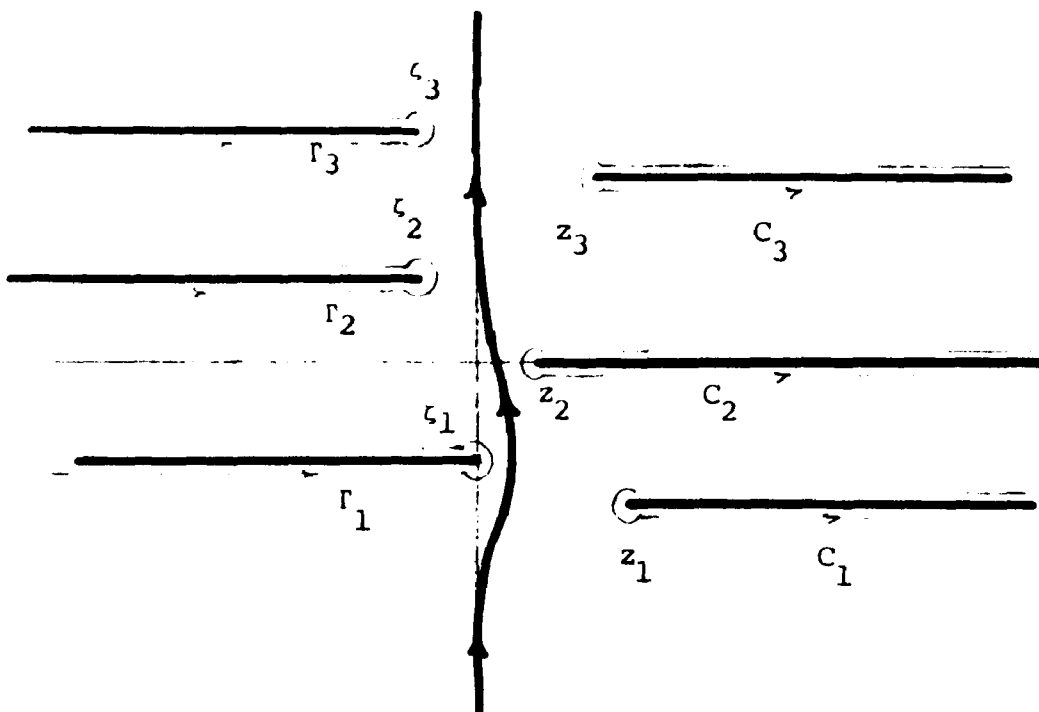
As $n \rightarrow \infty$

$$\alpha_n(u=1) \rightarrow \alpha(u=1) = 0$$

$$\beta_n(u=1) \rightarrow \beta(u=1) = -1/2 \quad (\text{II.5})$$

which satisfy our extrapolation calculations in Part I.

Appendix III. Laplace's Method



Consider the integral $I(\beta)$ has the form

$$I(\beta) = \int_{-i\infty}^{i\infty} dz f(z) \exp(-\beta z) \quad (\text{III.1})$$

where $|\beta|$ is large and real and $f(z)$ has many branch points like: z_1, z_2, z_3, \dots and $\zeta_1, \zeta_2, \zeta_3, \dots$ which are shown in above figure. We are going to calculate the asymptotic behaviors of this integral for $|\beta|$ is very large. Then we can write the above integral into

$$I(\beta) = \begin{cases} \int_{C_1 + C_2 + C_3 + \dots} \exp(-\beta z) f(z) dz & \beta > 0 \\ \int_{r_1 + r_2 + r_3 + \dots} \exp(-\beta z) f(z) dz & \beta < 0 \end{cases} \quad (\text{III.2})$$

For $\beta > 0$, near those branch points z_i , $f(z)$ can be written as

$$f(z) = (z - z_i)^v \sum_{p=0}^{\infty} a_p (z - z_i)^p \quad (\text{III.3})$$

with $\operatorname{Re} v > -1$, then the contribution from the contour C_i to $I(\beta)$ is

$$I_{C_i} = \int_{C_i} e^{-\beta z} (z - z_i)^v \sum_{p=0}^{\infty} a_p (z - z_i)^p dz \quad (\text{III.4})$$

This integral can be done and gives

$$I_{C_i} = -2 \sin \pi v \exp(-\beta z_i - iv - \frac{\pi}{2}) \int_0^\infty e^{-\beta r} r^v \sum_{p=0}^{\infty} a_p (ir)^p dr \quad (\text{III.5})$$

$$= -\frac{2 \sin \pi v}{\beta^{v+1}} \exp(-\beta z_i - iv - \frac{\pi}{2}) \sum_{p=0}^{\infty} \frac{a_p i^p r^{v+p+1}}{\beta^p} \quad (\text{III.6})$$

When the asymptotic contributions from the other z_i are added, so as to give an asymptotic expression for $I(\beta)$ itself. If poles are present, residues are easily included.

APPENDIX IV Calculation of $z_n(\ell, u)$ in the case of very strong coupling

In the case of very strong coupling, the un-normalized probability distribution $z_n(\ell, u)$ may be calculated by considering the diagrams which contain Q_2 only. The generating function $F(z, w)$ has the form of

$$F(z, w) = \sum_{p,q=0}^{\infty} (z^2 u)^{p+q} \sum_{r=1}^{\infty} (zw)^r \quad (\text{IV.1})$$

$$= \frac{zw}{(1-z^2 u)^2 (1-zw)} \quad (\text{IV.2})$$

Similarly, the probability distribution $z_n(\ell, u)$ can be written as a double integration with respect to the variables z and w , i.e.,

$$z_n(\ell, u) = \frac{1}{2\pi i} \oint_C \frac{dz}{z^{n+1}} \frac{1}{2\pi i} \oint_C \frac{dw}{w^{\ell+1}} \frac{zw}{(1-z^2 u)^2 (1-zw)} \quad (\text{IV.3})$$

where C is the circle around the origin.

In order to calculate this integral, we may apply the same technique as before and calculate the residue with respect to the singularity $w=1/z$, namely,

$$z_n(\ell, u) = \frac{1}{2\pi i} \oint_C \frac{dz}{z^{n-\ell+1}} \frac{1}{(1-z^2 u)^2} \quad (\text{IV.4})$$

The complex-integral in the z -plane can be calculated in the same way.

Finally, we obtain

$$z_n(\ell, u) = \frac{\partial}{\partial u} \frac{1}{2\pi i} \oint_C \frac{dz}{z^{n-\ell+1}} \frac{1}{(1-z^2 u)^2} \quad (\text{IV.5})$$

$$= \frac{\partial}{\partial u} (u^{\frac{n-\ell}{2} + 1}) = (m+1) u^m \quad (\text{IV.6})$$

As $\ell \rightarrow n$, $m \rightarrow 0$, $z_n(n, u) \rightarrow 1$ and $\ell \rightarrow 0$, $z_n(0, u) = (\frac{n}{2} + 1) \exp(-\frac{n}{2} V) \rightarrow 0$, where V is the strength of the coupling interaction.

The above equation is plotted in the case of $n=15$ for different values of interaction V in Fig. 28 and compares with those of considering the higher order diagrams Q_3 , Q_4 and the exact counting results.

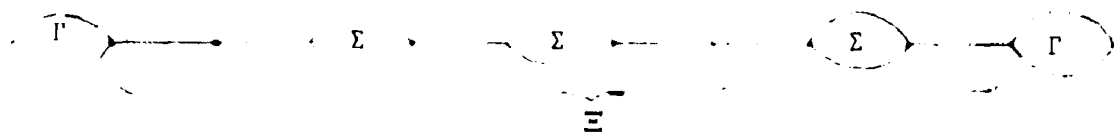
Appendix V. Generating function of summing over the diagrams containing

Q_2 , Q_3 and Q_4

In general, all the diagrams can be classified into two types:

1. All the diagrams which contain at least one single-step.

The general form of such diagrams has the form of



which is identical as before, except the vertex part should be modified. Similarly, we may write

$$F_1 = \Gamma \Xi \Gamma \quad (V.1)$$

where Ξ has the same form as eq. (2.15), namely,

$$\Xi = \frac{zw}{1-zw-\Sigma zw} = \frac{Q_1}{1 - Q_1 - \Sigma Q_1} \quad (2.15)$$

where $Q_1 = zw$. The vertex part may be written as the form similar to eq. (2.18), i.e.,

$$\Gamma = 1 + S + \Sigma + S^* \Sigma \quad (V.2)$$

where S is the sum of the diagrams which contain Q_2 and Q_4 and it is equivalent to Λ in eq. (2.18) which is the sum of the

diagrams containing Q_2 only. The diagrams of S are shown in Fig. 47. Each line represents a two-line bubble with a factor $z^2 u$ and G_0 and G_1 can be defined as follows:

$$G_0 = \sum_{p=0} Q_2^p = \frac{1}{1 - Q_2} \quad (V.3)$$

and

$$G_1 = \sum_{p=1} Q_2^p = \frac{Q_2}{1 - Q_2} \quad (V.4)$$

The corresponding self-energy part denotes as ϕ if it occurs at the middle of the diagrams and denotes as ψ if it occurs at the end. Then

$$\begin{aligned} 1 + S &= 1 + G_1 + G_1 \phi G_0 + G_1 \phi G_1 \phi G_0 + \dots \\ &\quad + \psi G_0 + \psi G_1 \phi G_0 + \psi G_1 \phi G_1 \phi G_0 + \dots \\ &= G_0 + G_0 (\psi + G_1 \phi) (1 + G_1 \phi + G_1 \phi G_1 \phi + \dots) \\ &= G_0 + G_0 \frac{\psi + G_1 \phi}{1 - G_1 \phi} \\ &= G_0 \frac{1 + \psi}{1 - G_1 \phi} \end{aligned} \quad (V.5)$$

The diagrams of ϕ which is connected by two G -lines (either G_0, G_1 or G_1, G_1) can be written as

$$\phi = 2Q_4 + 2Q_4 * Q_4 + 2Q_4 * Q_4 * Q_4 + \dots \quad (V.6)$$

Similarly, the diagrams of ψ which is connected only by one

G-line (either G_0 or G_1 -line) and can be written as

$$\psi = Q_4 + Q_4^* Q_4 + Q_4^* Q_4^* Q_4 + \dots \dots \dots \quad (\text{V.7})$$

where the asterisk '*' is defined same as before and the product of the Q_4 's has the simple formula as follows:

$$Q_4^* Q_4^* Q_4^* \dots \dots \cdot Q_4 = 3^{q-1} Q_4^q \quad (\text{V.8})$$

Then ϕ and ψ may reduce to

$$\phi = 2 \sum_{q=1}^{\infty} 3^{q-1} Q_4^q = \frac{2 Q_4}{1 - 3Q_4} \quad (\text{V.9})$$

and

$$\psi = \sum_{q=1}^{\infty} 3^{q-1} Q_4^q = \frac{Q_4}{1 - 3Q_4} \quad (\text{V.10})$$

By substituting eqs. (V.3), (V.4), (V.9) and (V.10) into eq. (V.5), we have

$$1 + S = \frac{1 - 2Q_4}{1 - Q_2 - 3Q_4 + Q_2 Q_4} \quad (\text{V.11})$$

If set $Q_4 \rightarrow 0$, then

$$1 + S \rightarrow \frac{1}{1 - Q_2} = 1 + \Lambda \quad (\text{V.12})$$

This agrees our previous calculations (eq.(2.22)).

The diagrams of $S^*\Sigma$ part are shown in Fig. 48, which can be obtained by the same way, namely,

$$\begin{aligned}
 S^*\Sigma &= G_1^0 + G_1\phi G_1^0 + G_1\phi G_1\phi G_1^0 + \dots \\
 &\quad + \psi G_1^0 + \psi G_1\phi G_1^0 + \psi G_1\phi G_1\phi G_1^0 + \dots + \Delta \\
 &= \Delta + \frac{\theta G_1 (1+\psi)}{1 - G_1\phi} \tag{V.13}
 \end{aligned}$$

where θ is defined in Fig. 49 which connects a G-line and can be written as:

$$\begin{aligned}
 \theta &= 2(Q_3 + Q_3^*Q_3 + Q_3^*Q_3^*Q_3 + \dots) * (1 + Q_4 \\
 &\quad + Q_4^*Q_4 + Q_4^*Q_4^*Q_4 + \dots) \tag{V.14}
 \end{aligned}$$

and Δ has almost same diagrams as θ , except it connects no G-line. Then Δ may be written in terms of

$$\Delta = \theta/2 - \Sigma \tag{V.15}$$

The product of the Q_3 's and Q_4 's has the property of

$$(Q_3^* Q_3^* Q_3^* \dots Q_3^*)^p * (Q_4^* Q_4^* Q_4^* \dots Q_4^*)^q = 2^{p-1} 3^{q+1} Q_3^p Q_4^q \tag{V.16}$$

and

$$Q_3^* Q_3^* Q_3^* \dots \dots \dots Q_3 = 2^{p-1} Q_3^p \quad (\text{V.17})$$

p

Then the eqs. (V.14) and (V.15) can be carried out quite easily, namely,

$$\theta = \frac{2Q_3}{1 - 2Q_3} + \frac{6Q_3Q_4}{1 - 3Q_4} - \frac{1}{1 - 2Q_3} \quad (\text{V.18})$$

$$= \frac{2Q_3}{(1-3Q_4)(1-2Q_3)} \quad (\text{V.19})$$

$$\Delta = \frac{3Q_3Q_4}{(1-3Q_4)(1-2Q_3)} \quad (\text{V.20})$$

Substituting eqs. (V.18), (V.19), (V.9) and (V.10) into (V.13), we obtain

$$S^* \Sigma = \frac{3Q_3Q_4}{(1-3Q_4)(1-2Q_3)} + \frac{2Q_2Q_3(1-2Q_4)}{(1-3Q_4)(1-2Q_3)(1-Q_2-3Q_4+Q_2Q_4)} \quad (\text{V.21})$$

Finally, combining eqs. (V.11), (V.20) and (V.21), we get the complete vertex part Γ , such that

$$\Gamma = \frac{1-Q_3(1-Q_2)-2Q_4(1-2Q_3)}{(1-2Q_3)(1-Q_2-3Q_4+Q_2Q_4)} \quad (\text{V.22})$$

It can be shown that if $Q_4 \rightarrow 0$, the above equation reduces to

$$\Gamma = \frac{1-Q_3(1-Q_2)}{(1-2Q_3)(1-Q_2)} \quad (\text{V.23})$$

It agrees to eq. (2.30) which takes into account the diagrams containing Q_2 and Q_3 only.

By substituting Σ in eq. (V.20) into eq. (2.15), we obtain

$$\Xi' = \frac{Q_1(1-2Q_3)}{1 - Q_1 - 2Q_3 + Q_1Q_3} \quad (\text{V.24})$$

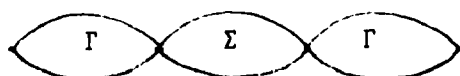
Now, we get the final form of F_1 , such that

$$F_1 = \Gamma^2 \Xi' \\ = \frac{Q_1(1-2Q_3) [1-Q_3(1-Q_2)-2Q_4(1-2Q_3)]^2}{(1-2Q_3)^2 (1-Q_2-3Q_4+Q_2Q_4)^2 (1-Q_1-2Q_3+Q_1Q_3)} \quad (\text{V.25})$$

Substituting all the values of $Q_1 = zw$, $Q_2 = z^2u$, $Q_3 = w z^3 u^3$ and $Q_4 = z^4 u^6$, we have

$$F_1 = \frac{[1-wz^3u^3(1-z^2u)-2z^4u^6(1-2wz^3u^3)]^2}{zw} \\ = \frac{(1-2wz^3u^3)(1-z^2u-3z^4u^6+z^6u^7)^2}{(1-zw-2wz^3u^3+w^2z^4u^7)} \quad (\text{V.26})$$

2. All the diagrams which contains no single-step. The general type of such diagrams has the form of



The diagrams of this kind are shown in Fig. 47, which can be written as:

$$\Phi = \mathcal{L} \Sigma \mathcal{L} + C \quad (V.27)$$

where

$$\begin{aligned} \mathcal{L} &= G_1 \delta + \psi G_1 \delta + G_1 \phi G_1 \delta + \psi G_1 \phi G_1 \delta + G_1 \phi G_1 \phi G_1 \delta \\ &\quad + \dots \dots \dots + \delta' \\ &= \frac{G_1 (1+\psi) \delta}{1 - \phi G_1} + \delta' \end{aligned} \quad (V.28)$$

$$\begin{aligned} \delta &= 2(1+3Q_4 + 3^2 Q_4^2 + \dots \dots \dots) \\ &= \frac{2}{1-3Q_4} \end{aligned} \quad (V.29)$$

$$\delta' = \delta/2 = \frac{1}{1-3Q_4} \quad (V.30)$$

and $C(z)$ will be the sum of the diagrams which does not contain Q_3 , then it reduces to the case of the walk returning to the origin. Summing over those diagrams is quite difficult, since every lattice point on the graphs can be considered as the starting point (same as the end point). Fortunately, this term always vanish for $\ell \neq 0$. Suppose we are interested in calculating the total number of walks which returns to origin, $U_n(u)$, then the generating function $F(z,w)$ reduces to $C(z)$. Now, it is not necessary to calculate the exact form of $C(z)$, since the

asymptotic behavior of $U_n(u)$ is most interesting and the singularities of the generating function $C(z)$ plays an important role in calculating those coefficients $U_n(u)$. From eq. (V.22), we may obtain $C(z)$ has the approximate form of

$$C(z) \sim \frac{C'}{(1-z^2 u - 3z^4 u^6 + z^6 u^7)^2} \quad (\text{V.31})$$

Substituting the values of G_1 , ϕ , ψ , δ , and δ' into eq. (V.28), we have

$$\begin{aligned} \mathcal{L} &= \frac{1+Q_2}{1-Q_2-3Q_4+Q_2Q_4} \\ &= \frac{1+z^2 u}{1-z^2 u - 3z^4 u^6 + z^6 u^7} \end{aligned} \quad (\text{V.32})$$

and $\phi(z, w)$ has the form of

$$\begin{aligned} \phi &= \frac{Q_3(1+Q_2)^2}{(1-2Q_3)(1-Q_2-3Q_4+Q_2Q_4)^2} + C(z) \\ &= \frac{wz^3 u^3 (1+z^2 u)^2}{(1-2wz^3 u^3)(1-z^2 u - 3z^4 u^6 + z^6 u^7)^2} + \frac{C'}{(1-z^2 u - 3z^4 u^6 + z^6 u^7)^2} \end{aligned} \quad (\text{V.33})$$

Setting $Q_4 \rightarrow 0$, above equation reduces to eq. (2.41), i.e.,

$$\phi = \frac{Q_3(1+Q_2)^2}{(1-2Q_3)(1-Q_2)^2} + \frac{Q_2}{(1-Q_2)^2} \quad (\text{V.34})$$

which agrees to our previous calculation.

The complete generating function $F(z, w)$ can be written as the

sum of $F_1(z, w)$ (eq. (V.26) and $\phi(z, w)$ (eq. (V.33)), namely,

$$\begin{aligned}
 F(z, w) &= F_1(z, w) + \phi(z, w) \\
 &= \frac{\left[1-wz^3u^3(1-z^2u)-2z^4u^6(1-2wz^3u^3) \right]^2}{(1-2wz^3u^3)(1-z^2u-3z^4u^6+z^6u^7)^2} \frac{zw}{1-zw-2wz^3u^3+w^2z^4u^3} \\
 &+ \frac{wz^3u^3(1+z^2u)^2}{(1-2wz^3u^3)(1-z^2u-3z^4u^6+z^6u^7)^2} \\
 &+ \frac{C'}{(1-z^2u-3z^4u^6+z^6u^7)^2} \tag{V.35}
 \end{aligned}$$

The un-normalized probability distribution $Z_n(\ell, u)$ may be obtained in the same way, such that

$$Z_n(\ell, u) = \frac{1}{2\pi i} \oint_C \frac{dz}{z^{n+1}} \frac{1}{2\pi i} \oint_C \frac{dw}{w^{\ell+1}} F(z, w) \tag{2.11}$$

The poles of $F(z, w)$ in the complex w -plane are the same as that in the Sec. II. D. which are

$$w_1 = \frac{1}{2z^3u^3} \tag{2.54}$$

$$\text{and } w_{\pm} = \frac{\xi \pm \eta}{2z^3u^3} \tag{2.55}$$

where $\xi = 1 + 2z^2u^3$

$$\eta = (1 + 4z^4u^6)^{1/2} \tag{2.56}$$

In order to calculate this integral, we may deform the contour C to C' , which includes all the singularities of $F(z,w)$ except at $w = 0$. The residue at $w = w_1$ vanishes, since that of $F_1(z,w)$ and $\Phi(z,w)$ have the same magnitude but different in sign.

Then

$$z_n^{(\ell, u)} = -\frac{1}{2\pi i} \oint_C \frac{dz}{z^{n+1}} \frac{\left[1 - \frac{1}{2}(\xi+n)(1-z^2u) - 2z^4u^6(1-\xi-n) \right]^2}{(1-\xi-n)_n(1-z^2u-3z^4u^6+z^6u^7)^2 w_+^\ell} \\ + \frac{1}{2\pi i} \oint_C \frac{dz}{z^{n+1}} \frac{\left[1 - \frac{1}{2}(\xi-n)(1-z^2u) - 2z^4u^6(1-\xi-n) \right]^2}{(1-\xi+n)_n(1-z^2u-3z^4u^6+z^6u^7)^2 w_-^\ell} \quad (V.36)$$

which almost has the same form as eq. (2.57), except the pole of the integrand is shifted from

$$z_p^2 = 1/u \text{ to } z_p^2 = (1+2u^4)/u \quad (V.37)$$

and the integral may be carried out in the same way by the method of complex integration.

Appendix VI. Punching Through Analytical Continuation

Consider a model integral has the form of

$$I(a) = \frac{1}{2\pi i} \int_{-i\infty}^{i\infty} e^{z^2} \frac{dz}{z-a} \quad (\text{VI.1})$$

The path of the integration is along the imaginal axis, and the pole at $z = a$ lies on the real axis. Suppose $a > 0$, we determine the analytical continuation value of this integral as $a \rightarrow 0^+$ (Fig. 51). Substitute $z \rightarrow iy$, and $y = x a$, the integral reduces to

$$\begin{aligned} I(a) &= \frac{1}{2\pi i} \int_{-\infty}^{\infty} e^{-y^2} \frac{dy}{y+ia} = -\frac{a}{2\pi} \int_{-\infty}^{\infty} \frac{dy}{y^2+a^2} e^{-y^2} \\ &= -\frac{1}{2} \operatorname{sgn}(a) \int_{-\infty}^{\infty} \frac{dx e^{-a^2 x^2}}{x^2+1} \end{aligned} \quad (\text{VI.2})$$

where the function $\operatorname{sgn}(a)$ is defined as

$$\operatorname{sgn}(a) = \begin{cases} 1 & \text{for } a > 0 \\ -1 & \text{for } a < 0 \end{cases} \quad (\text{VI.3})$$

In the case of $a^2 \ll 1$, eq. (VI.2) has a simple form

$$I(a) \approx -\frac{1}{2\pi} \operatorname{sgn}(a) \int_{-\infty}^{\infty} \frac{dx}{x^2+1} = -\frac{1}{2} \operatorname{sgn}(a) = -\frac{1}{2} \quad \text{for } a > 0 \quad (\text{VI.4})$$

Now, if $a < 0$, we determine the analytical continuation value of

this integral as $a \rightarrow 0^-$. In this case, the contour of integration may be distorted in order to pass around the singularity on the negative axis (Fig. 48). The result can be obtained by the same way, except it contains an additional term due to the residue at the pole $z = a$, i.e.,

$$I(a) \approx -\frac{1}{2} \operatorname{sgn}(a) - e^{a^2} \quad (\text{VI.5})$$

$$\approx -\frac{1}{2} \quad \text{for } a < 0 \quad (\text{VI.6})$$

The integral is an analytical continuation function crossing the pole, $z = a$, such that

$$\lim_{a \rightarrow 0^+} I(a) = \lim_{a \rightarrow 0^-} I(a) \quad (\text{VI.7})$$

Now, we may combine both cases together, as $a \rightarrow 0$, namely,

$$I(a) = -\frac{1}{2} \operatorname{sgn}(a) - e^{a^2} \theta(-a) \quad (\text{VI.8})$$

where

$$\theta(-a) = \begin{cases} 1 & a < 0 \\ 0 & a > 0 \end{cases} \quad (\text{VI.9})$$

Next consider another model integral which has the form of

$$J(a) = \frac{1}{2\pi i} \int_{-i\infty}^{i\infty} \frac{e^{z^2} dz}{(z-a)^2} \quad (\text{VI.10})$$

which can be written as

$$J(a) = \frac{\partial}{\partial a} \left[\frac{1}{2\pi i} \int_{-i\infty}^{i\infty} -\frac{e^z}{z-a} dz \right] = \frac{\partial I(a)}{\partial a} \quad (\text{VI.11})$$

By substituting the value of the integral $I(a)$ in eq. (VI.8), we may obtain

$$J(a) = -\frac{1}{2} \frac{\partial}{\partial a} \operatorname{sgn}(a) - e^{a^2} \frac{\partial}{\partial a} \theta(-a) - \frac{\partial}{\partial a} e^{a^2} \quad (\text{VI.12})$$

$$= -\frac{\partial}{\partial a} (\text{Residue of the integrand of } I(a) \text{ at } z=a)$$

$$(\text{VI.13})$$

since the first two terms in eq. (VI.12) cancel each other.

Now, we consider our probability distribution function which has the form of

$$z_n^{(2)}(\ell, u) = \frac{1}{2\pi i} \oint_C dz e^{F(z)} \frac{(\xi-\eta)(\xi+\eta-1)}{uz\eta(z-1/u)} \quad (\text{VI.14})$$

where $F(z)$, ξ and η have been defined before. Suppose $F(z)$ has a minimum at $z = z_s$ at the real axis, such that $F(z_s) = 0$.

Then the contour C may be deformed to C' in order to pass the saddle point z_s . Because the saddle point z_s is a function of ℓ and u , which may lie either inside or outside the pole $z_p = 1/u$ depending on the value of ℓ ; if $\ell > \bar{\ell}$, $z_p > z_s$, the result of the integral is equal to

$$z_n^{(2)}(\ell, u) \simeq e^{F(z_s)} \frac{M(z_s, u)}{(2\pi F''(z_s))^{1/2}} \frac{1}{z_s - \frac{1}{u}} \quad (\text{VI.15})$$

where

$$M(z_s, u) = \left[\frac{(\xi - n)(\xi + n - 1)}{uz^n} \right] \quad \text{evaluated at } z_s \quad (\text{VI.16})$$

if $\ell < \bar{\ell}$, $z_p < z_s$, the results of the integral yields two terms; one is due to integrating through the saddle point, the other is due to the residue at the pole, namely,

$$z_n^{(2)}(\ell, u) \approx e^{F(z_s)} \frac{M(z_s, u)}{(2 F''(z_s))^{1/2}} - e^{F(z_p)} M(z_p, u) \quad (\text{VI.17})$$

Suppose $\ell \rightarrow \bar{\ell}$, $z_n^{(2)}(\ell, u)$ will diverge which is not expected. We would predict that $z_n^{(2)}(\ell, u)$ should be a smooth function of ℓ , by applying the same trick as the model integral and introducing a new variable

$$a = z_p - z_s \quad (\text{VI.18})$$

Fix the saddle point z_s and let the pole z_p vary along the real axis. We will obtain the analytical continuation value of $z_n^{(2)}(\ell, u)$ as $a \rightarrow 0$, $z_p \rightarrow z_s$, such that,

$$z_n^{(2)}(\ell, u) = - \frac{e^{F(z_s)}}{2} M(z_s, u) \operatorname{sgn}(a) - e^{F(z_p)} M(z_p, u) \theta(-a) \quad (\text{VI.19})$$

At $a \rightarrow 0$, it reduces to

$$z_n^{(2)}(\ell, u) = - \frac{1}{2} e^{F(z_p)} M(z_p, u) \quad (\text{VI.20})$$

Similarly, we may consider the integral as follows:

$$z_n^{(3)}(\ell, u) = \frac{1}{2\pi i} \oint_C dz e^{F(z)} \frac{\xi+\eta-1}{u^2 z^n (z-\frac{1}{u})^2} \quad (\text{VI.21})$$

It can be done in the same way and rewrite this integral into

$$z_n^{(3)}(\ell, u) = \frac{\partial}{\partial z_p} \left[\frac{1}{2\pi i} \oint_C dz e^{F(z)} \frac{\xi+\eta-1}{u^2 z^n (z-\frac{1}{u})^2} \right] \quad (\text{VI.22})$$

While the pole is closing the saddle point, $a \rightarrow 0$, the analytical continuation value of this integral has the form of

$$z_n^{(3)}(\ell, u) = \frac{e^{F(z_p)}}{n} \left[n + (\xi-1) \frac{4u^4}{n} \right] \quad (\text{VI.23})$$

Now, we may conclude that the integral in eq. (2.59) can be written as the sum of

$$z_n(\ell, u) = z_n^{(1)}(\ell, u) + z_n^{(2)}(\ell, u) + z_n^{(3)}(\ell, u) \quad (\text{VI.24})$$

as $z_p \rightarrow z_s$, $a \rightarrow 0$, where

$$z_n^{(1)}(\ell, u) \simeq \frac{e^{F(z_s)}}{(2\pi F''(z_s))^{1/2}} \frac{(\xi-\eta)^2 (\xi+\eta-1)}{4z_s^n} \quad (\text{VI.25})$$

is a smooth function of ℓ and $z_n^{(2)}(\ell, u)$, $z_n^{(3)}(\ell, u)$ are defined in eqs. (VI.20) and (VI.25).

TABLE I.

$$c_1 = 2z_1(1)$$

$$z_1(1) = 1$$

$$c_2 = z_2(0) + 2z_2(2)$$

$$z_2(0) = 2u$$

$$z_2(2) = 1$$

$$c_3 = 2z_3(1) + 2z_3(3)$$

$$z_3(1) = 2u + u^3$$

$$z_3(3) = 1$$

$$c_4 = z_4(0) + 2z_4(2) + 2z_4(4)$$

$$z_4(0) = 4u^2 + 2u^6$$

$$z_4(2) = 2u + 2u^3$$

$$z_4(4) = 1$$

$$c_5 = 2z_5(1) + 2z_5(3) + 2z_5(5)$$

$$z_5(1) = 3u^3 + 4u^4 + 2u^6 + u^{10}$$

$$z_5(3) = 2u + 3u^3$$

$$z_5(5) = 1$$

$$c_6 = z_6(0) + 2z_6(2) + 2z_6(4) + 2z_6(6)$$

$$z_6(0) = 6u^3 + 12u^7 + 2u^{15}$$

$$z_6(2) = 3u^2 + 6u^4 + 4u^6 + 2u^{10}$$

$$z_6(4) = 2u + 4u^3$$

$$z_6(6) = 1$$

$$\begin{aligned}
c_7 &= 2z_7(1) + 2z_7(3) + 2z_7(5) + 2z_7(7) \\
z_7(1) &= 4 u^3 + 8 u^5 + 8 u^7 + 6 u^9 + 6 u^{11} + 2 u^{15} + u^{21} \\
z_7(3) &= 3 u^2 + 8 u^4 + 7 u^6 + 3 u^{10} \\
z_7(5) &= 5 u^3 + 2 u \\
z_7(7) &= 1
\end{aligned}$$

$$\begin{aligned}
c_8 &= z_8(0) + 2z_8(2) + 2z_8(4) + 2z_8(6) + 2z_8(8) \\
z_8(0) &= 8 u^4 + 32 u^8 + 12 u^{12} + 16 u^{16} + 2 u^{28} \\
z_8(2) &= 4 u^3 + 10 u^5 + 16 u^7 + 8 u^9 + 8 u^{11} + 6 u^{13} + 2 u^{15} \\
&\quad + 2 u^{21} \\
z_8(4) &= 3 u^2 + 10 u^4 + 11 u^6 + 4 u^{10} \\
z_8(6) &= 2 u + 6 u^3 \\
z_8(8) &= 1
\end{aligned}$$

$$\begin{aligned}
c_9 &= 2z_9(1) + 2z_9(3) + 2z_9(5) + 2z_9(7) + 2z_9(9) \\
z_9(1) &= 5 u^4 + 12 u^6 + 18 u^8 + 28 u^{10} + 22 u^{12} + 22 u^{16} \\
&\quad 8 u^{18} + 8 u^{22} + 2 u^{28} + u^{36} \\
z_9(3) &= 4 u^3 + 13 u^5 + 24 u^7 + 14 u^9 + 10 u^{11} + 14 u^{13} \\
&\quad + 2 u^{15} + 3 u^{21} \\
z_9(5) &= 3 u^2 + 12 u^4 + 16 u^6 + 5 u^{10} \\
z_9(7) &= 2 u + 7 u^3 \\
z_9(9) &= 1
\end{aligned}$$

$$\begin{aligned}
c_{10} &= z_{10}(0) + 2z_{10}(2) + 2z_{10}(4) + 2z_{10}(6) + 2z_{10}(8) + 2z_{10}(10) \\
z_{10}(0) &= 10 u^5 + 60 u^9 + 70 u^{13} + 50 u^{17} + 40 u^{21} + 20 u^{29} \\
&\quad + 2 u^{45} \\
z_{10}(2) &= 5 u^4 + 14 u^6 + 34 u^8 + 32 u^{10} + 33 u^{12} + 30 u^{14}
\end{aligned}$$

$$+ 24 u^{16} + 10 u^{18} + 6 u^{20} + 10 u^{22} + 8 u^{24} + 2 u^{28} \\ + 2 u^{36}$$

$$z_{10}(4) = 4 u^3 + 16 u^5 + 34 u^7 + 24 u^9 + 12 u^{11} + 24 u^{13} \\ + 2 u^{15} + 4 u^{21}$$

$$z_{10}(6) = 3 u^2 + 14 u^4 + 22 u^6 + 6 u^{10}$$

$$z_{10}(8) = 2 u + 8 u^3$$

$$z_{10}(10) = 1$$

$$c_{11} = 2z_{11}(1) + 2z_{11}(3) + 2z_{11}(5) + 2z_{11}(7) + 2z_{11}(9) + 2z_{11}(11)$$

$$z_{11}(1) = 6 u^5 + 16 u^7 + 32 u^9 + 68 u^{11} + 58 u^{13} + 27 u^{15} \\ + 90 u^{17} + 44 u^{19} + 22 u^{21} + 24 u^{23} + 20 u^{25} \\ + 20 u^{27} + 12 u^{29} + 10 u^{31} + 10 u^{37} + 2 u^{45} \\ + u^{55}$$

$$z_{11}(3) = 5 u^4 + 18 u^6 + 46 u^8 + 56 u^{10} + 46 u^{12} + 52 u^{14} \\ + 47 u^{16} + 12 u^{18} + 13 u^{20} + 12 u^{22} + 18 u^{24} \\ + 2 u^{28} + 3 u^{36}$$

$$z_{11}(5) = 4 u^3 + 19 u^5 + 46 u^7 + 39 u^9 + 14 u^{11} + 36 u^{13} \\ + 2 u^{15} + 5 u^{21}$$

$$z_{11}(7) = 3 u^2 + 16 u^4 + 29 u^6 + 7 u^{10}$$

$$z_{11}(9) = 2 u + 9 u^3$$

$$z_{11}(11) = 1$$

$$c_{12} = z_{12}(0) + 2z_{12}(2) + 2z_{12}(4) + 2z_{12}(6) + 2z_{12}(8) + 2z_{12}(10) \\ + 2z_{12}(12)$$

$$z_{12}(0) = 12 u^6 + 96 u^{10} + 204 u^{14} + 150 u^{18} + 264 u^{22} + 112 u^{30} \\ + 60 u^{24} + 24 u^{46} + 2 u^{66}$$

$$\begin{aligned}
z_{12}(2) &= 6 u^5 + 18 u^7 + 56 u^9 + 72 u^{11} + 110 u^{13} + 96 u^{15} \\
&\quad + 78 u^{17} + 102 u^{19} + 74 u^{21} + 18 u^{23} + 70 u^{25} \\
&\quad + 22 u^{27} + 12 u^{29} + 32 u^{31} + 12 u^{37} + 10 u^{39} \\
&\quad + 2 u^{45} + 2 u^{55} \\
z_{12}(4) &= 5 u^4 + 22 u^6 + 62 u^8 + 88 u^{10} + 69 u^{12} + 78 u^{14} \\
&\quad + 86 u^{16} + 14 u^{18} + 21 u^{20} + 14 u^{22} + 30 u^{24} \\
&\quad + 2 u^{28} + 4 u^{36} \\
z_{12}(6) &= 4 u^3 + 22 u^5 + 60 u^7 + 60 u^9 + 10 u^{11} + 50 u^{13} \\
&\quad + 2 u^{15} + 6 u^{21} \\
z_{12}(8) &= 3 u^2 + 18 u^4 + 37 u^6 + 8 u^{10} \\
z_{12}(10) &= 2 u + 10 u^3 \\
z_{12}(12) &= 1
\end{aligned}$$

$$\begin{aligned}
c_{13} &= 2z_{13}(1) + 2z_{13}(3) + 2z_{13}(5) + 2z_{13}(7) + 2z_{13}(9) + 2z_{13}(11) \\
&\quad + 2z_{13}(13) \\
z_{13}(1) &= 7 u^6 + 20 u^8 + 50 u^{10} + 124 u^{12} + 126 u^{14} + 144 u^{16} \\
&\quad + 236 u^{18} + 112 u^{20} + 184 u^{22} + 136 u^{24} + 126 u^{26} \\
&\quad + 128 u^{28} + 51 u^{30} + 64 u^{32} + 32 u^{34} + 40 u^{36} \\
&\quad + 65 u^{38} + 30 u^{42} + 14 u^{46} + 12 u^{48} \\
&\quad + 12 u^{56} + 2 u^{66} + u^{78} \\
z_{13}(3) &= 6 u^5 + 23 u^7 + 72 u^9 + 122 u^{11} + 150 u^{13} + 155 u^{15} \\
&\quad + 182 u^{17} + 142 u^{19} + 104 u^{21} + 66 u^{23} + 100 u^{25} \\
&\quad + 56 u^{27} + 12 u^{29} + 56 u^{31} + 14 u^{37} + 22 u^{39} \\
&\quad + 2 u^{45} + 3 u^{55} \\
z_{13}(5) &= 5 u^4 + 26 u^6 + 81 u^8 + 132 u^{10} + 106 u^{12} + 108 u^{14} \\
&\quad + 144 u^{16} + 16 u^{18} + 30 u^{20} + 16 u^{22} + 44 u^{24} \\
&\quad + 2 u^{28} + 5 u^{36}
\end{aligned}$$

$$z_{13}(7) = 4 u^3 + 25 u^5 + 76 u^7 + 88 u^9 + 18 u^{11} + 66 u^{15} \\ + 2 u^{15} + 7 u^{21}$$

$$z_{13}(9) = 3 u^2 + 20 u^4 + 46 u^6 + 9 u^{10}$$

$$z_{13}(11) = 2 u + 11 u^3$$

$$z_{13}(13) = 1$$

$$c_{14} = z_{14}(0) + 2z_{14}(2) + 2z_{14}(4) + 2z_{14}(6) + 2z_{14}(8) + 2z_{14}(10) \\ + 2z_{14}(12) + 2z_{14}(14)$$

$$z_{14}(0) = 14 u^7 + 140 u^{11} + 434 u^{15} + 490 u^{19} + 784 u^{23} \\ + 336 u^{27} + 434 u^{31} + 448 u^{35} + 140 u^{43} + 98 u^{47} \\ + 84 u^{51} + 28 u^{67} + 2u^{91}$$

$$z_{14}(2) = 7 u^6 + 22 u^8 + 82 u^{10} + 128 u^{12} + 255 u^{14} + 248 u^{16} \\ 240 u^{18} + 374 u^{20} + 344 u^{22} + 132 u^{24} + 284 u^{26} \\ + 166 u^{28} + 155 u^{30} + 208 u^{32} + 52 u^{34} + 42 u^{36} \\ + 54 u^{38} + 70 u^{40} + 52 u^{42} + 44 u^{46} + 14 u^{48} \\ + 14 u^{56} + 12 u^{58} + 2 u^{66} + 2 u^{78}$$

$$z_{14}(4) = 6 u^5 + 28 u^7 + 94 u^9 + 180 u^{11} + 234 u^{13} + 236 u^{15} \\ + 306 u^{17} + 246 u^{19} + 138 u^{21} + 138 u^{23} + 134 u^{25} \\ + 110 u^{27} + 12 u^{29} + 82 u^{31} + 61 u^{37} + 36 u^{39} \\ + 2 u^{45} + 4 u^{55}$$

$$z_{14}(6) = 5 u^4 + 30 u^6 + 103 u^8 + 190 u^{10} + 163 u^{12} \\ + 142 u^{14} + 224 u^{16} + 18 u^{18} + 40 u^{20} + 18 u^{22} \\ + 60 u^{24} + 2 u^{28} + 6 u^{36}$$

$$z_{14}(8) = 4 u^3 + 28 u^5 + 94 u^7 + 124 u^9 + 20 u^{11} + 84 u^{13} \\ + 2 u^{15} + 8 u^{21}$$

$$z_{14}(10) = 3 u^2 + 22 u^4 + 56 u^6 + 10 u^{10}$$

$$z_{14}(12) = 2 u + 12 u^3$$

$$z_{14}(14) = 1$$

$$c_{15} = 2z_{15}(1) + 2z_{15}(3) + 2z_{15}(5) + 2z_{15}(7) + 2z_{15}(9) + 2z_{15}(11)$$

$$+ 2z_{15}(13) + 2z_{15}(15)$$

$$\begin{aligned} z_{15}(1) = & 8 u^7 + 24 u^9 + 72 u^{11} + 196 u^{13} + 238 u^{15} + 408 u^{17} \\ & + 512 u^{19} + 312 u^{21} + 708 u^{23} + 592 u^{25} + 476 u^{27} \\ & + 336 u^{29} + 458 u^{31} + 424 u^{33} + 168 u^{35} + 448 u^{37} \\ & + 276 u^{39} + 292 u^{43} + 36 u^{47} + 158 u^{49} + 114 u^{51} \\ & + 42 u^{55} + 2 u^{59} + u^{105} \end{aligned}$$

$$\begin{aligned} z_{15}(3) = & 7 u^6 + 28 u^8 + 102 u^{10} + 208 u^{12} + 336 u^{14} \\ & + 428 u^{16} + 495 u^{18} + 480 u^{20} + 574 u^{22} + 424 u^{24} \\ & + 346 u^{26} + 374 u^{28} + 233 u^{30} + 274 u^{32} + 230 u^{34} \\ & + 44 u^{36} + 59 u^{38} + 104 u^{40} + 120 u^{42} + 76 u^{46} \\ & + 16 u^{48} + 16 u^{56} + 26 u^{58} + 2 u^{66} + 3 u^{78} \end{aligned}$$

$$\begin{aligned} z_{15}(5) = & 6 u^5 + 33 u^7 + 120 u^9 + 258 u^{11} + 358 u^{13} + 353 u^{15} \\ & + 476 u^{17} + 428 u^{19} + 176 u^{21} + 237 u^{23} + 172 u^{25} \\ & + 187 u^{27} + 12 u^{29} + 110 u^{31} + 18 u^{37} + 52 u^{39} \\ & + 2 u^{45} + 5 u^{55} \end{aligned}$$

$$\begin{aligned} z_{15}(7) = & 5 u^4 + 34 u^6 + 128 u^8 + 264 u^{10} + 247 u^{12} + 180 u^{14} \\ & + 329 u^{16} + 20 u^{18} + 51 u^{20} + 20 u^{22} + 78 u^{24} \\ & + 2 u^{28} + 7 u^{36} \end{aligned}$$

$$\begin{aligned} z_{15}(9) = & 4 u^3 + 31 u^5 + 114 u^7 + 169 u^9 + 22 u^{11} + 104 u^{13} \\ & 2 u^{15} + 9 u^{21} \end{aligned}$$

$$z_{15}(11) = 3 u^2 + 24 u^4 + 67 u^6 + 11 u^{10}$$

$$z_{15}(13) = 2 u + 13 u^3$$

$$z_{15}(15) = 1$$

TABLE II

$$u_2 = 2u$$

$$u_4 = 4 u^2 + 2 u^6$$

$$u_6 = 6 u^3 + 12 u^7 + 2 u^{15}$$

$$u_8 = 8 u^4 + 32 u^8 + 12 u^{12} + 16 u^{16} + 2 u^{28}$$

$$u_{10} = 10 u^5 + 60 u^9 + 70 u^{13} + 50 u^{17} + 40 u^{21} + 20 u^{29} + 2 u^{45}$$

$$\begin{aligned} u_{12} = & 12 u^6 + 96 u^{10} + 204 u^{14} + 150 u^{18} + 264 u^{22} + 112 u^{30} \\ & + 60 u^{34} + 24 u^{46} + 2 u^{66} \end{aligned}$$

$$\begin{aligned} u_{14} = & 14 u^7 + 140 u^{11} + 434 u^{15} + 784 u^{23} + 490 u^{19} + 336 u^{27} \\ & + 434 u^{31} + 448 u^{35} + 140 u^{43} + 98 u^{47} + 84 u^{51} + 28 u^{67} \\ & + 2 u^{91} \end{aligned}$$

$$\begin{aligned} u_{16} = & 16 u^8 + 192 u^{12} + 784 u^{16} + 1312 u^{20} + 1848 u^{24} + 2144 u^{28} \\ & + 1136 u^{32} + 2112 u^{36} + 640 u^{40} + 1152 u^{44} + 192 u^{48} \\ & + 704 u^{52} + 140 u^{56} + 224 u^{60} + 128 u^{68} + 112 u^{72} + 32 u^{92} \\ & + 2 u^{120} \end{aligned}$$

$$\begin{aligned} u_{18} = & 18 u^9 + 252 u^{13} + 1278 u^{17} + 2898 u^{21} + 4338 u^{25} \\ & + 6822 u^{29} + 4104 u^{33} + 7920 u^{37} + 4068 u^{41} + 4308 u^{45} \\ & + 3546 u^{49} + 2124 u^{53} + 2412 u^{57} + 2052 u^{61} + 252 u^{69} \\ & + 1548 u^{73} + 336 u^{81} + 162 u^{93} + 144 u^{97} + 36 u^{121} + 2 u^{153} \end{aligned}$$

$$\begin{aligned}
u_{20} = & 20 u^{10} + 320 u^{14} + 1940 u^{18} + 5600 u^{22} + 9820 u^{26} \\
& + 16570 u^{30} + 16640 u^{34} + 21040 u^{38} + 19800 u^{42} + 15580 u^{46} \\
& + 22840 u^{50} + 4240 u^{54} + 15460 u^{58} + 10550 u^{62} + 6360 u^{66} \\
& + 400 u^{70} + 8240 u^{74} + 1890 u^{78} + 3400 u^{82} + 504 u^{90} + 1160 u^{94} \\
& + 1480 u^{98} + 480 u^{106} + 200 u^{122} + 180 u^{126} + 40 u^{154} \\
& + 2 u^{190}
\end{aligned}$$

TABLE III

v	$\mu(u)$	v	$\mu(u)$
0.00	2.0000	1.05	1.0369
0.05	1.7237	1.10	1.0322
0.10	1.5637	1.15	1.0281
0.15	1.4577	1.20	1.0245
0.20	1.3812	1.25	1.0214
0.25	1.3228	1.30	1.0186
0.30	1.2765	1.35	1.0161
0.35	1.2387	1.40	1.0140
0.40	1.2072	1.45	1.0122
0.45	1.1806	1.50	1.0106
0.50	1.1578	1.55	1.0091
0.55	1.1381	1.60	1.0079
0.60	1.1211	1.65	1.0068
0.65	1.1062	1.70	1.0059
0.70	1.0931	1.75	1.0051
0.75	1.0831	1.80	1.0044
0.80	1.0717	1.85	1.0038
0.85	1.0628	1.90	1.0033
0.90	1.0551	1.95	1.0028
0.95	1.0482	2.00	1.0024
1.00	1.0422	2.50	1.0006
		3.00	1.0001
		3.50	1.0000
		4.00	1.0000

TABLE IV

V	$\mu'(u)$
0.00	1.9980
0.05	1.6314
0.10	1.4374
0.15	1.3084
0.20	1.2077
0.25	1.1263
0.30	1.0605
0.35	1.0027
0.40	0.9523
0.45	0.9066
0.50	0.8687
0.55	0.8322
0.60	0.7991
0.65	0.7710
0.70	0.7434
0.75	0.7185
0.80	0.6956
0.85	0.6748
0.90	0.6553
0.95	0.6373
1.00	0.6178

TABLE V

$$\langle r_1^2 \rangle = 2/c_1 = 1$$

$$\langle r_2^2 \rangle = 8/c_2$$

$$\langle r_3^2 \rangle = 2/c_3 (9 + 2 u + u^3)$$

$$\langle r_4^2 \rangle = 2/c_4 (16 + 8 u + 8 u^3)$$

$$\langle r_5^2 \rangle = 2/c_5 (25 + 18 u + 3 u^2 + 27 u^3 + 4 u^4 + 2 u^6 + u^{10})$$

$$\langle r_6^2 \rangle = 2/c_6 (36 + 32 u + 12 u^2 + 64 u^3 + 24 u^4 + 16 u^6 + 8 u^{10})$$

$$\begin{aligned} \langle r_7^2 \rangle = 2/c_7 (49 + 50 u + 27 u^2 + 129 u^3 + 72 u^4 + 8 u^5 + 63 u^6 \\ + 8 u^7 + 6 u^9 + 27 u^{10} + 6 u^{11} + 2 u^{15} + u^{21}) \end{aligned}$$

$$\begin{aligned} \langle r_8^2 \rangle = 2/c_8 (64 + 72 u + 48 u^2 + 232 u^3 + 160 u^4 + 40 u^5 \\ + 176 u^6 + 64 u^7 + 32 u^9 + 64 u^{10} + 32 u^{11} \\ + 24 u^{13} + 8 u^{15} + 8 u^{21}) \end{aligned}$$

$$\begin{aligned} \langle r_9^2 \rangle = 2/c_9 (81 + 98 u + 75 u^2 + 379 u^3 + 305 u^4 + 117 u^5 \\ + 412 u^6 + 216 u^7 + 18 u^8 + 126 u^9 + 153 u^{10} \\ + 90 u^{11} + 22 u^{12} + 126 u^{13} + 18 u^{15} + 22 u^{16} \\ + 8 u^{18} + 27 u^{21} + 8 u^{22} + .2 u^{28} + u^{36}) \end{aligned}$$

$$\langle r_{10}^2 \rangle = 2/c_{10} (100 + 128 u + 108 u^2 + 576 u^3 + 524 u^4 + 256 u^5 + 848 u^6 + 544 u^7 + 136 u^8 + 384 u^9 + 344 u^{10} + 192 u^{11} + 132 u^{12} + 384 u^{13} + 120 u^{14} + 32 u^{15} + 96 u^{16} + 40 u^{18} + 24 u^{20} + 64 u^{21} + 40 u^{22} + 32 u^{24} + 8 u^{28} + 8 u^{36})$$

$$\langle r_{11}^2 \rangle = 2/c_{11} (121 + 162 u + 147 u^2 + 829 u^3 + 829 u^4 + 481 u^5 + 1583 u^6 + 1166 u^7 + 414 u^8 + 1007 u^9 + 847 u^{10} + 418 u^{11} + 414 u^{12} + 958 u^{13} + 468 u^{14} + 77 u^{15} + 423 u^{16} + 108 u^{17} + 24 u^{18} + 44 u^{19} + 117 u^{20} + 147 u^{21} + 108 u^{22} + 24 u^{23} + 162 u^{24} + 20 u^{25} + 20 u^{27} + 18 u^{28} + 12 u^{29} + 10 u^{31} + 27 u^{36} + 10 u^{37} + 2 u^{45} + u^{55})$$

$$\langle r_{12}^2 \rangle = 2/c_{12} (144 + 200 u + 192 u^2 + 1144 u^3 + 1232 u^4 + 816 u^5 + 2720 u^6 + 2232 u^7 + 992 u^8 + 2384 u^9 + 1920 u^{10} + 864 u^{11} + 1104 u^{12} + 2240 u^{13} + 1248 u^{14} + 456 u^{15} + 1376 u^{16} + 312 u^{17} + 224 u^{18} + 408 u^{19} + 336 u^{20} + 512 u^{21} + 224 u^{22} + 72 u^{23} + 480 u^{24} + 280 u^{25} + 88 u^{27} + 32 u^{28} + 48 u^{29} + 128 u^{31} + 64 u^{36} + 48 u^{37} + 40 u^{39} + 8 u^{45} + 8 u^{55})$$

$$\begin{aligned}
\langle r_{13}^2 \rangle = 2/c_{13} & (169 + 242 u + 243 u^2 + 1527 u^3 + 1745 u^4 + 1279 u^5 \\
& + 4383 u^6 + 3931 u^7 + 2045 u^8 + 4960 u^9 \\
& + 4079 u^{10} + 1980 u^{11} + 2774 u^{12} + 4584 u^{13} \\
& + 2826 u^{14} + 1493 u^{15} + 3744 u^{16} + 1638 u^{17} \\
& + 636 u^{18} + 1278 u^{19} + 862 u^{20} + 1279 u^{21} \\
& + 584 u^{22} + 594 u^{23} + 1236 u^{24} + 900 u^{25} + 126 u^{26} \\
& + 504 u^{27} + 178 u^{28} + 108 u^{29} + 51 u^{30} + 504 u^{31} \\
& + 64 u^{32} + 32 u^{34} + 165 u^{36} + 126 u^{37} + 65 u^{38} \\
& + 198 u^{39} + 30 u^{42} + 18 u^{45} + 14 u^{46} + 12 u^{48} \\
& + 27 u^{55} + 12 u^{56} + 2 u^{66} + u^{78})
\end{aligned}$$

$$\begin{aligned}
\langle r_{14}^2 \rangle = 2/c_{14} & (196 + 288 u + 300 u^2 + 1984 u^3 + 2380 u^4 + 1888 u^5 \\
& + 6708 u^6 + 6464 u^7 + 3796 u^8 + 9440 u^9 \\
& + 8168 u^{10} + 4160 u^{11} + 6380 u^{12} + 9120 u^{13} \\
& + 6132 u^{14} + 3904 u^{15} + 9056 u^{16} + 4896 u^{17} \\
& + 1608 u^{18} + 3936 u^{19} + 2936 u^{20} + 2720 u^{21} \\
& + 2024 u^{22} + 2208 u^{23} + 2688 u^{24} + 2144 u^{25} \\
& + 1136 u^{26} + 1760 u^{27} + 736 u^{28} + 192 u^{29} \\
& + 620 u^{30} + 1312 u^{31} + 832 u^{32} + 208 u^{34} + 384 u^{36} \\
& + 256 u^{37} + 216 u^{38} + 576 u^{39} + 280 u^{40} + 208 u^{42} \\
& + 32 u^{45} + 176 u^{46} + 56 u^{48} + 64 u^{55} + 56 u^{56} \\
& + 48 u^{58} + 8 u^{66} + 8 u^{78})
\end{aligned}$$

$$\begin{aligned}
\langle r_{15}^2 \rangle = & \frac{2}{c_{15}} (225 + 338 u + 363 u^2 + 2521 u^3 + 3149 u^4 + 2661 u^5 \\
& + 9836 u^6 + 10067 u^7 + 6524 u^8 + 16713 u^9 \\
& + 15185 u^{10} + 8304 u^{11} + 13975 u^{12} + 17570 u^{13} \\
& + 11844 u^{14} + 9225 u^{15} + 19973 u^{16} + 12308 u^{17} \\
& + 5435 u^{18} + 11212 u^{19} + 6819 u^{20} + 5441 u^{21} \\
& + 6146 u^{22} + 6633 u^{23} + 7638 u^{24} + 4892 u^{25} \\
& + 3114 u^{26} + 5151 u^{27} + 3464 u^{28} + 636 u^{29} \\
& + 2097 u^{30} + 3208 u^{31} + 2466 u^{32} + 424 u^{33} \\
& + 2070 u^{34} + 168 u^{35} + 739 u^{36} + 898 u^{37} \\
& + 531 u^{38} + 1576 u^{39} + 936 u^{40} + 1080 u^{42} \\
& + 292 u^{43} + 50 u^{45} + 684 u^{46} + 36 u^{47} + 144 u^{48} \\
& + 158 u^{49} + 114 u^{51} + 167 u^{55} + 144 u^{56} + 48 u^{57} \\
& + 234 u^{58} + 42 u^{61} + 18 u^{66} + 16 u^{67} + 14 u^{69} \\
& + 27 u^{78} + 14 u^{79} + 2 u^{91} + u^{105})
\end{aligned}$$

TABLE VI

$$\langle r_2^2 \rangle = 0$$

$$\langle r_4^2 \rangle = 1/u_4(u^2)$$

$$\langle r_6^2 \rangle = 1/u_6(12 u^3 + 8 u^7)/3$$

$$\langle r_8^2 \rangle = 1/u_8(10 u^4 + 19 u^8 + 3 u^{12} + 3 u^{16})$$

$$\begin{aligned} \langle r_{10}^2 \rangle = 1/u_{10}(100 u^5 + 344 u^9 + 208 u^{13} + 124 u^{17} + 48 u^{21} \\ + 16 u^{29})/5 \end{aligned}$$

$$\begin{aligned} \langle r_{12}^2 \rangle = 1/u_{12}(105 u^6 + 540 u^{10} + 677 u^{14} + 396 u^{18} + 422 u^{22} \\ + 120 u^{30} + 40 u^{34} + 10 u^{46})/3 \end{aligned}$$

$$\begin{aligned} \langle r_{14}^2 \rangle = 1/u_{14}(392 u^7 + 2720 u^{11} + 5484 u^{15} + 4508 u^{19} + 5432 u^{23} \\ + 1488 u^{27} + 1900 u^{31} + 1472 u^{35} + 240 u^{43} \\ + 244 u^{47} + 120 u^{51} + 24 u^{67})/7 \end{aligned}$$

$$\begin{aligned} \langle r_{16}^2 \rangle = 1/u_{16}(336 u^8 + 2954 u^{12} + 8416 u^{16} + 10126 u^{20} + 11816 u^{24} \\ + 9106 u^{28} + 4648 u^{32} + 6672 u^{36} + 1460 u^{40} \\ + 2160 u^{44} + 592 u^{48} + 1168 u^{52} + 140 u^{56} + 210 u^{60} \\ + 158 u^{68} + 84 u^{72} + 14 u^{92})/4 \end{aligned}$$

$$\langle r_{18}^2 \rangle = 1/u_{18} (1080 u^9 + 11536 u^{13} + 42988 u^{17} + 71704 u^{21} + 88944 u^{25} + 102692 u^{29} + 52704 u^{33} + 83856 u^{37} + 35264 u^{41} + 30792 u^{45} + 21060 u^{49} + 15032 u^{53} + 10368 u^{57} + 7944 u^{61} + 1560 u^{69} + 4592 u^{73} + 672 u^{81} + 396 u^{93} + 224 u^{97} + 32 u^{121})/9$$

$$\langle r_{20}^2 \rangle = 1/u_{20} (825 u^{10} + 10392 u^{14} + 48149 u^{18} + 105296 u^{22} + 150503 u^{26} + 203736 u^{30} + 159244 u^{34} + 181952 u^{38} + 139086 u^{42} + 93560 u^{46} + 109254 u^{50} + 28704 u^{54} + 60201 u^{58} + 35984 u^{62} + 17238 u^{66} + 2500 u^{70} + 22052 u^{74} + 4284 u^{78} + 6714 u^{82} + 630 u^{90} + 2000 u^{94} + 2458 u^{98} + 2016 u^{106} + 242 u^{122} + 144 u^{126} + 18 u^{154})/5$$

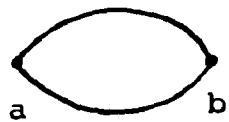


Figure 1. $U_2(u) = 2 u$

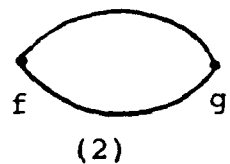
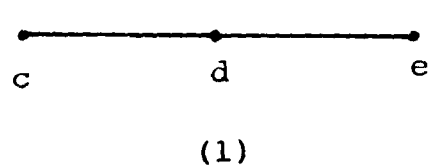
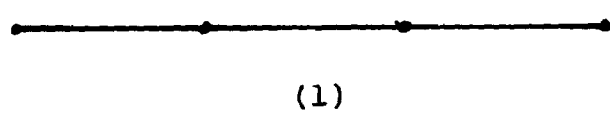


Figure 2. $U_4(u) = 4 u^2 + 2 u^6$



(1)



(2)



(3)

Figure 3. $U_6(u) = 6 u^3 + 12 u^7 + 2 u^{15}$

$$z_1(1) = 1$$

Figure 4. $c_1(u) = 2 z_1(1) = 2$

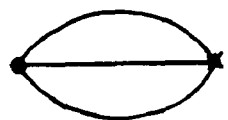
$$z_2(2) = 1$$

$$z_2(0) = 2 u$$

Figure 5. $c_2(u) = z_2(0) + 2 z_2(2) = 2 + 2 u$

$$z_3(3) = 1$$

$$z_3(1) = 2 u + u^3$$



(4)

Figure 6. $c_3(u) = 2 z_3(3) + 2 z_3(1) = 2 + 4 u + u^3$

Figure 7.

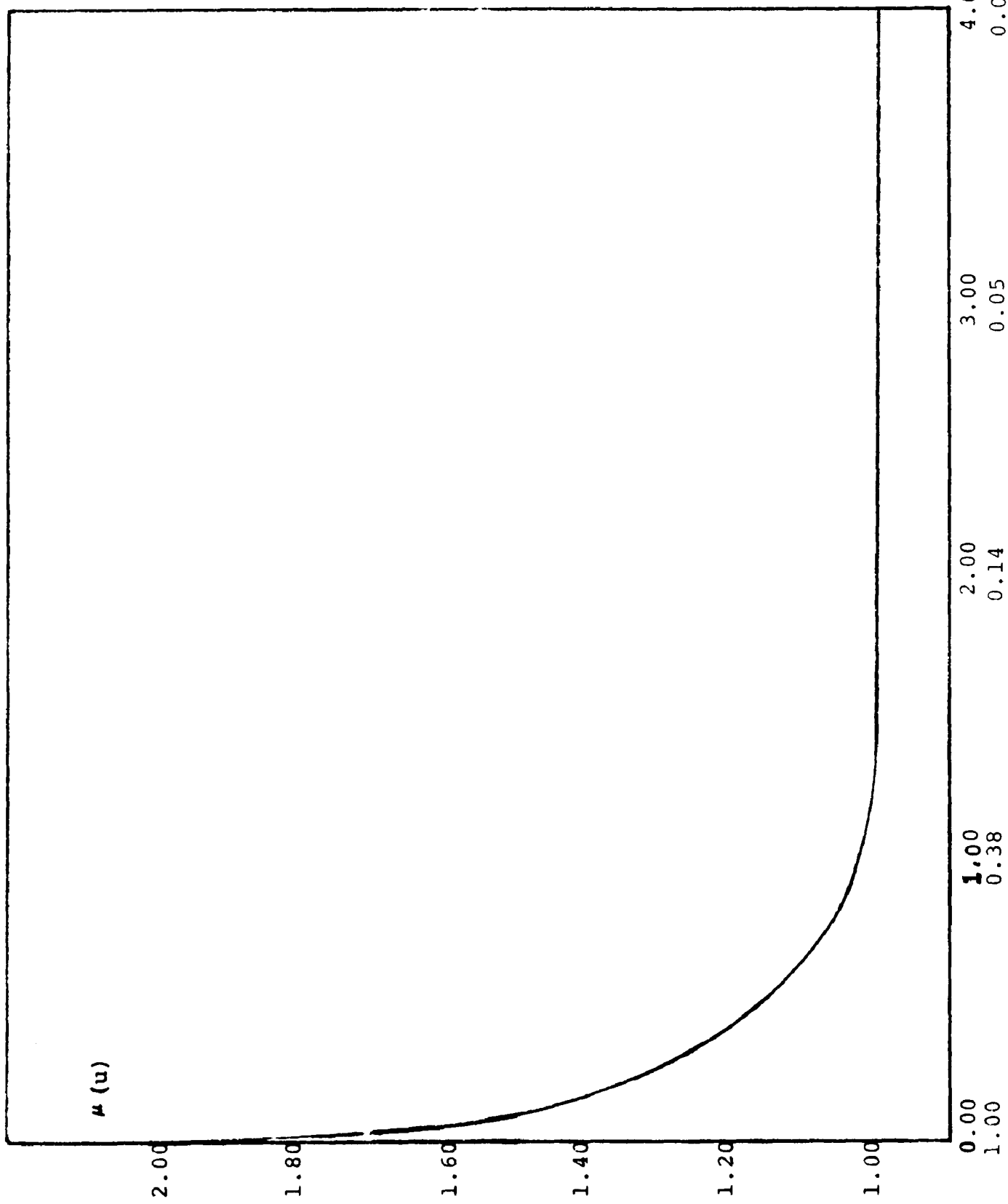


Figure 8

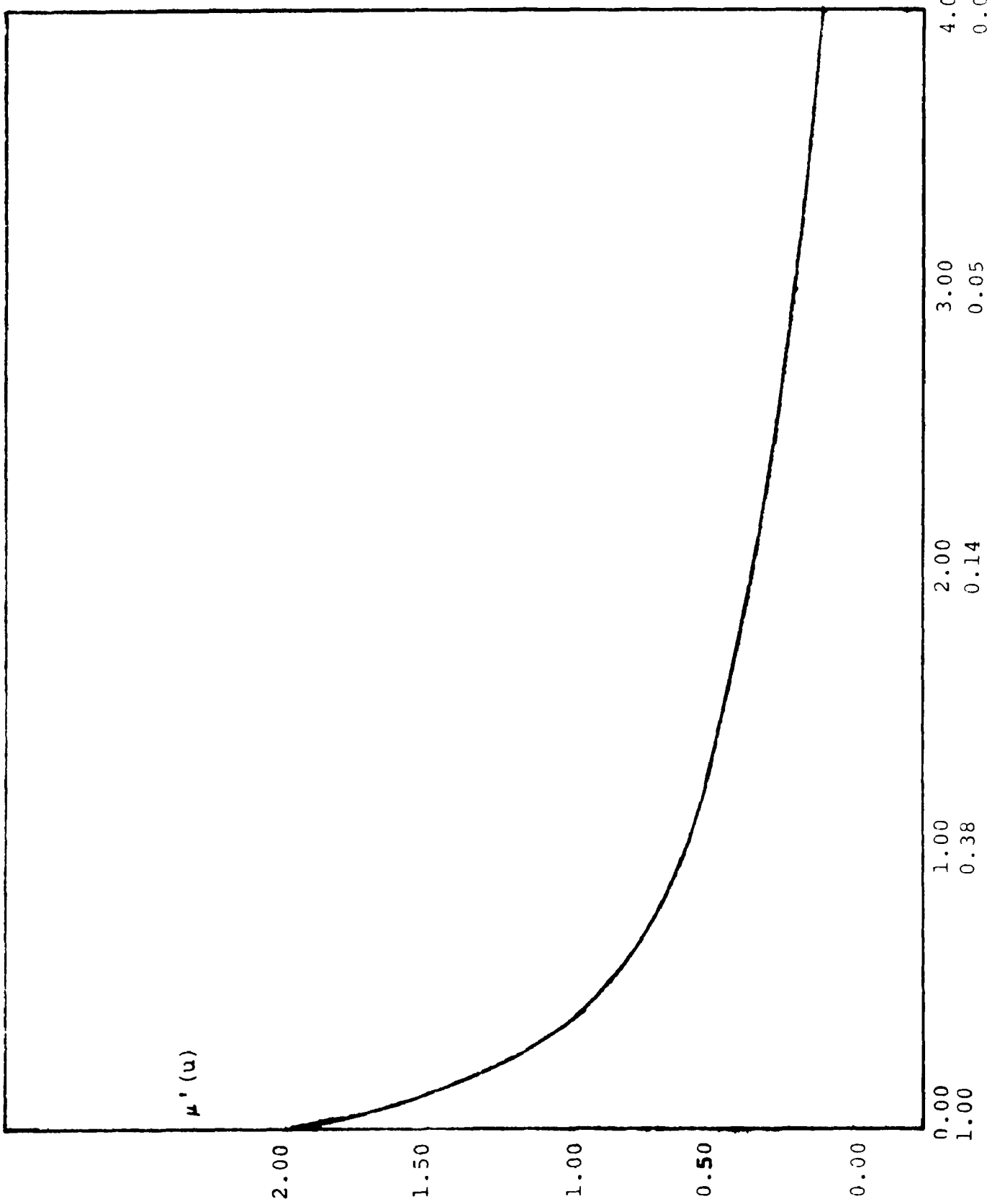
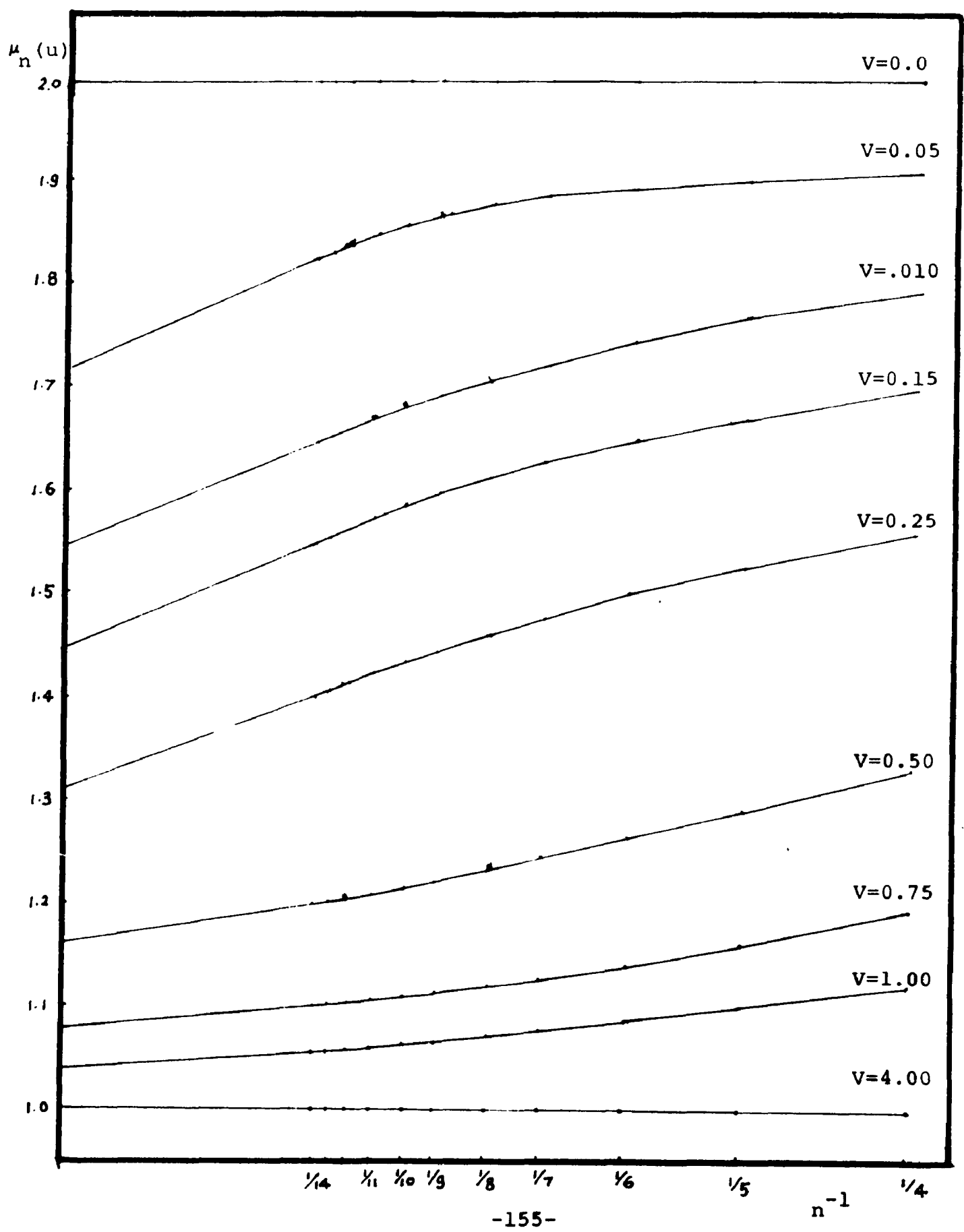


Figure 9



$\mu_n^2(u)$

Figure 10

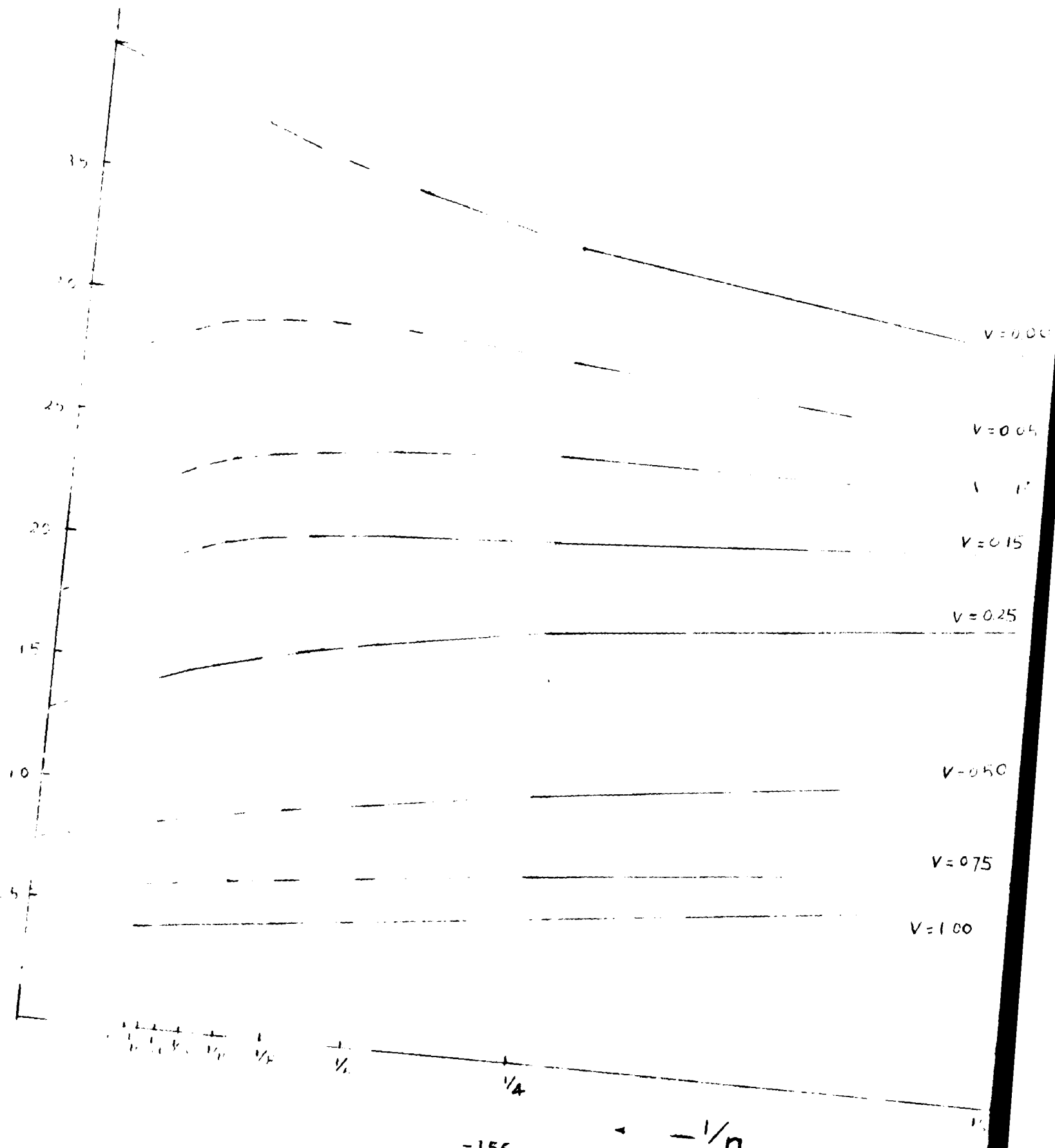


Figure 11

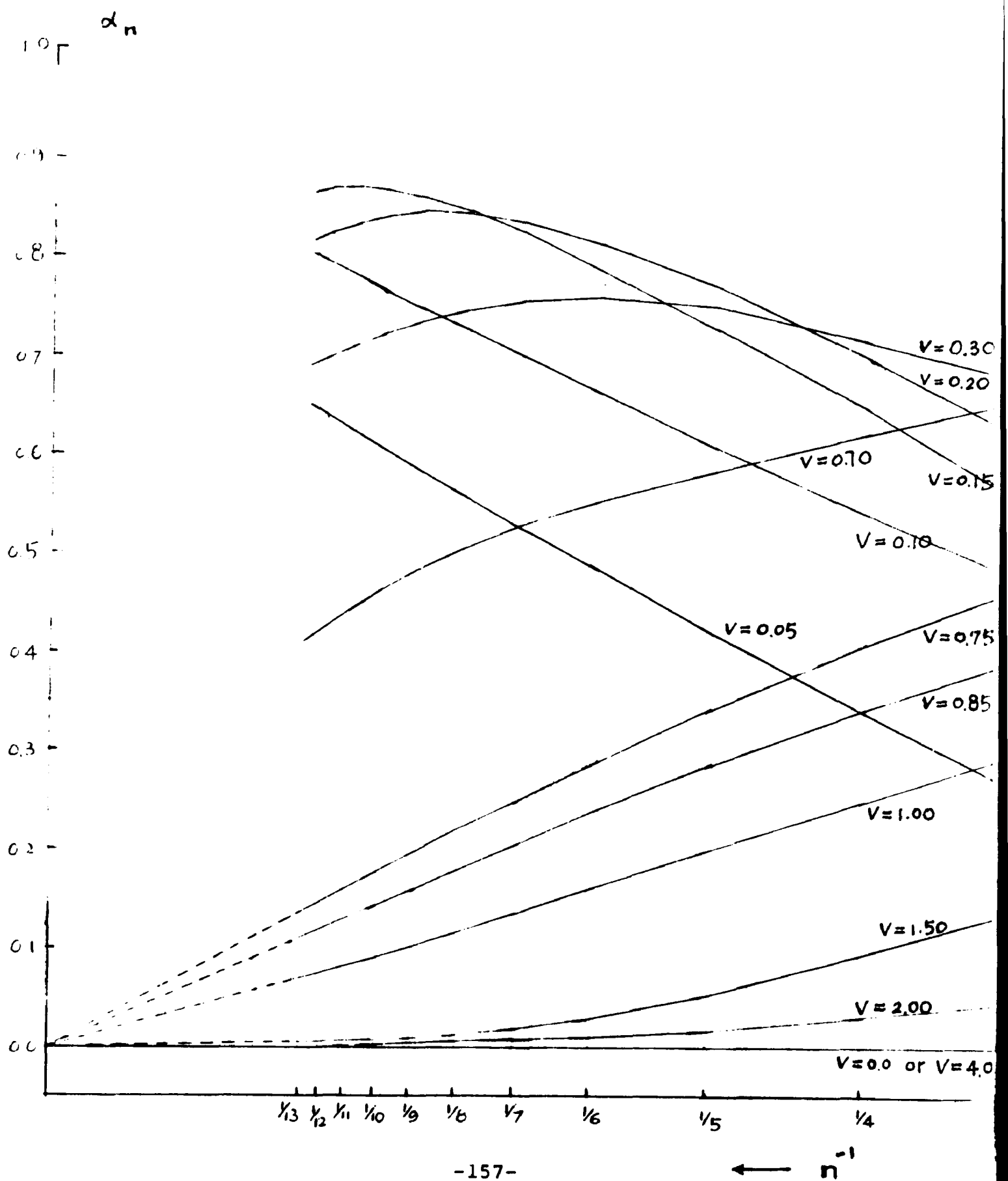


Figure 12

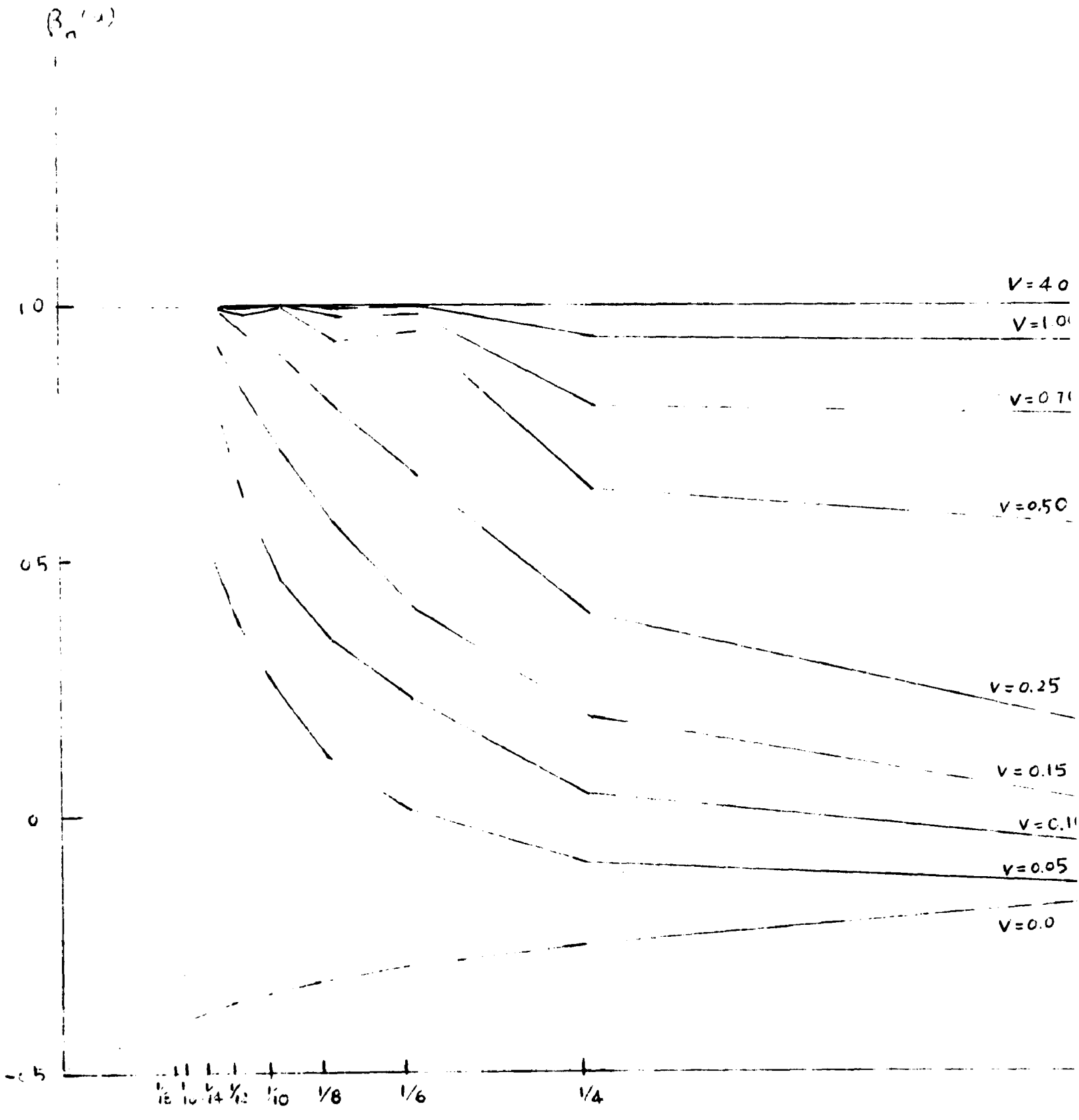


Figure 13

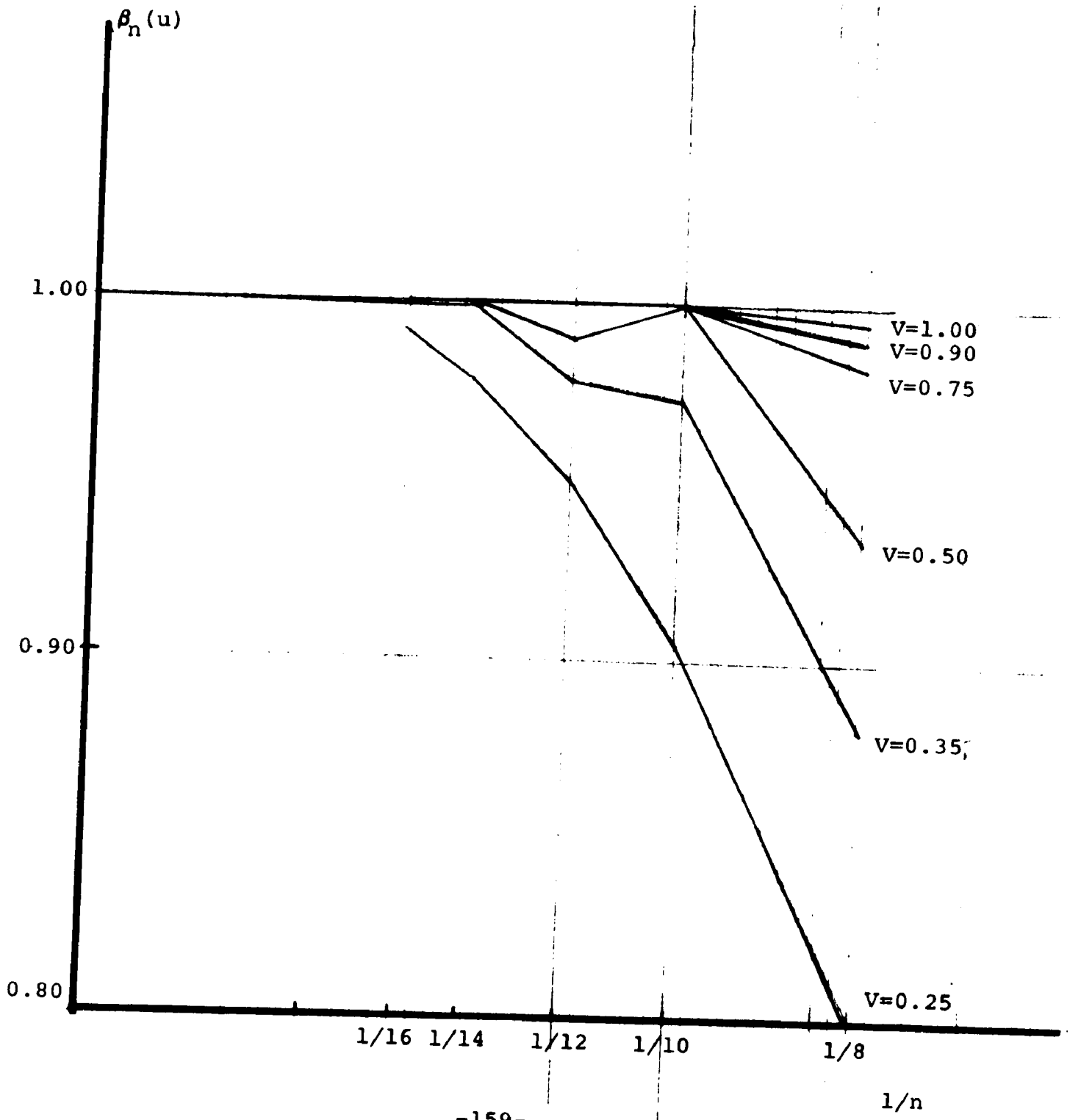
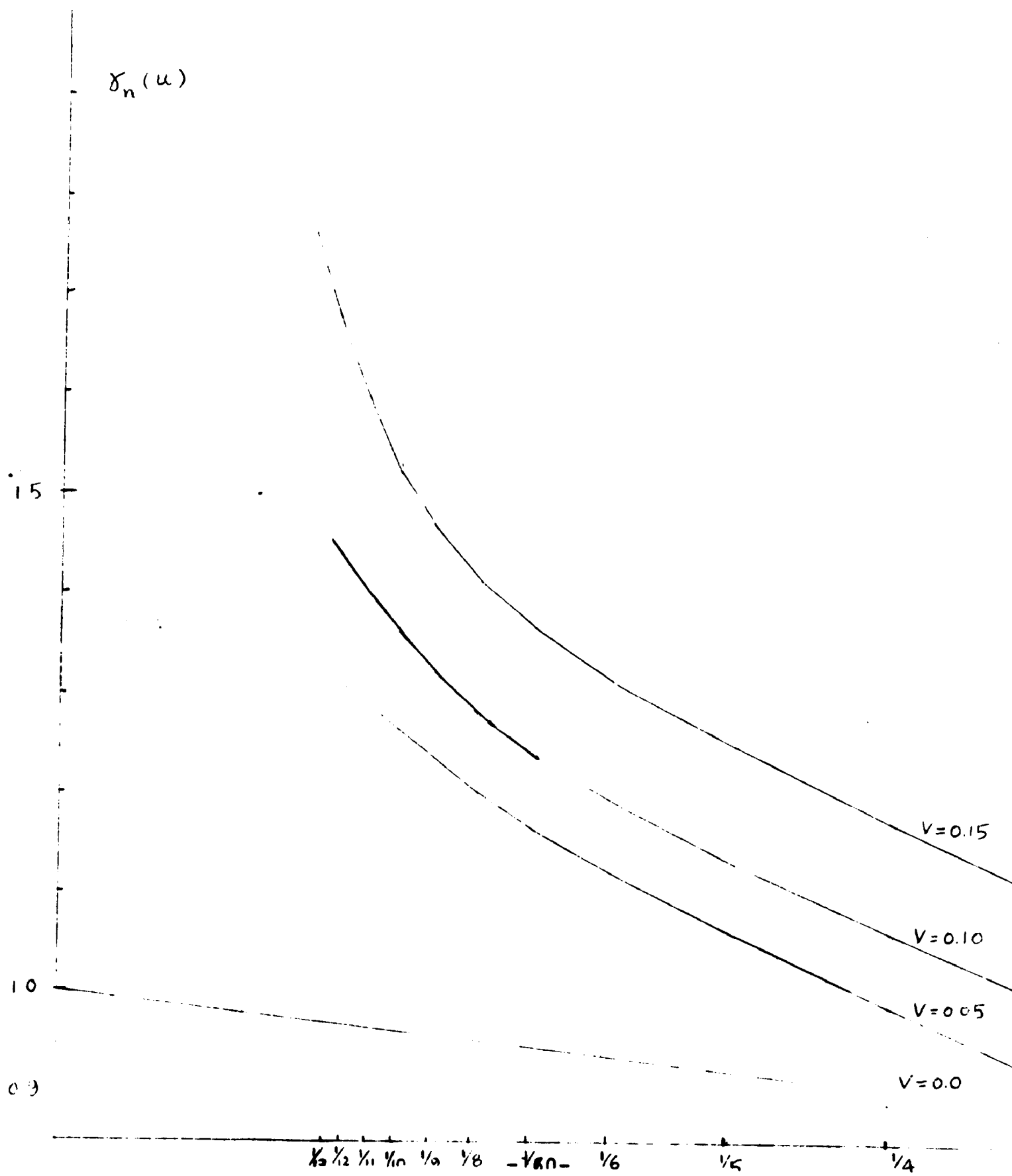


Figure 14



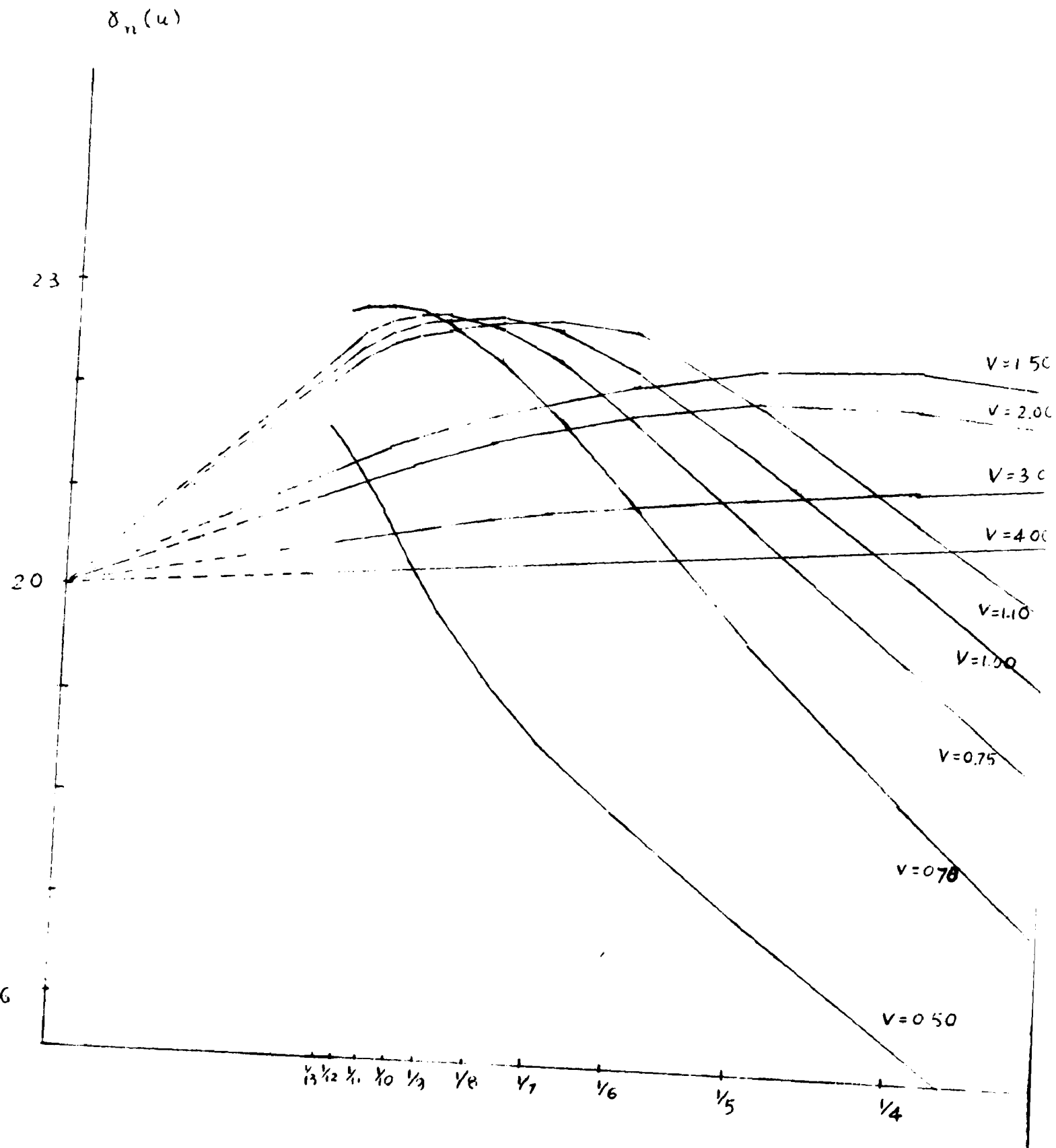


Figure 15

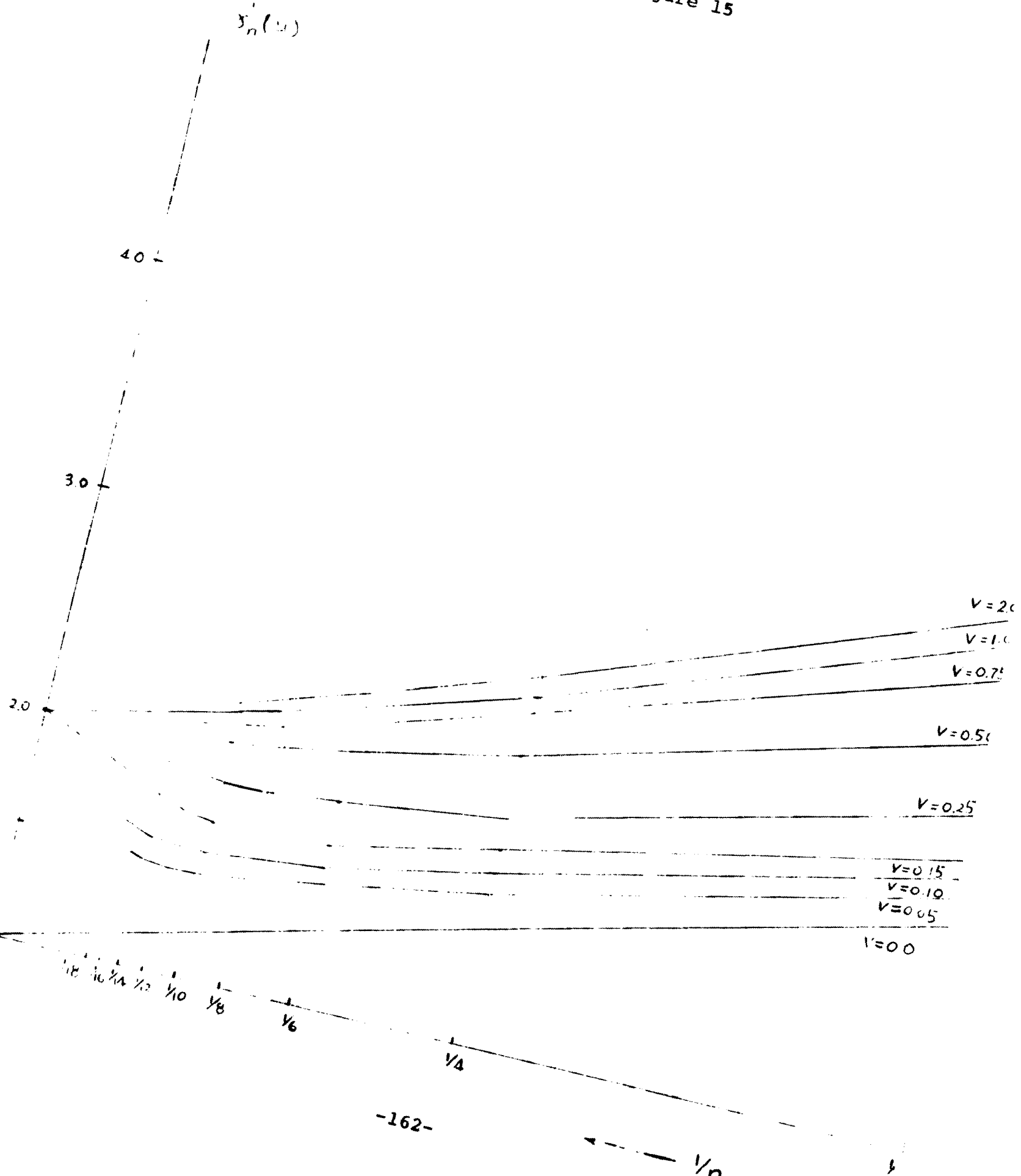
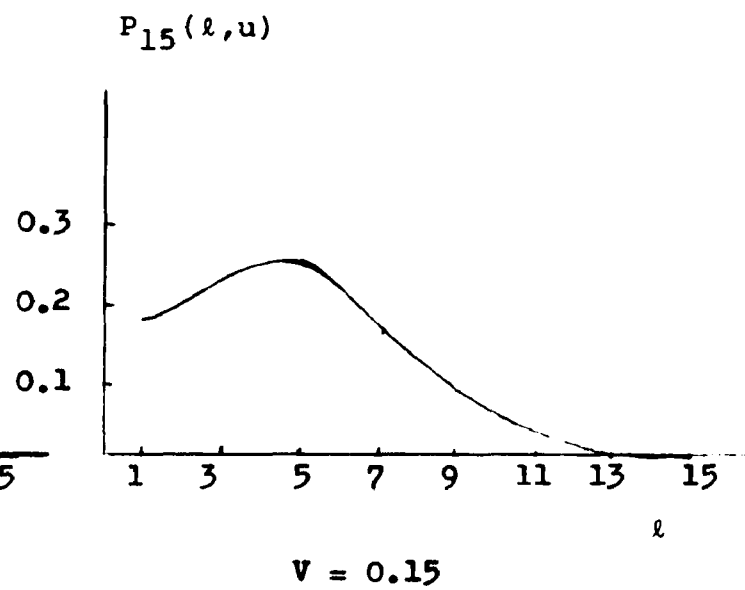
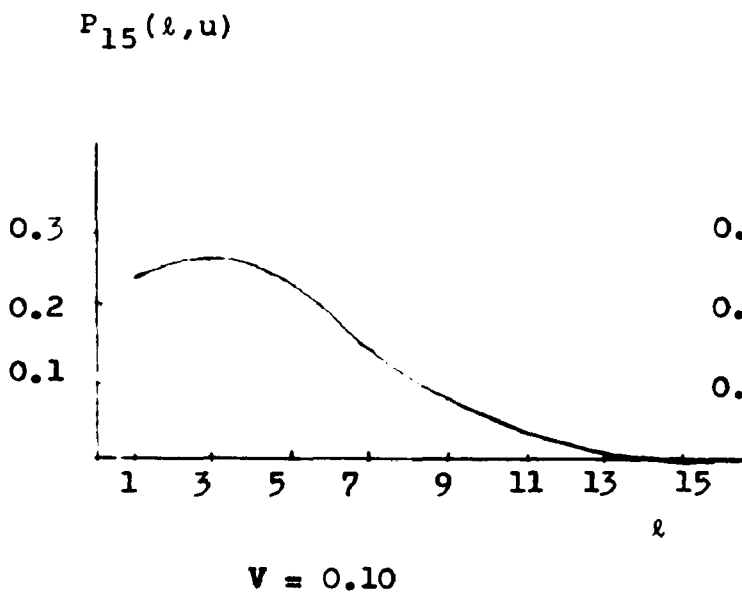
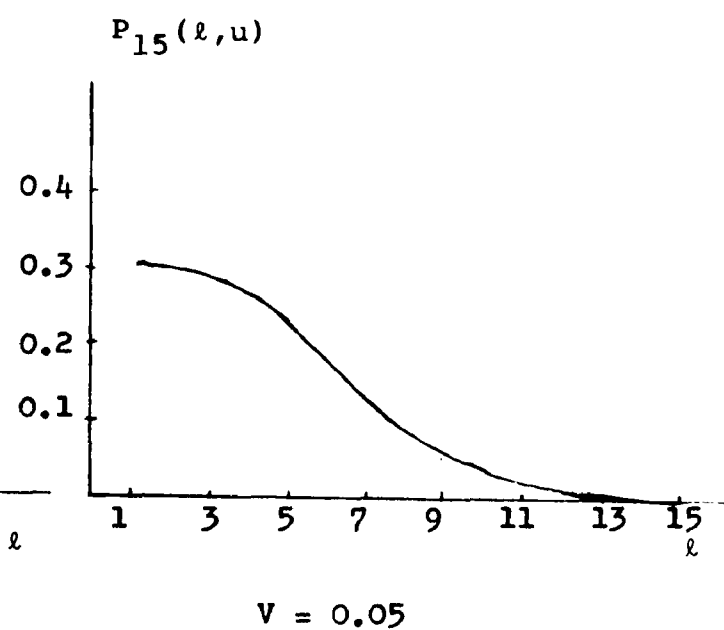
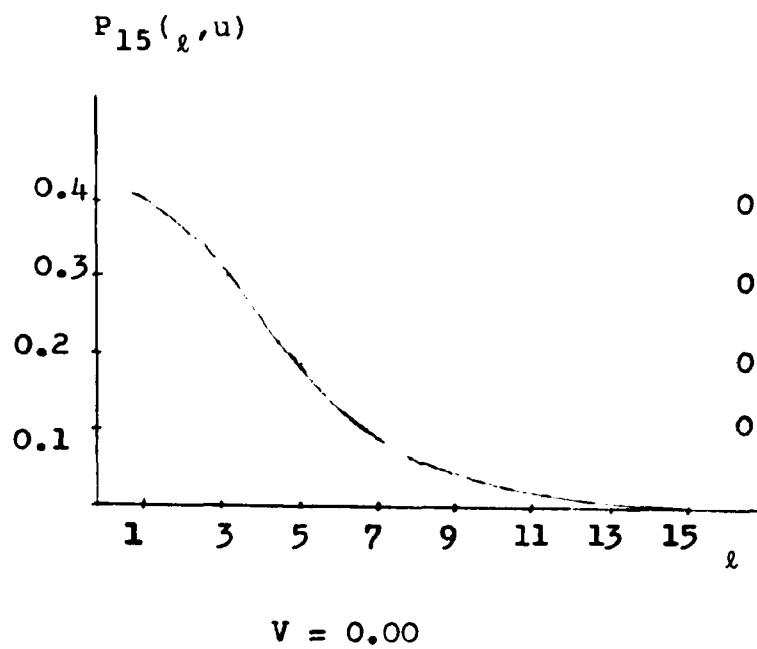
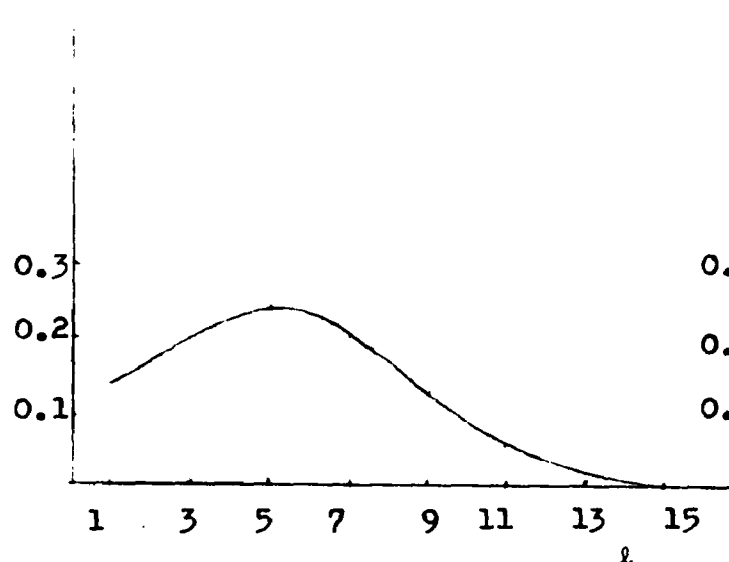


Figure 16

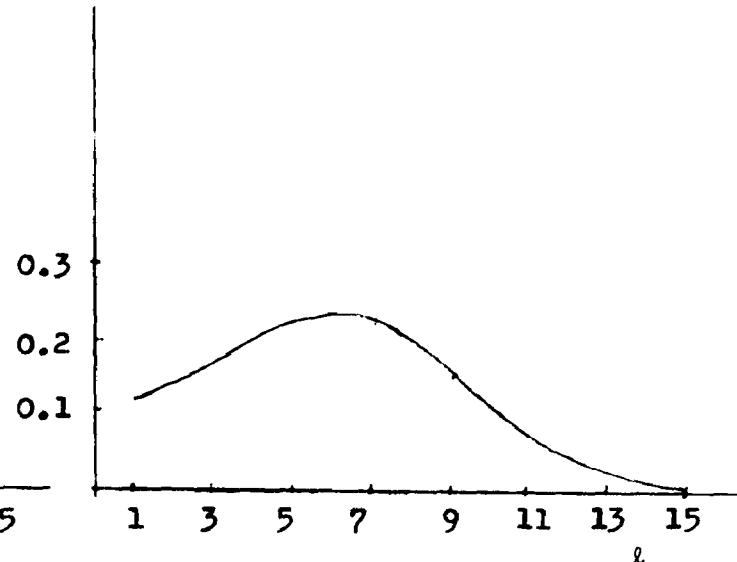


$P_{15}(\ell, u)$



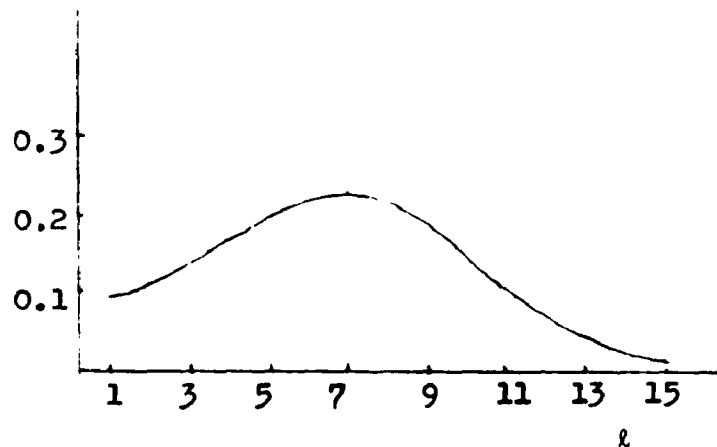
$v = 0.20$

$P_{15}(\ell, u)$



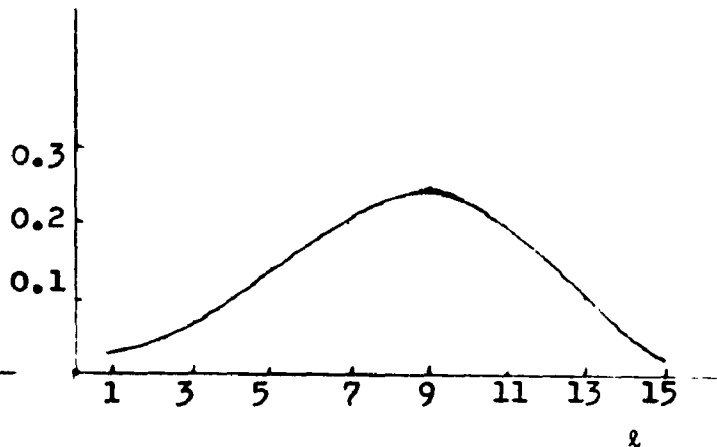
$v = 0.25$

$P_{15}(\ell, u)$



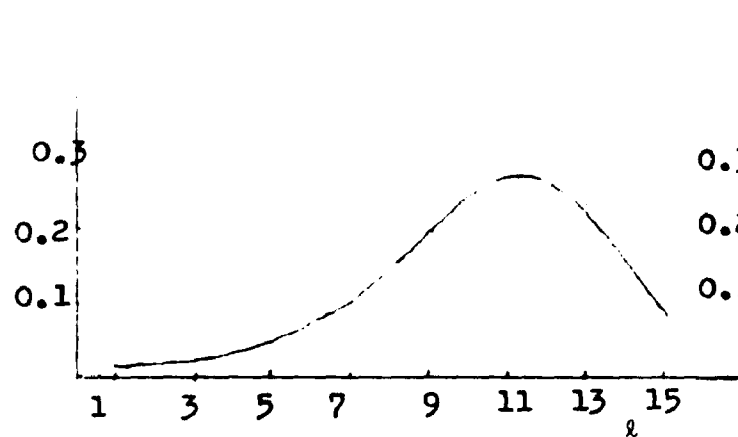
$v = 0.30$

$P_{15}(\ell, u)$

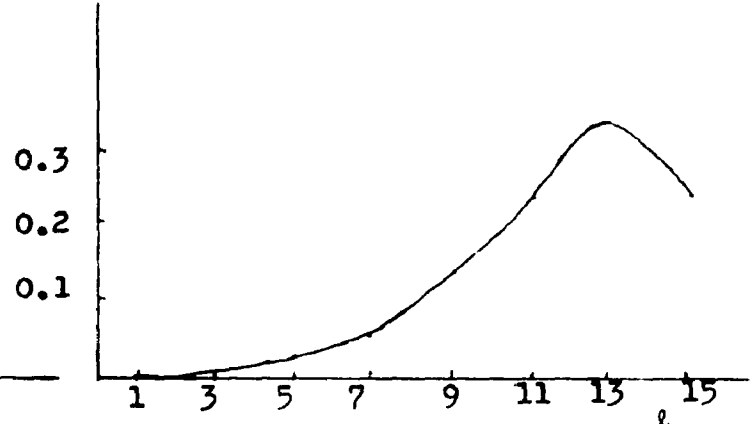


$v = 0.50$

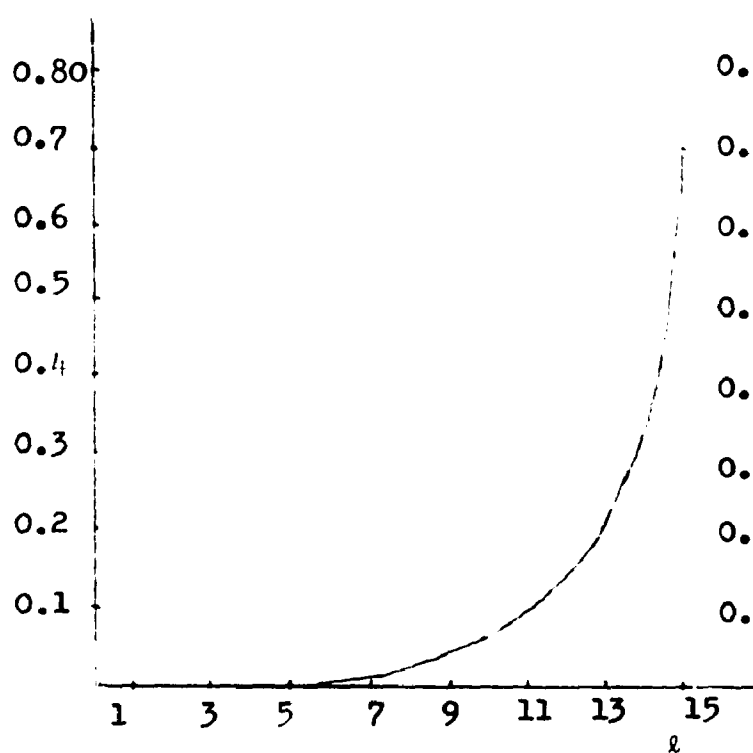
$P_{15}(\ell, u)$



$P_{15}(\ell, u)$

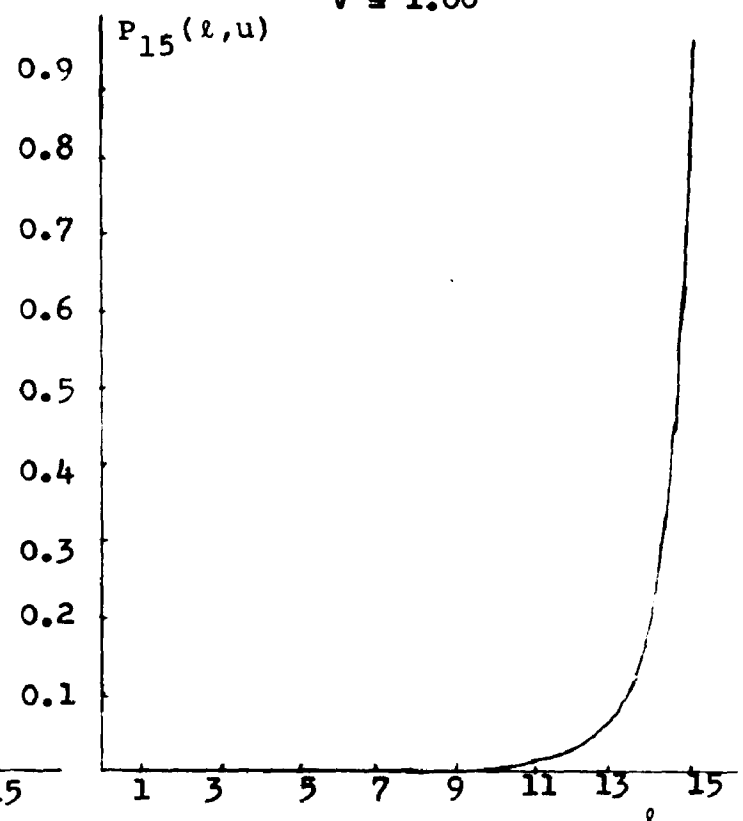


$P_{15}(\ell, u)$
 $v = 0.75$



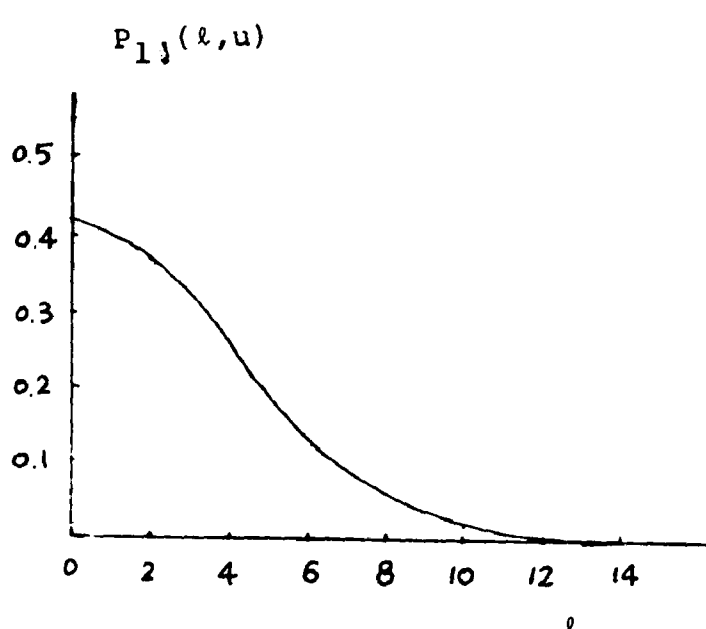
$v = 2.00$

$v = 1.00$

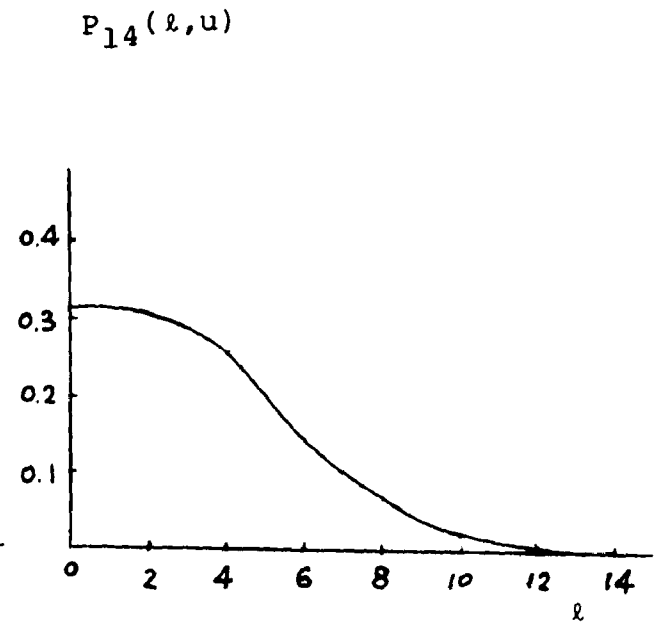


$v = 4.00$

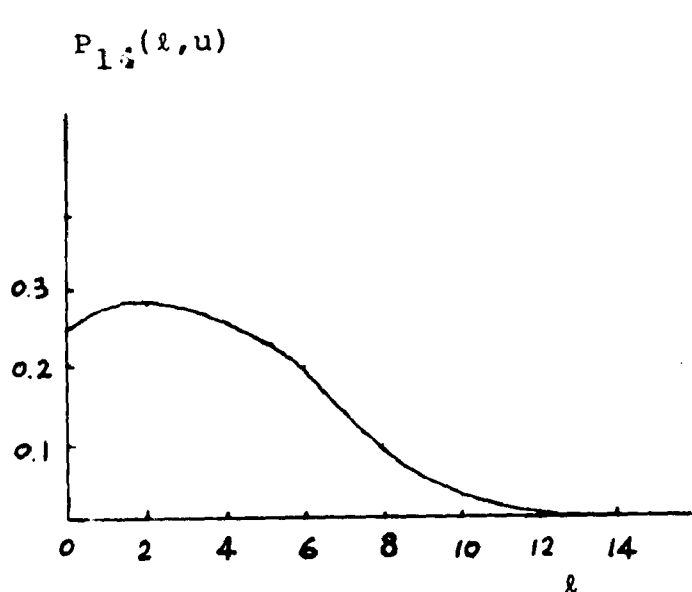
Figure 17



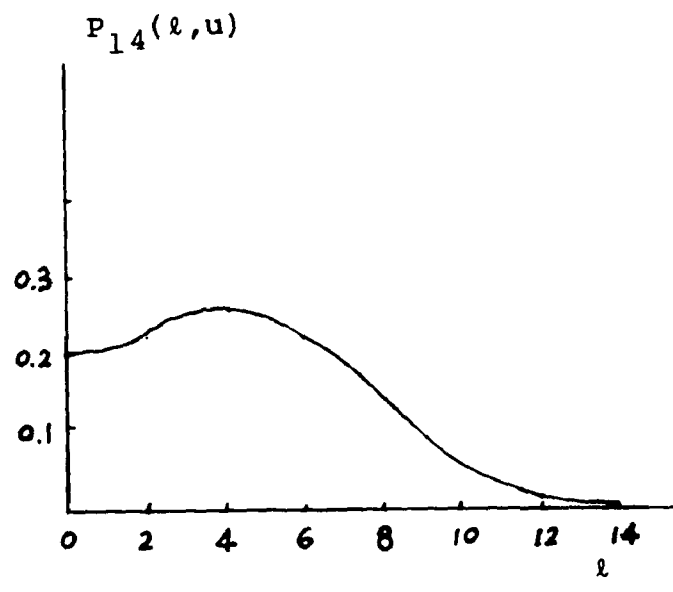
$V = 0.00$



$V = 0.05$

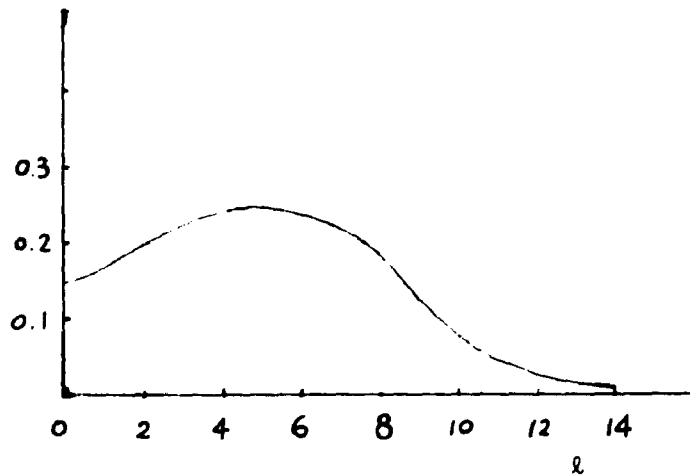


$V = 0.10$



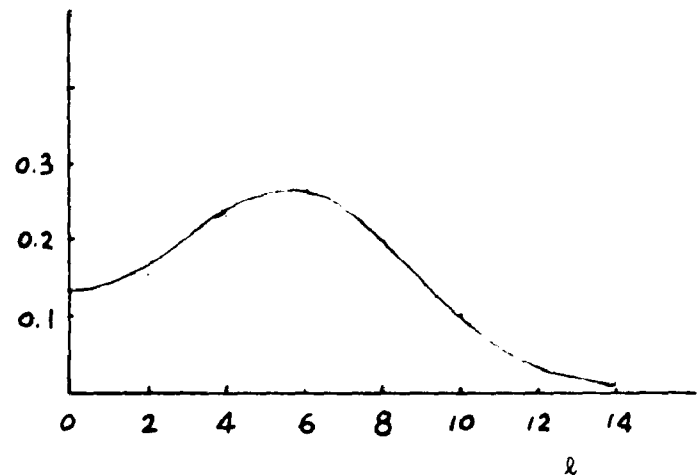
$V = 0.15$

$P_{14}(\ell, u)$



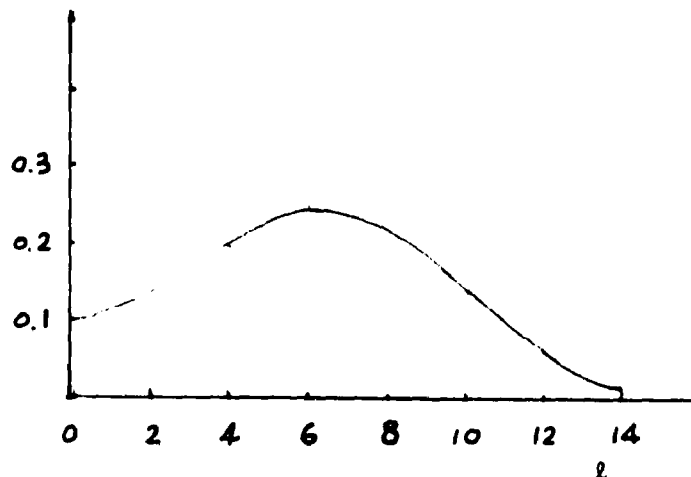
$V = 0.20$

$P_{14}(\ell, u)$



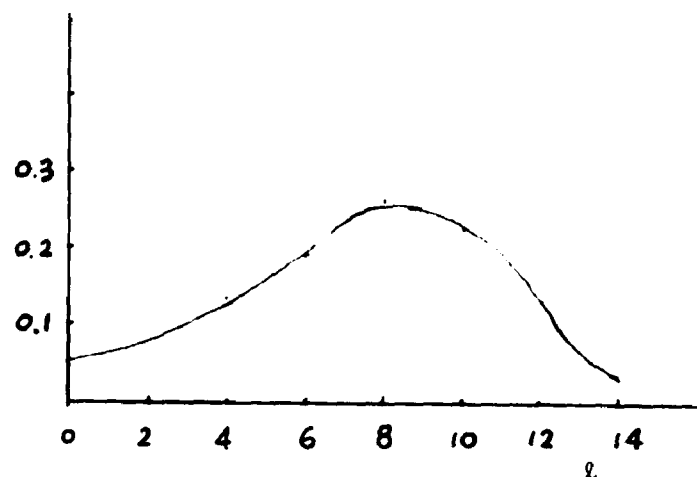
$V = 0.25$

$P_{14}(\ell, u)$



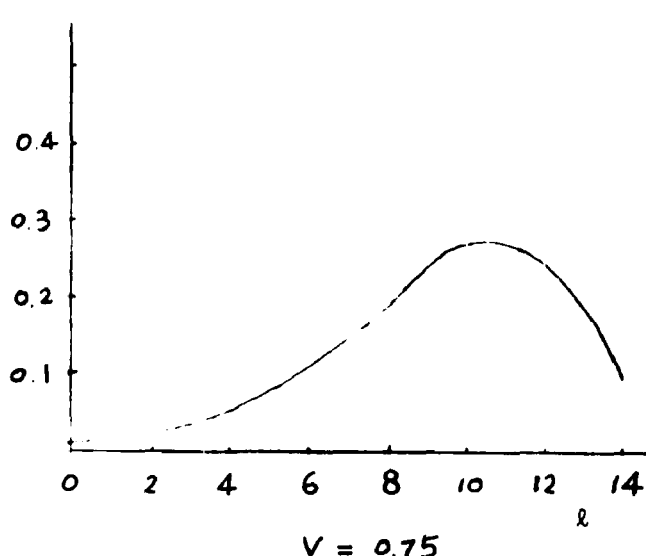
$V = 0.30$

$P_{14}(\ell, u)$

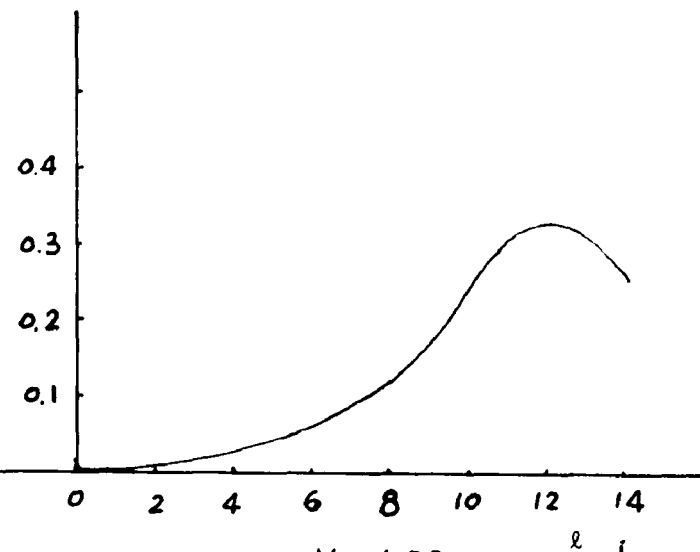


$V = 0.50$

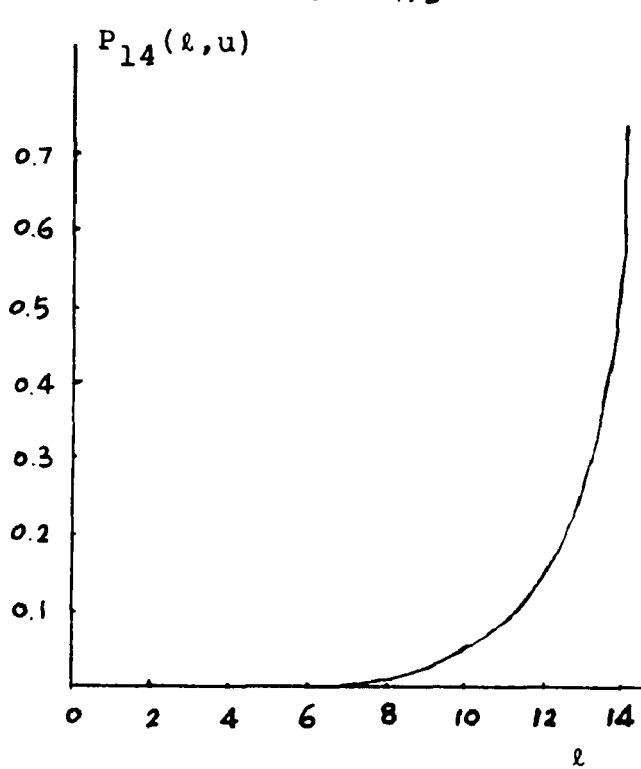
$P_{14}(\ell, u)$



$P_{14}(\ell, u)$

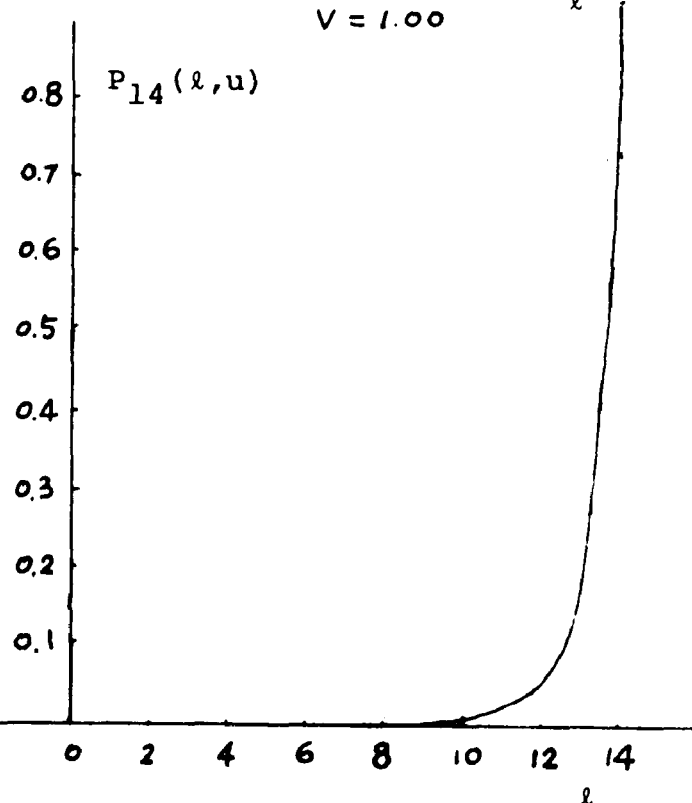


$P_{14}(\ell, u)$



$V = 2.00$

$P_{14}(\ell, u)$



$V = 4.00$

Figure 18

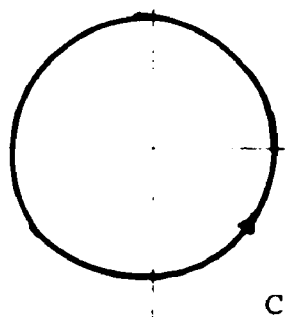


Figure 19

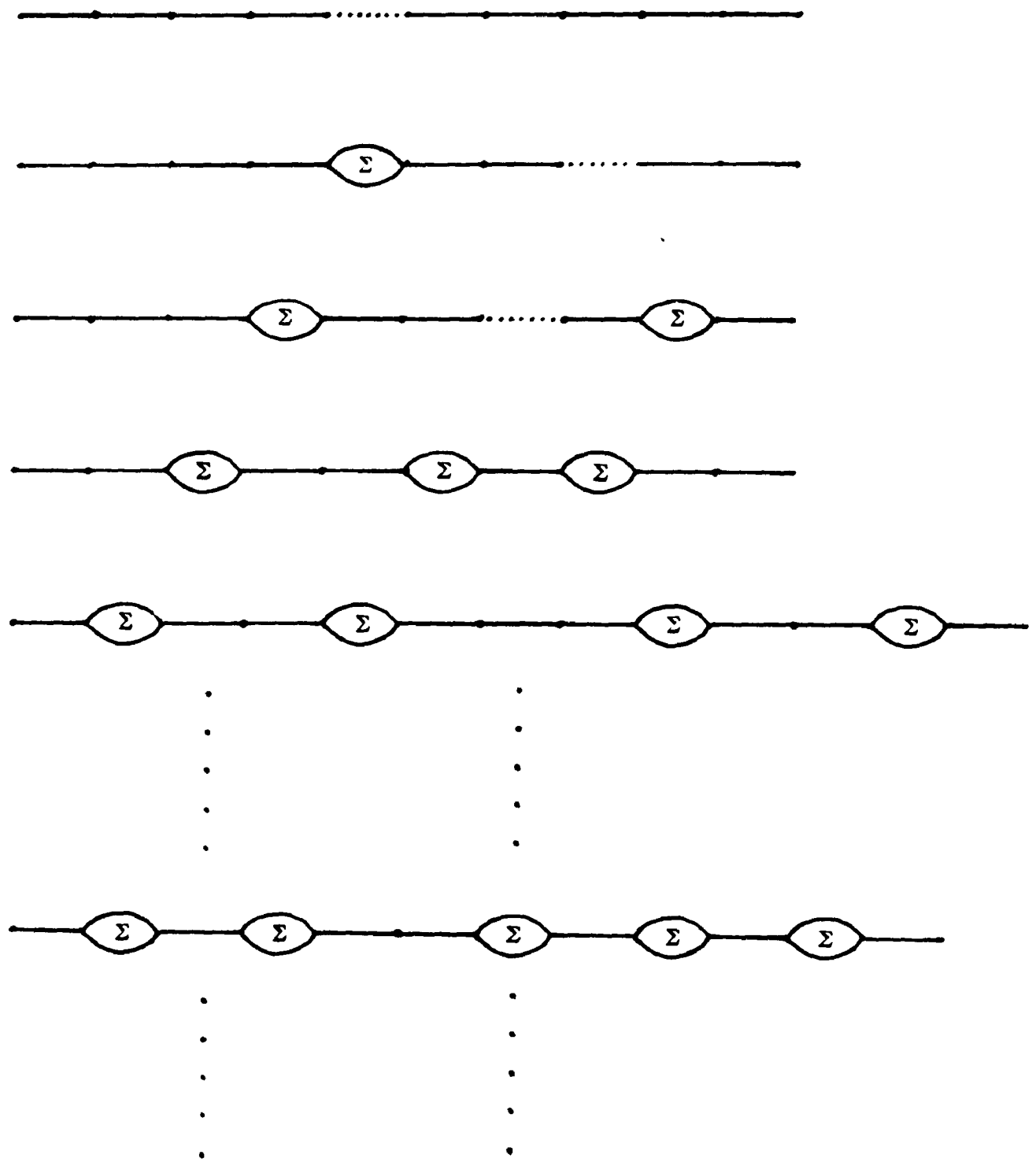


Figure 20

$$\begin{aligned}
 \sum = & \quad \text{Diagram 1} + \text{Diagram 2} + \text{Diagram 3} + \text{Diagram 4} + \dots \\
 & + \text{Diagram 5} + \text{Diagram 6} + \text{Diagram 7} + \text{Diagram 8} + \dots \\
 & + \text{Diagram 9} + \text{Diagram 10} + \text{Diagram 11} + \text{Diagram 12} + \dots \\
 & + \text{Diagram 13} + \text{Diagram 14} + \text{Diagram 15} + \text{Diagram 16} + \dots \\
 & + \text{Diagram 17} + \text{Diagram 18} + \dots \\
 & + \text{Diagram 19} + \text{Diagram 20} + \text{Diagram 21} + \text{Diagram 22} + \dots \\
 & + \dots
 \end{aligned}$$

Figure 21

Figure 22

$$\Sigma = \text{Diagram 1} + \text{Diagram 2} + \text{Diagram 3} + \\ + \text{Diagram 4} + \dots$$

The diagrams consist of two horizontal lines. Diagram 1 has a single oval loop connecting them. Diagram 2 has two ovals connected by a horizontal line. Diagram 3 has three ovals connected by a horizontal line. Diagram 4 has four ovals connected by a horizontal line.

Figure 23

$$\Lambda = \text{Diagram 1} + \text{Diagram 2} + \text{Diagram 3} + \\ + \text{Diagram 4} + \dots$$

The diagrams consist of two horizontal lines. Diagram 1 has a single oval loop connecting them. Diagram 2 has two ovals connected by a horizontal line. Diagram 3 has three ovals connected by a horizontal line. Diagram 4 has four ovals connected by a horizontal line. The diagrams are identical to those in Figure 22.

Figure 24

$$\Lambda * \Sigma = M_1 + M_2 + M_3 + M_4 + M_5 + \dots = \sum_{j=1} M_j$$

$$M_1 = \text{Diagram } 1 + \text{Diagram } 2 + \text{Diagram } 3 + \dots$$

$$+ \text{Diagram } 4 + \dots$$

$$M_2 = \text{Diagram } 1 + \text{Diagram } 2 + \dots$$

$$+ \text{Diagram } 3 + \text{Diagram } 4 + \dots$$

$$M_3 = \text{Diagram } 1 + \text{Diagram } 2 + \dots$$

$$+ \text{Diagram } 3 + \dots$$

$$M_4 = \text{Diagram } 1 + \dots$$

Figure 25

$$\Gamma = \bullet + \text{Diagram} + \text{Diagram} + \text{Diagram} + \dots$$
$$+ \text{Diagram} + \text{Diagram} + \text{Diagram} + \dots$$
$$+ \text{Diagram} + \text{Diagram} + \text{Diagram} + \dots$$
$$+ \text{Diagram} + \text{Diagram} + \dots$$
$$+ \text{Diagram} + \dots$$
$$+ \text{Diagram} + \dots$$

Figure 26

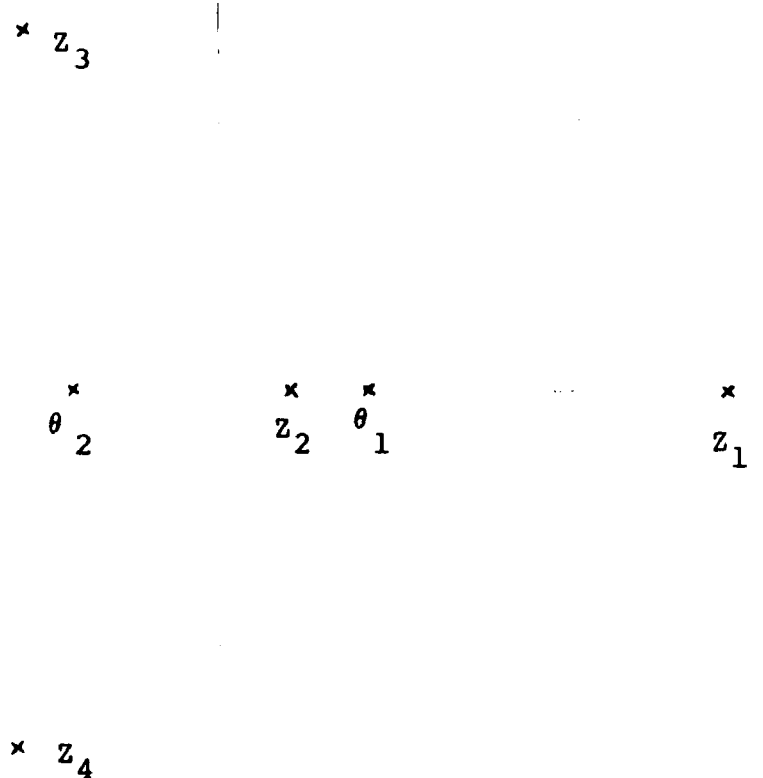


Figure 27



Figure 28

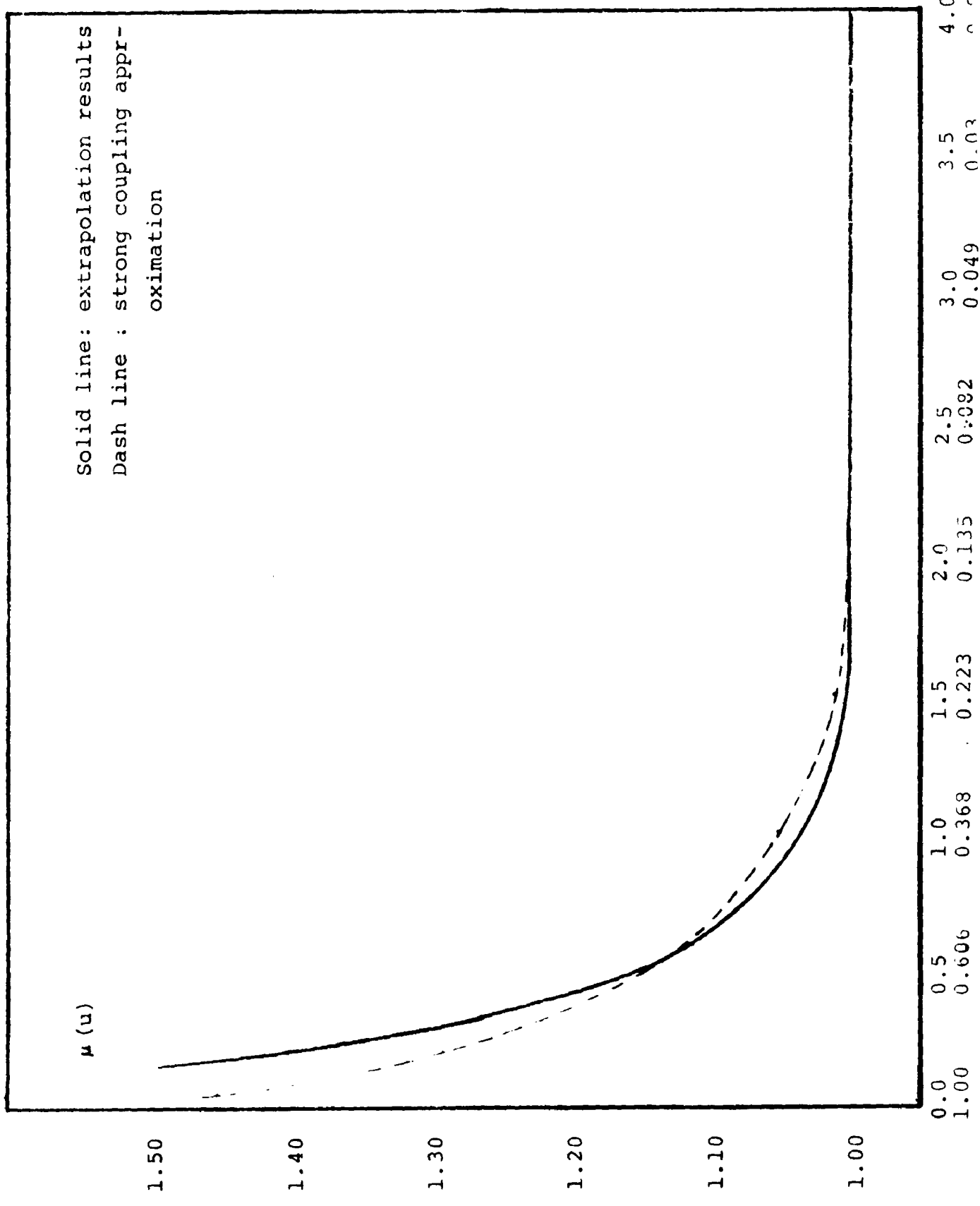


Figure 29

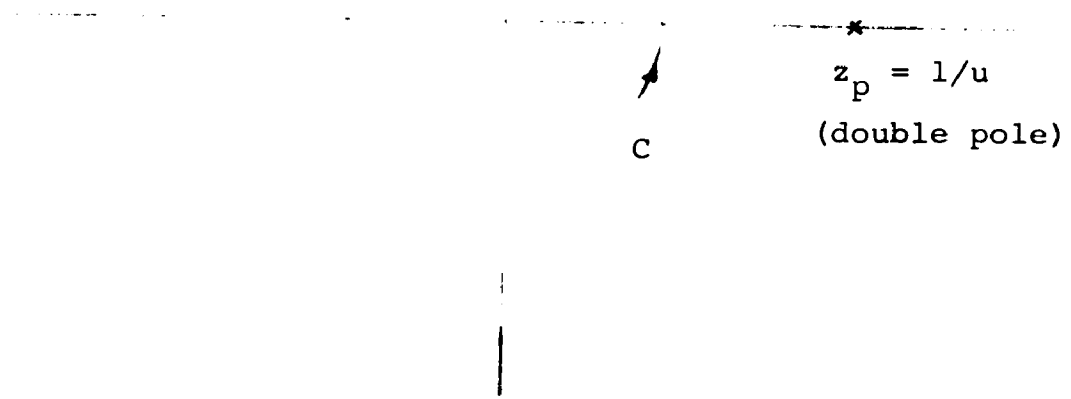
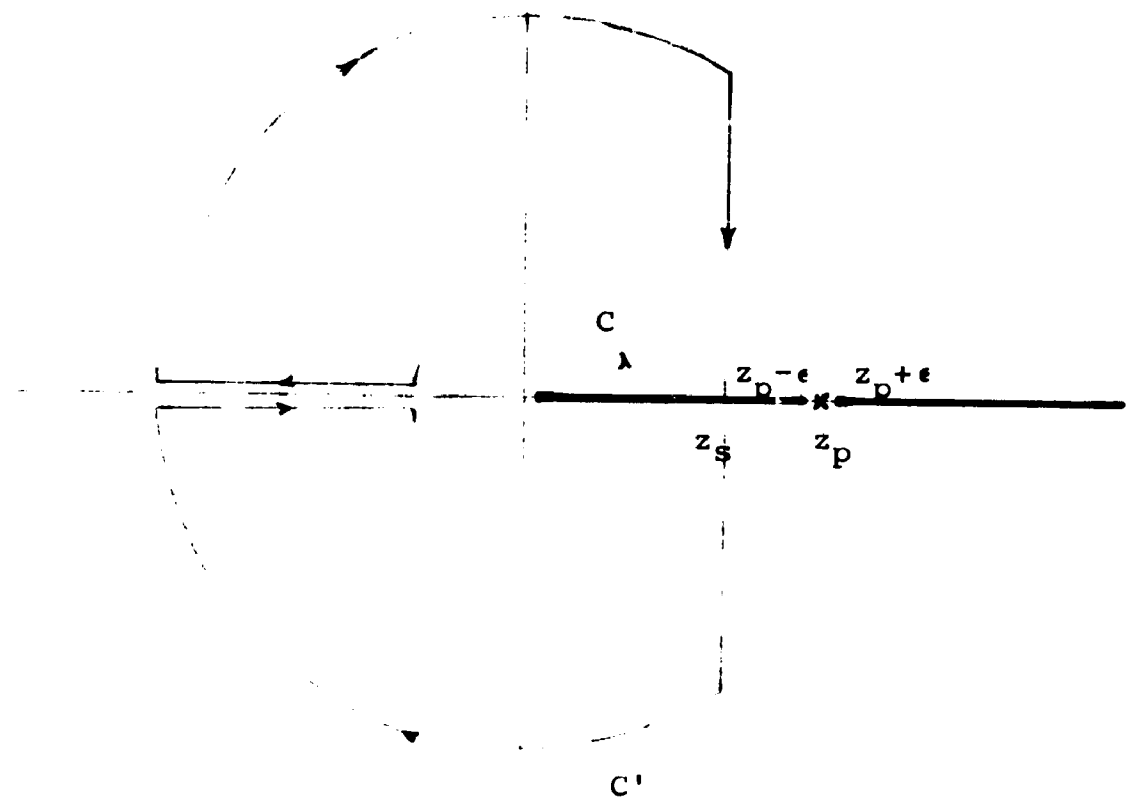


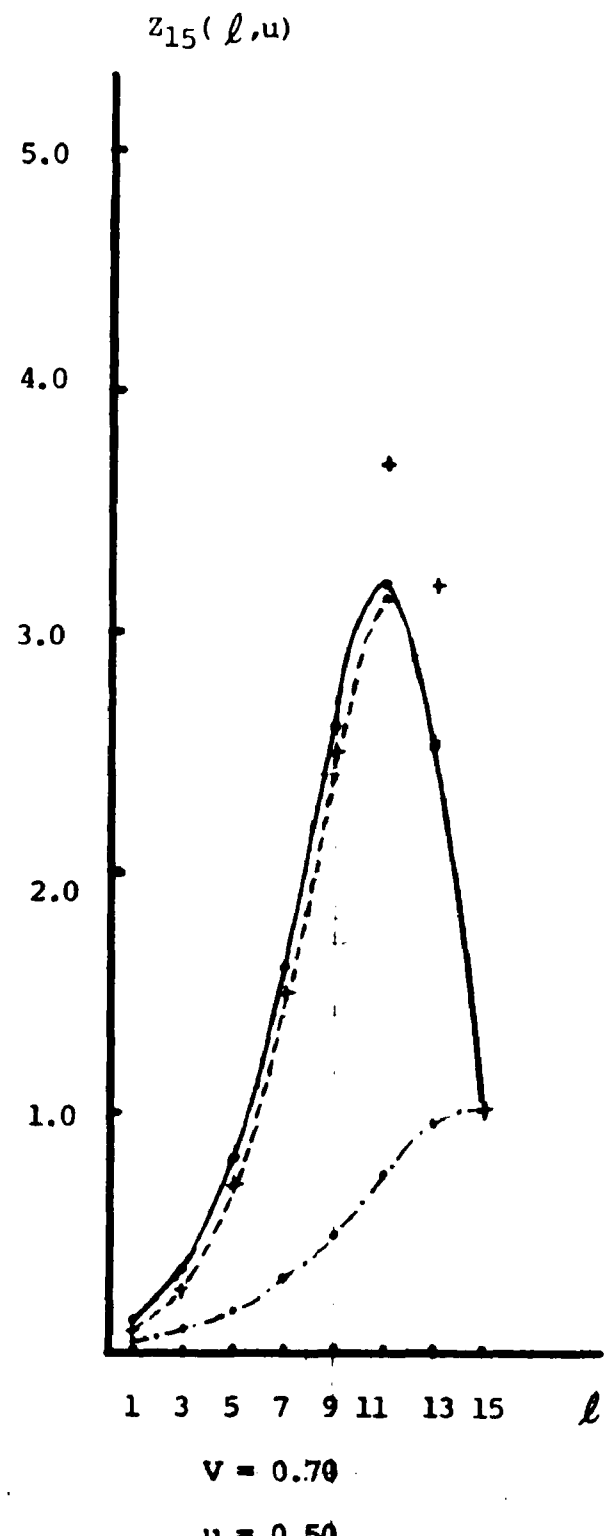
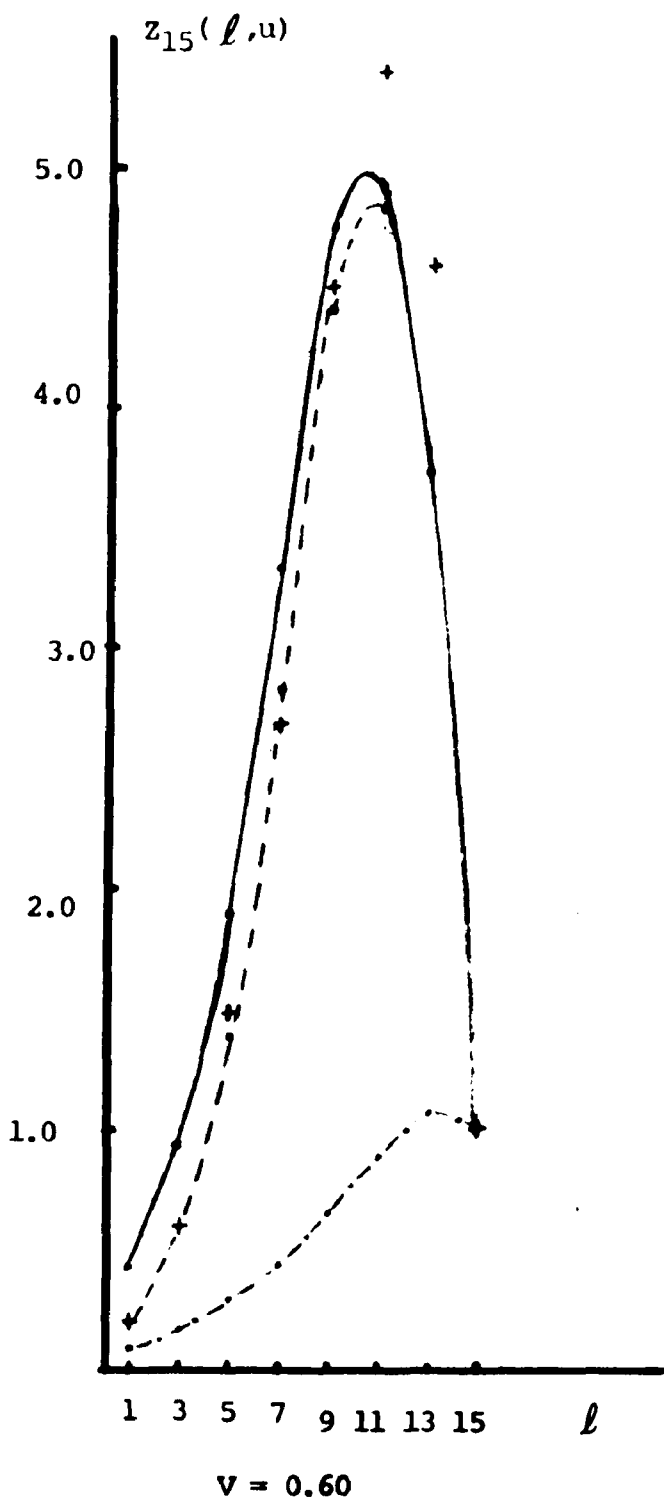
Figure 30



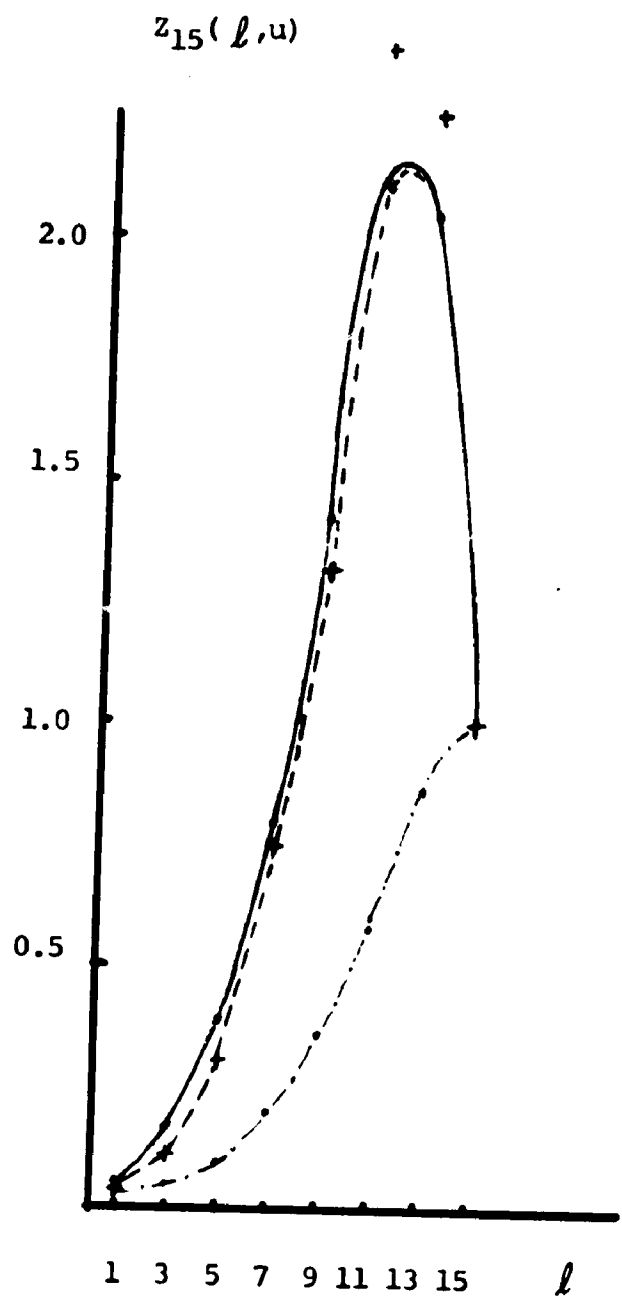
Saddle point z_s may lie in this region:

if $\ell > \bar{\ell}$, $0 < z_s \leq z_p - \epsilon$; $\ell < \bar{\ell}$, $z_p + \epsilon < z_s$.

Fig. 31

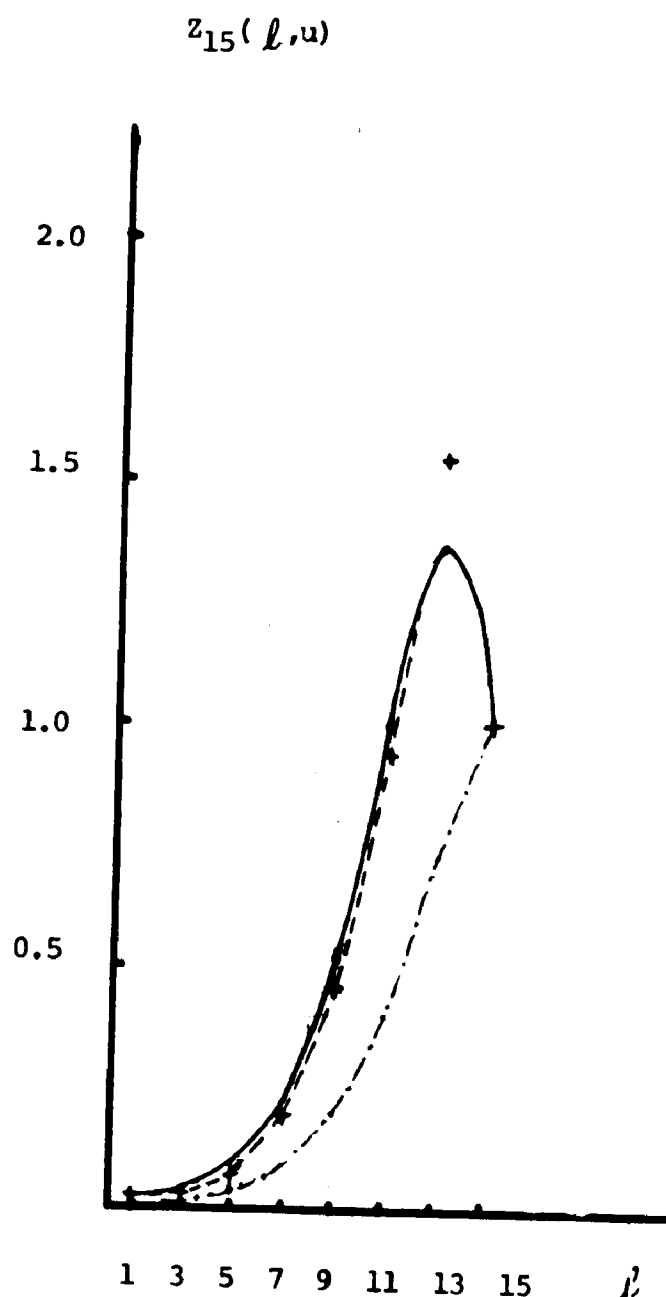


+
 denotes the generating function results
 Solid-line represents the exact counting results
 Dot-line represents the strong-coupling approximation containing Q_2 & Q_3
 Dot-dash-line represents the strong-coupling approximation containing Q_2



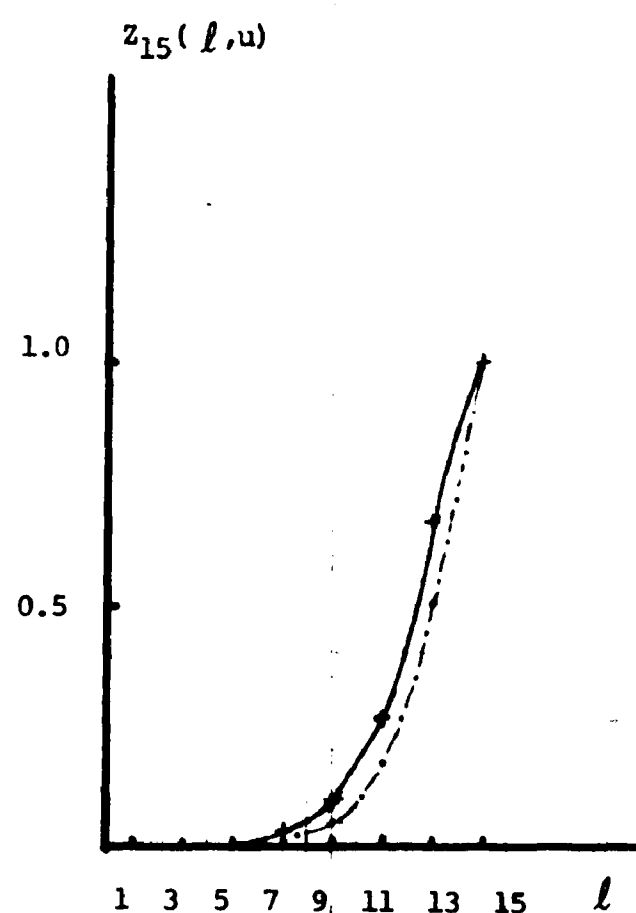
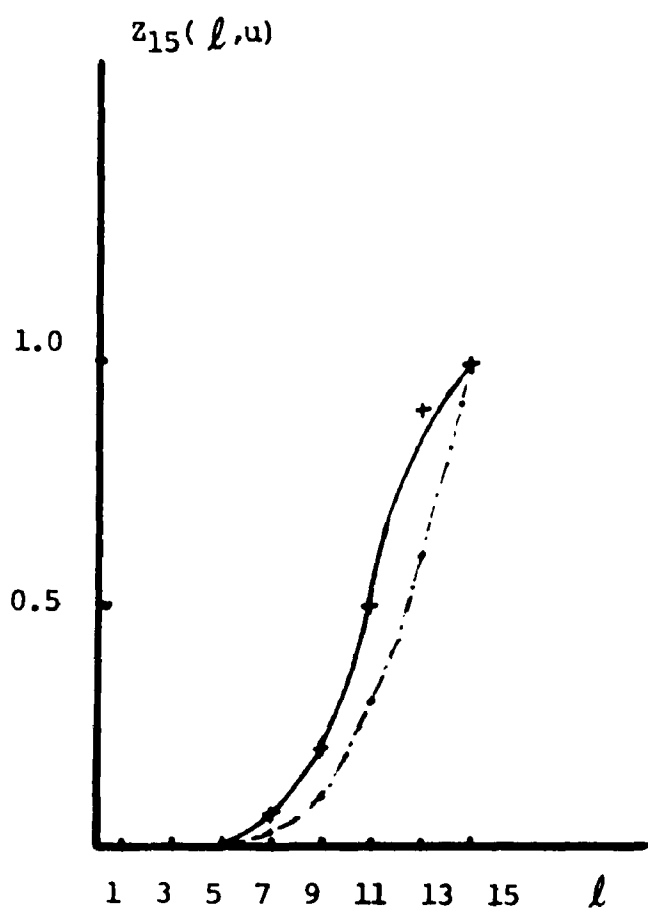
$v = 0.80$

$u = 0.45$

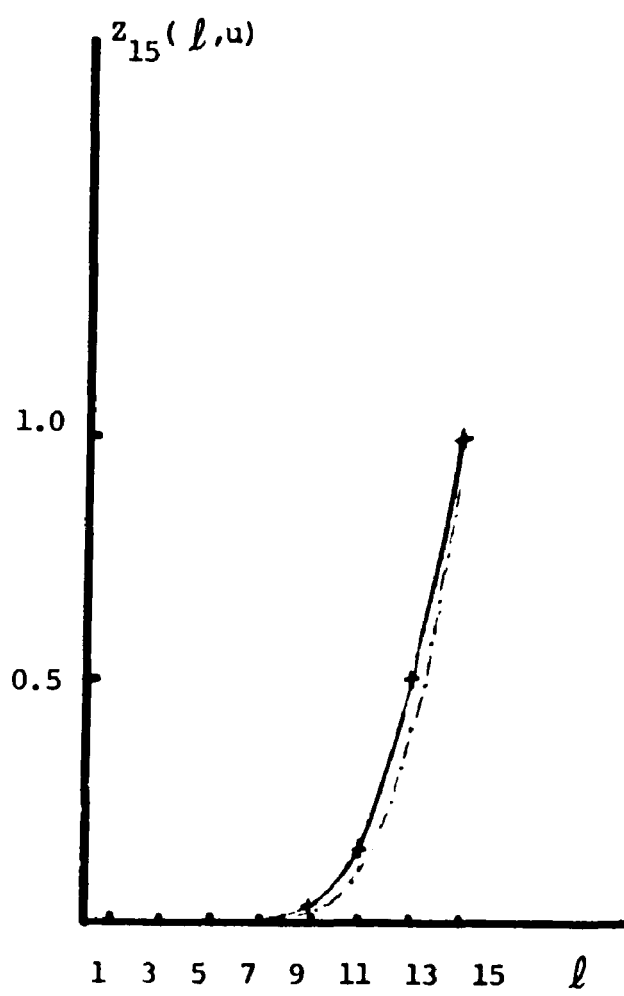


$v = 1.00$

$u = 0.37$



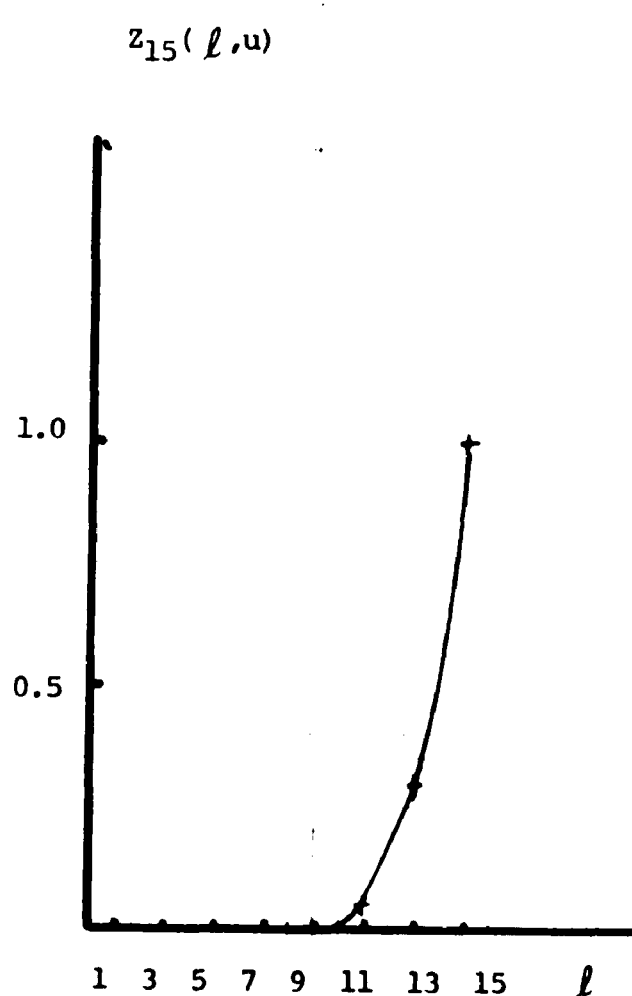
Solid-line and dot-line coincide



$v = 1.60$

$u = 0.20$

Dot-line coincides with solid-line



$v = 2.00$

$u = 0.14$

Both three lines coincide

Figure 32

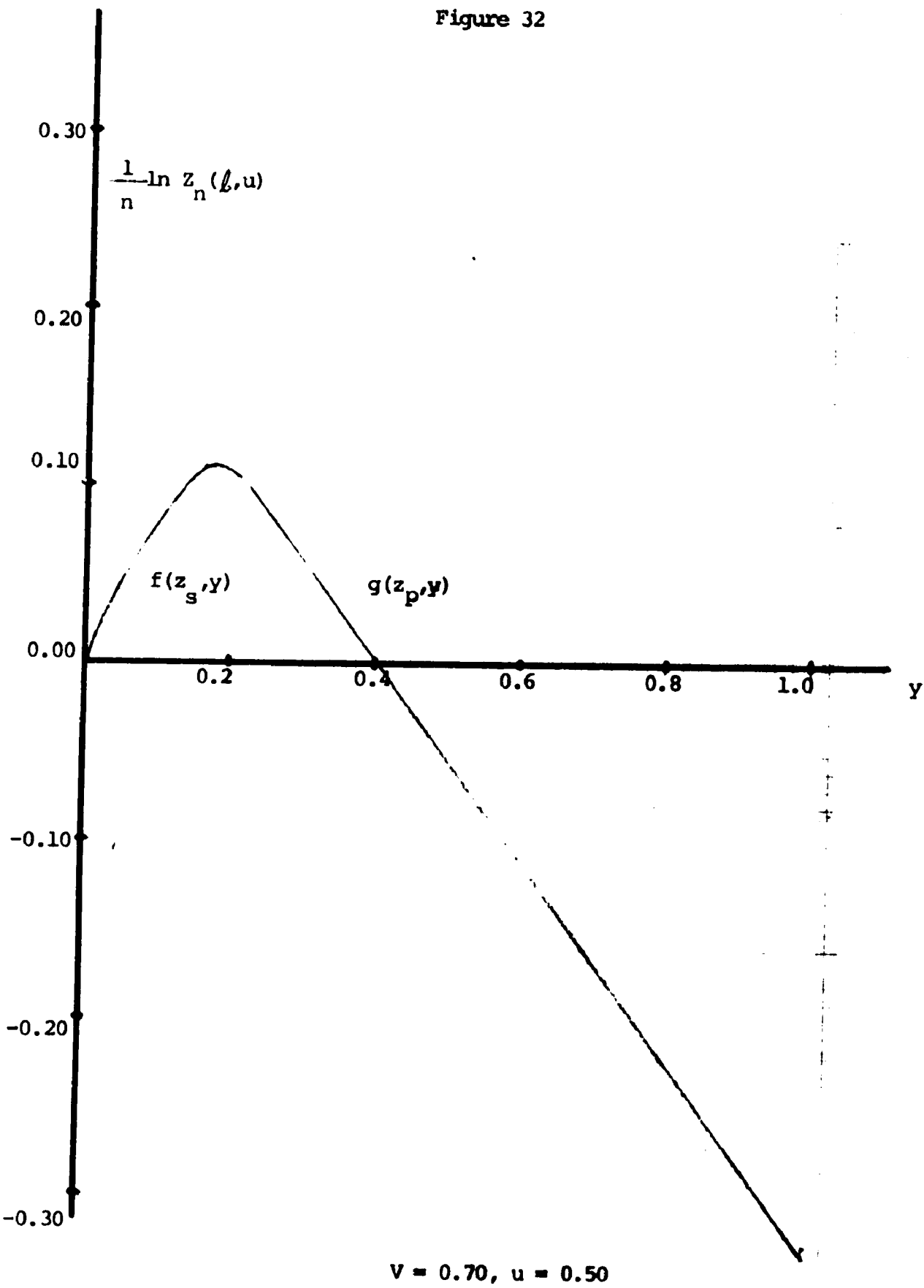


Figure 33

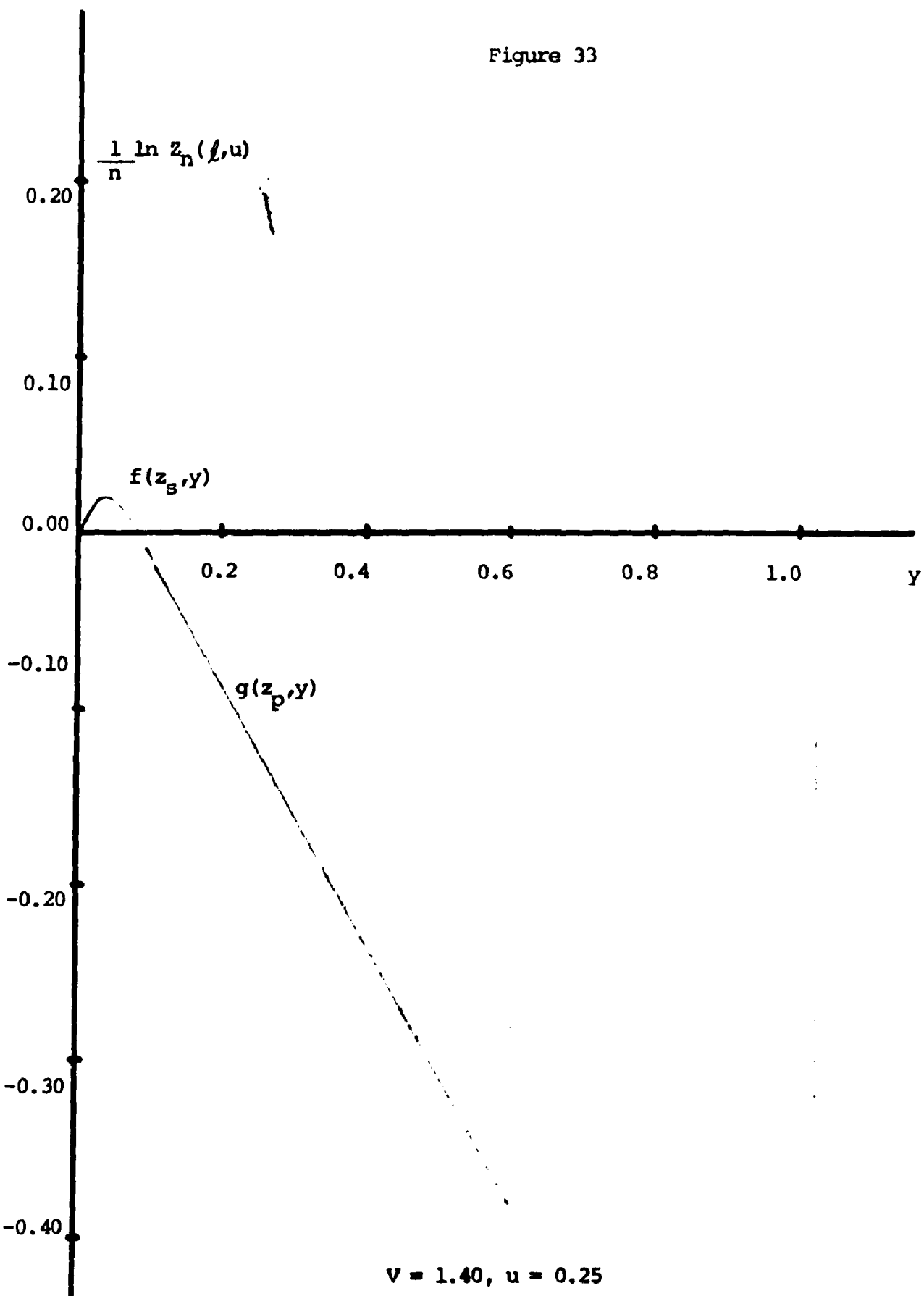


Figure 34

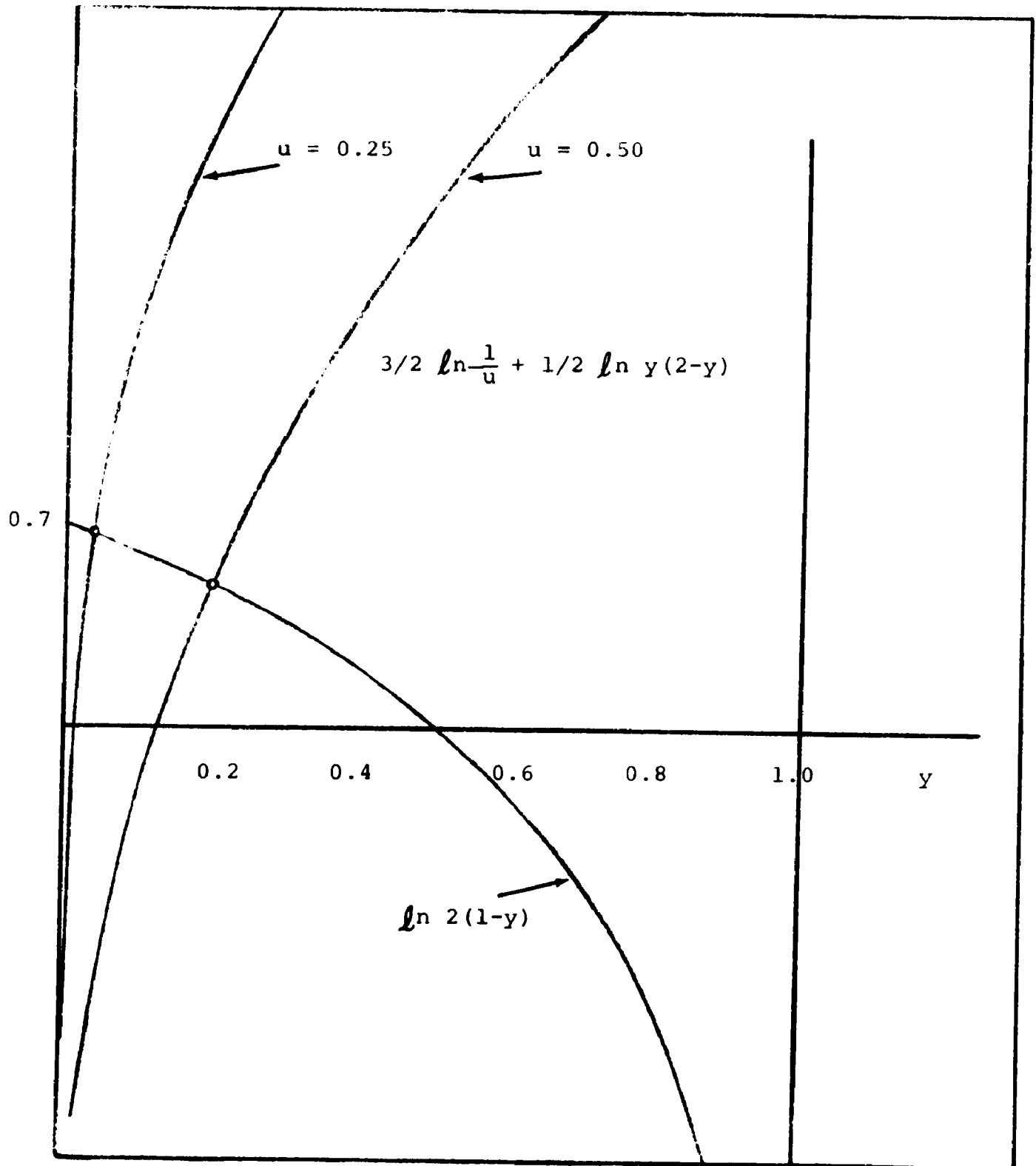


Figure 35

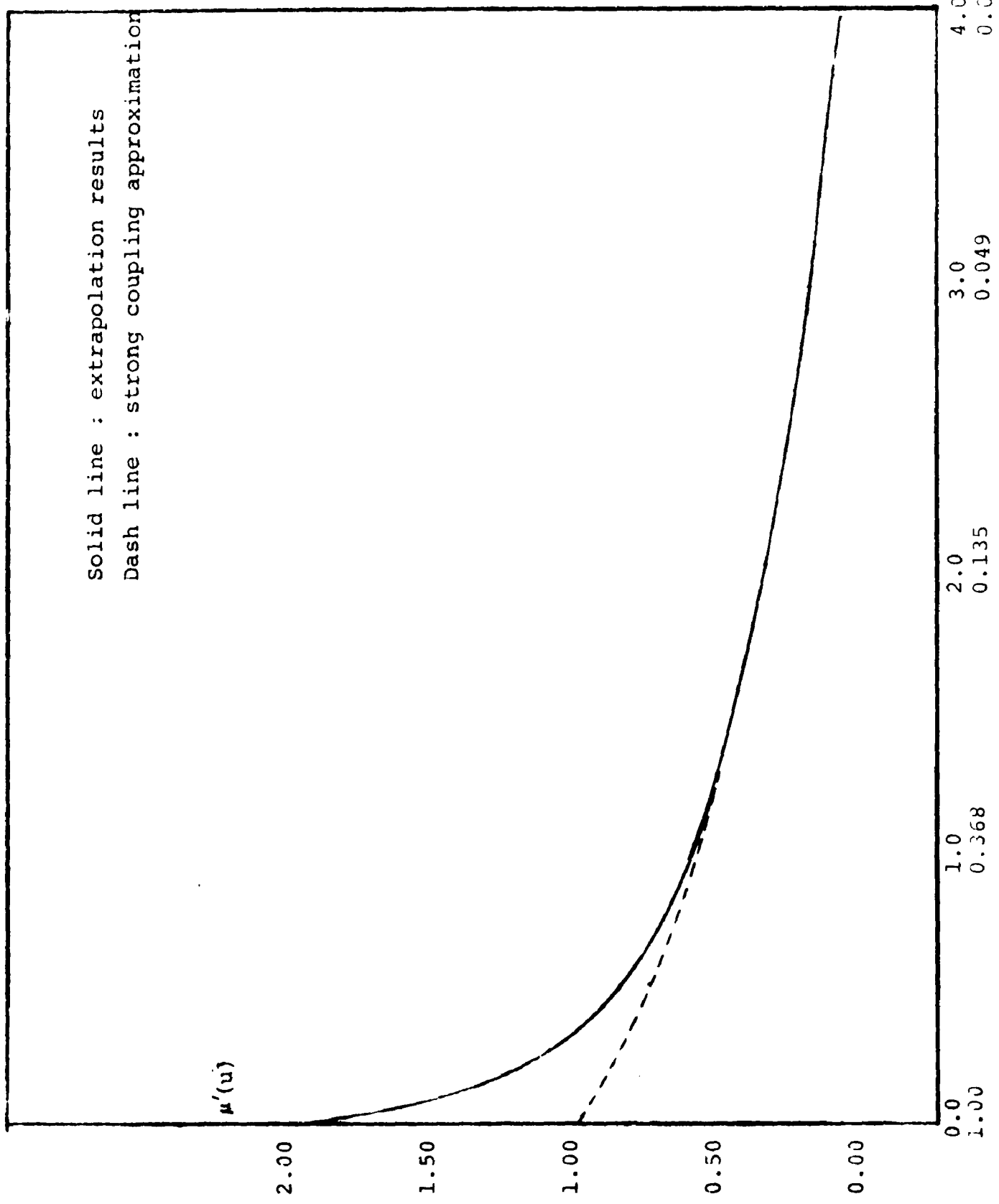


Figure 36

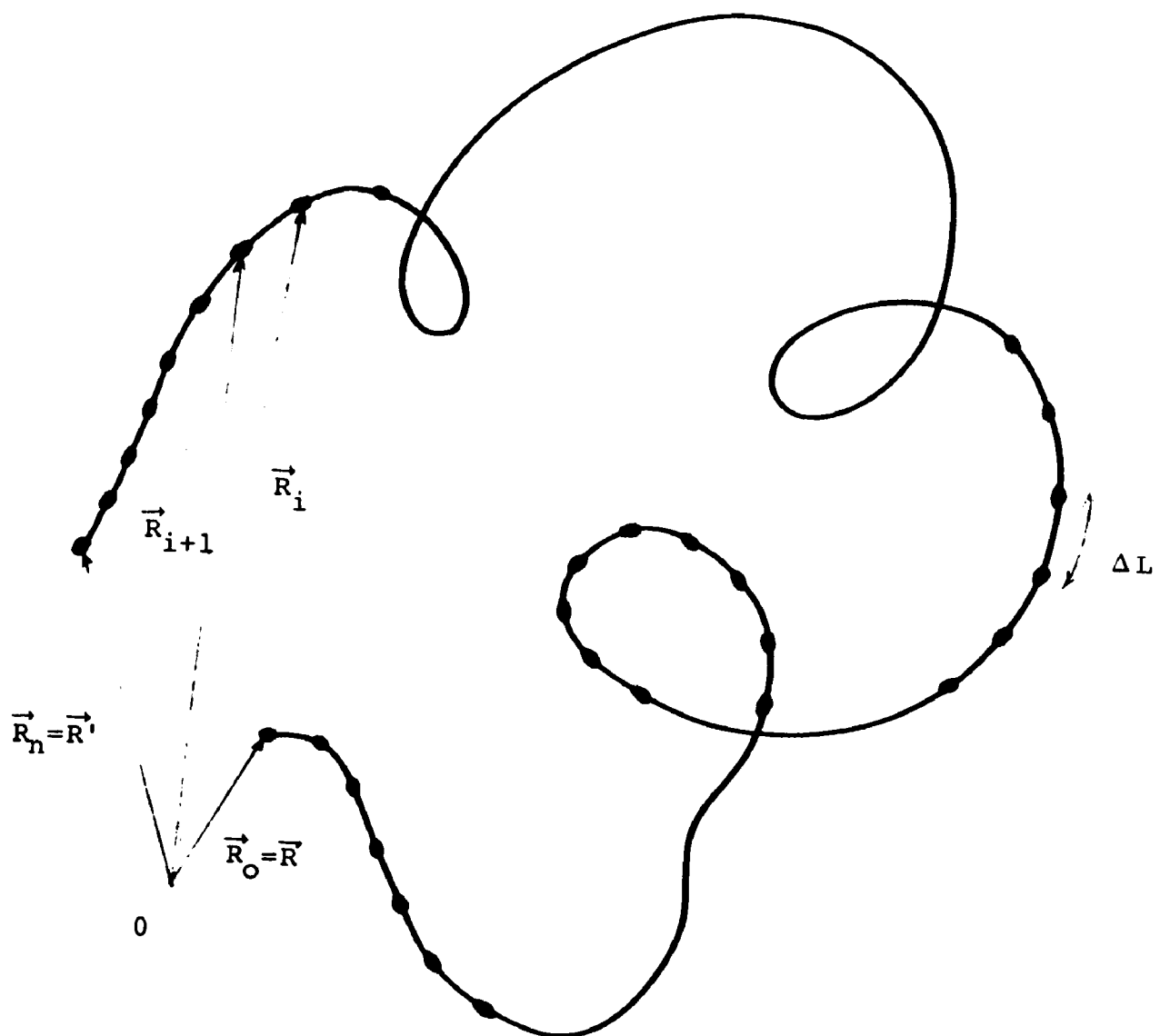


Figure 37

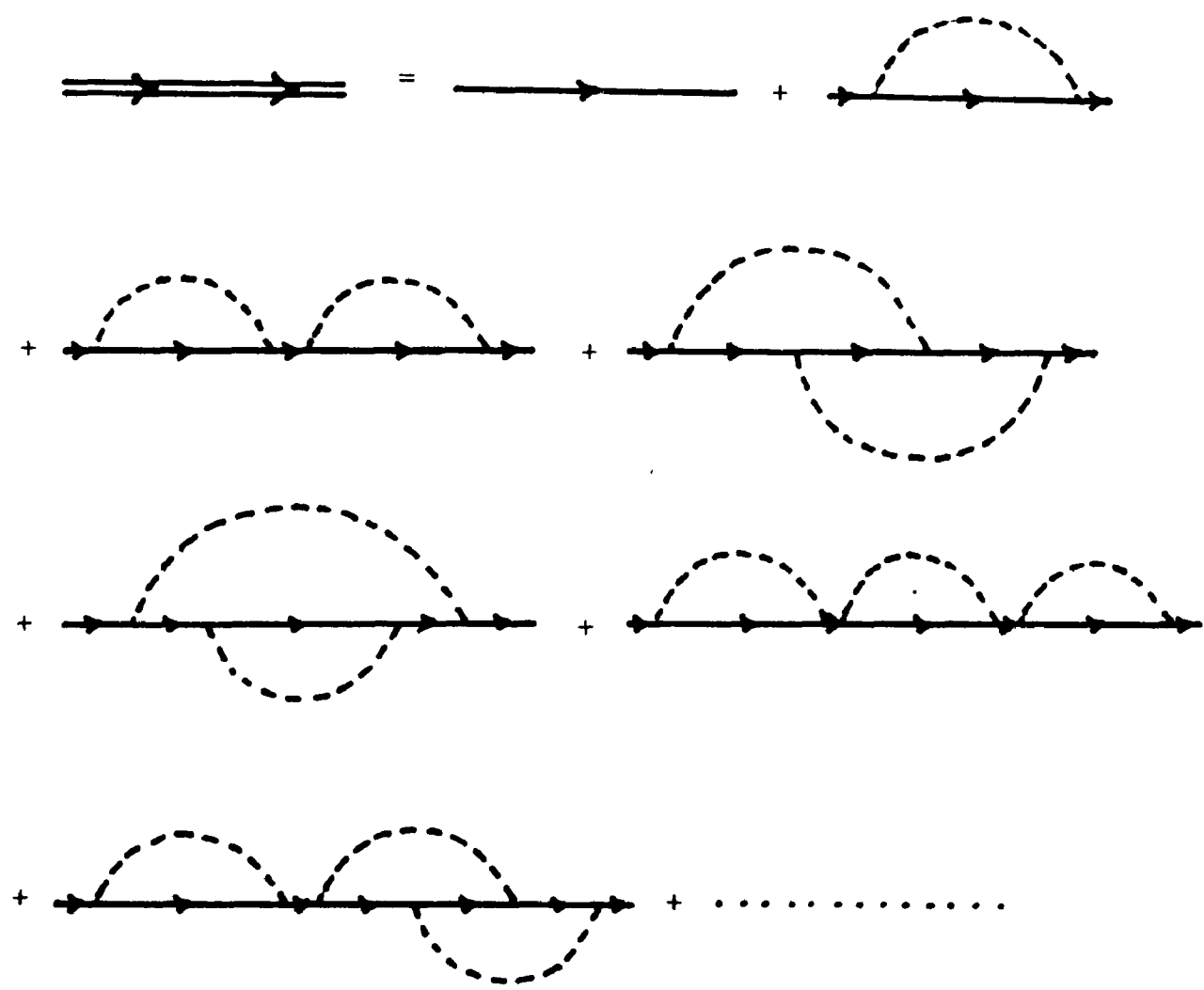


Figure 38

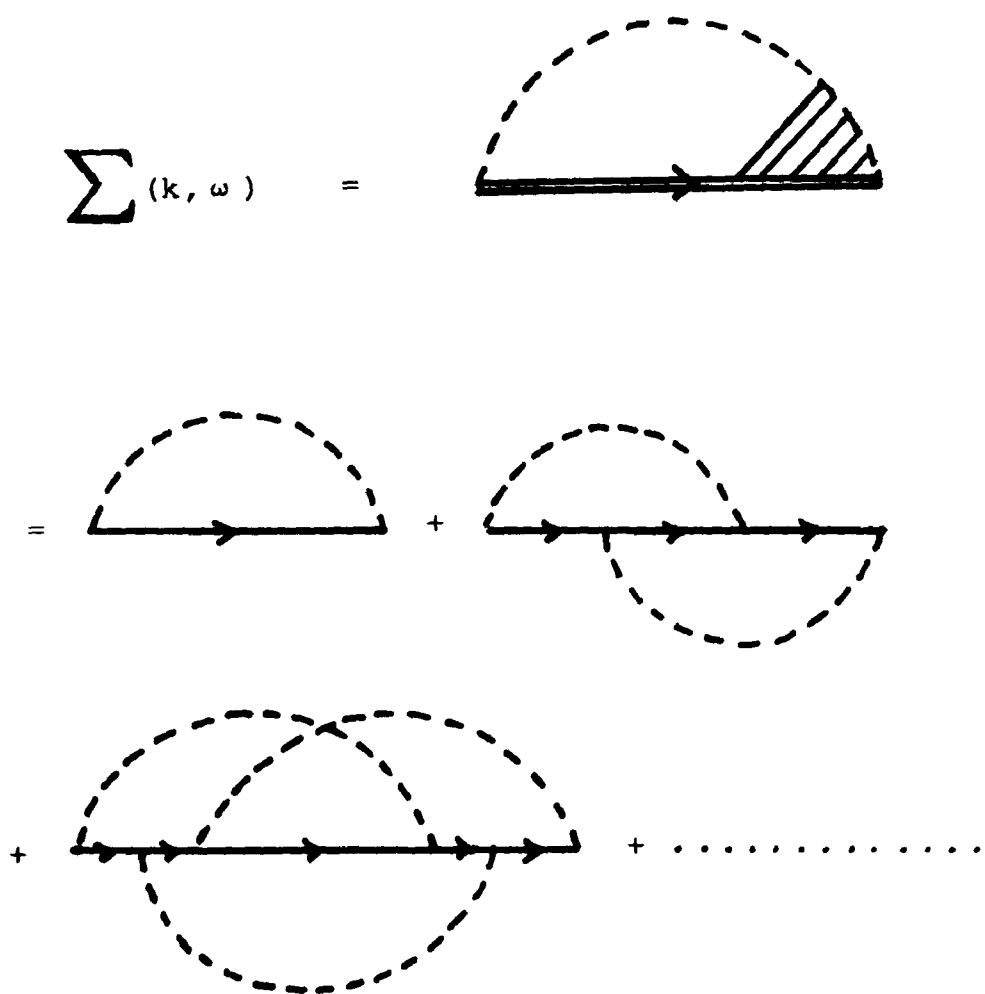


Figure 39

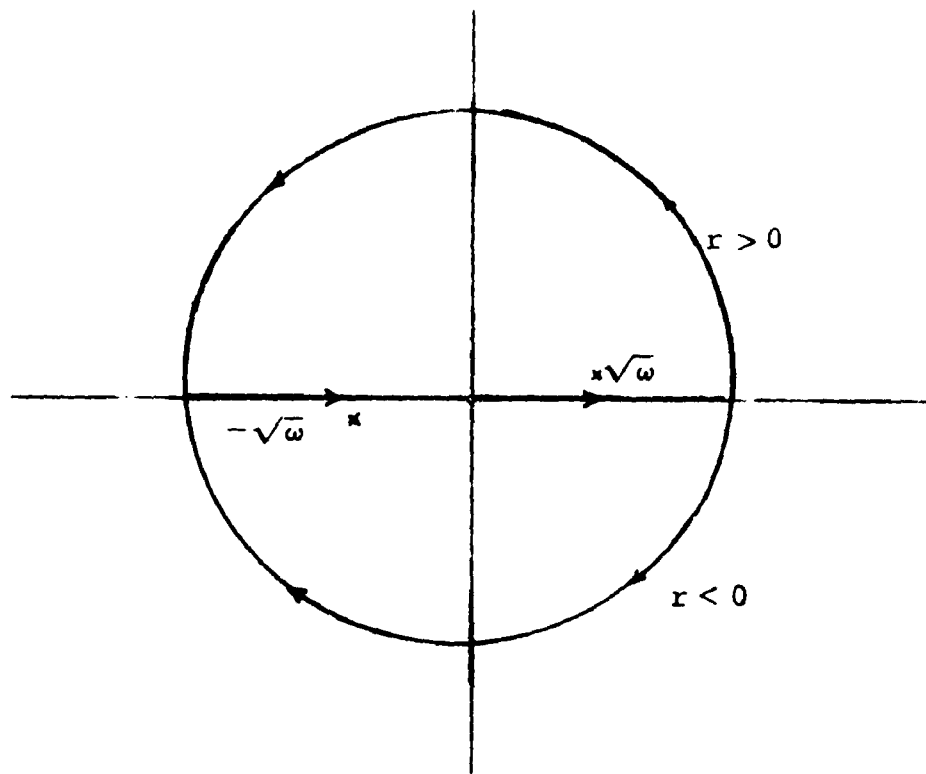


Figure 40

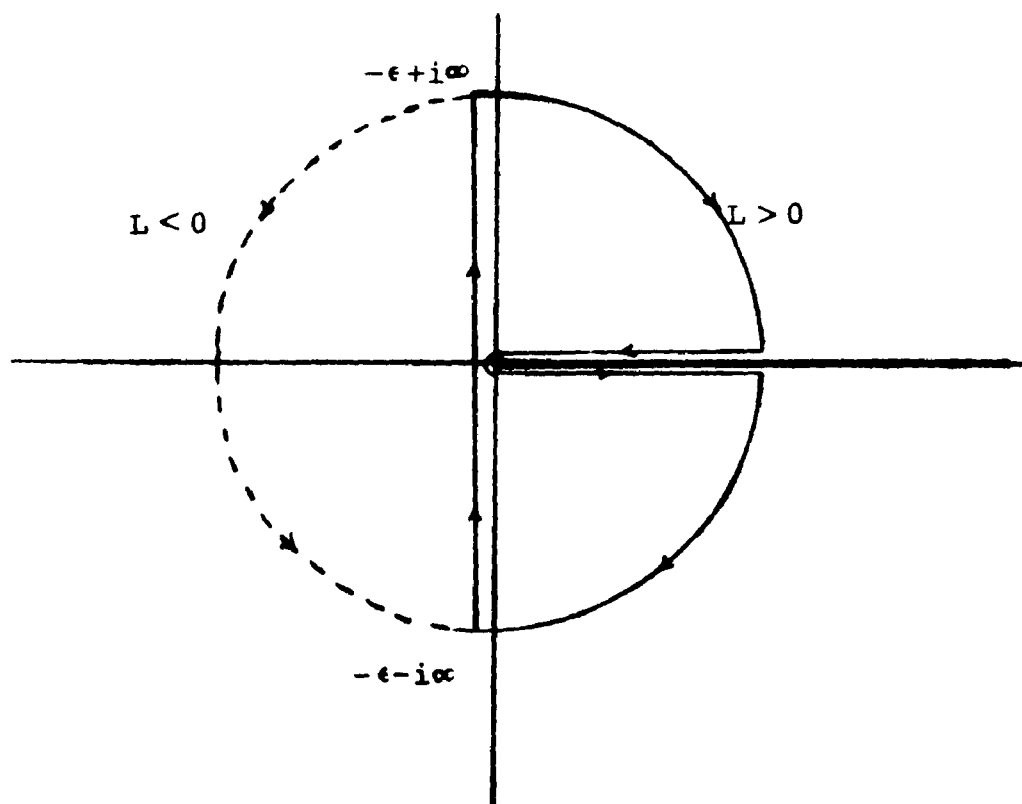


Figure 41

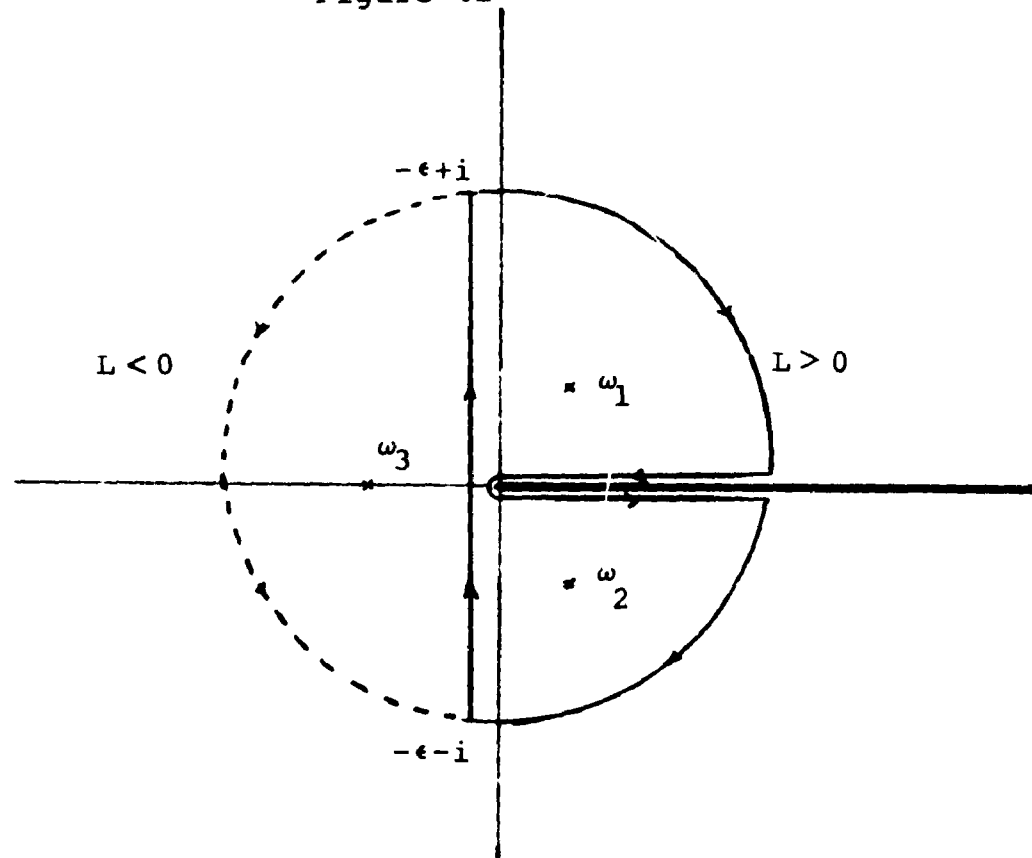


Figure 42

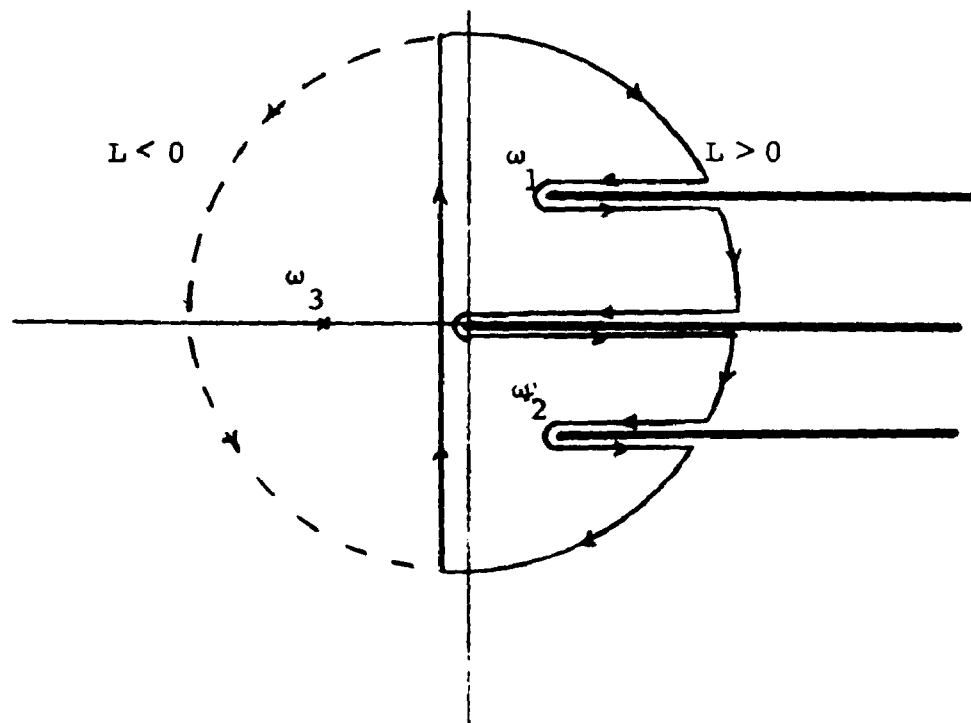


Figure 43

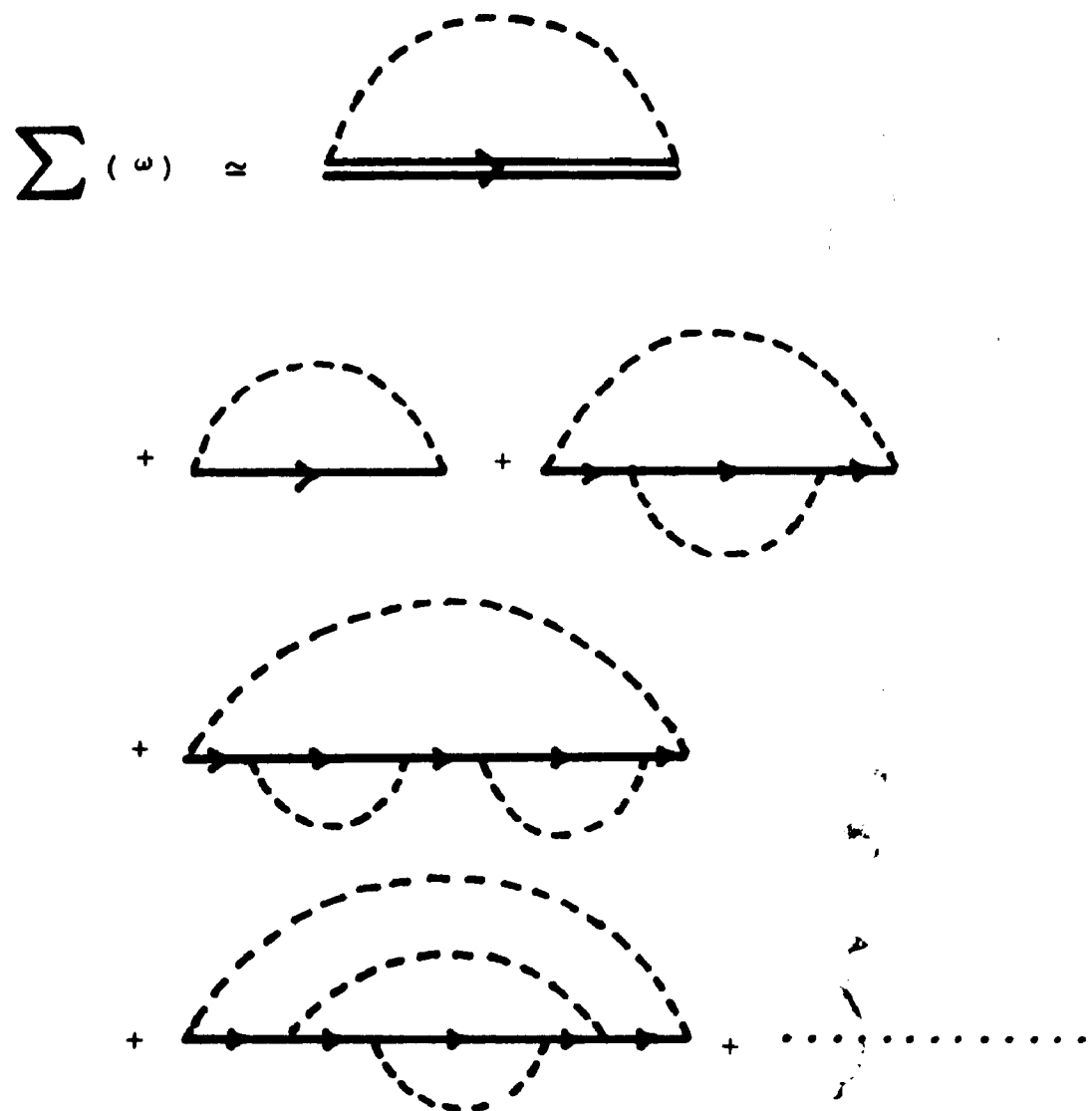


Figure 44

$$\sum_2 \text{(vertex)} = \begin{array}{c} \text{---} \\ \text{---} \end{array}$$

A Feynman diagram consisting of a horizontal solid line with three segments. The first segment is labeled $k-q_1$, the second $k-q_1-q_2$, and the third $k-q_2$. Above the line is a dashed arc with an arrow pointing right, labeled q_1 . Below the line is another dashed arc with an arrow pointing left, labeled q_2 .

$$\sum_2 = \begin{array}{c} \text{---} \\ \text{---} \end{array}$$

A Feynman diagram consisting of a horizontal solid line with three segments. The first segment is labeled $k-q_1$, the second $k-q_1-q_2$, and the third $k-q_1$. Above the line is a dashed arc with an arrow pointing right, labeled q_1 . Below the line is another dashed arc with an arrow pointing left, labeled q_2 .

Figure 45

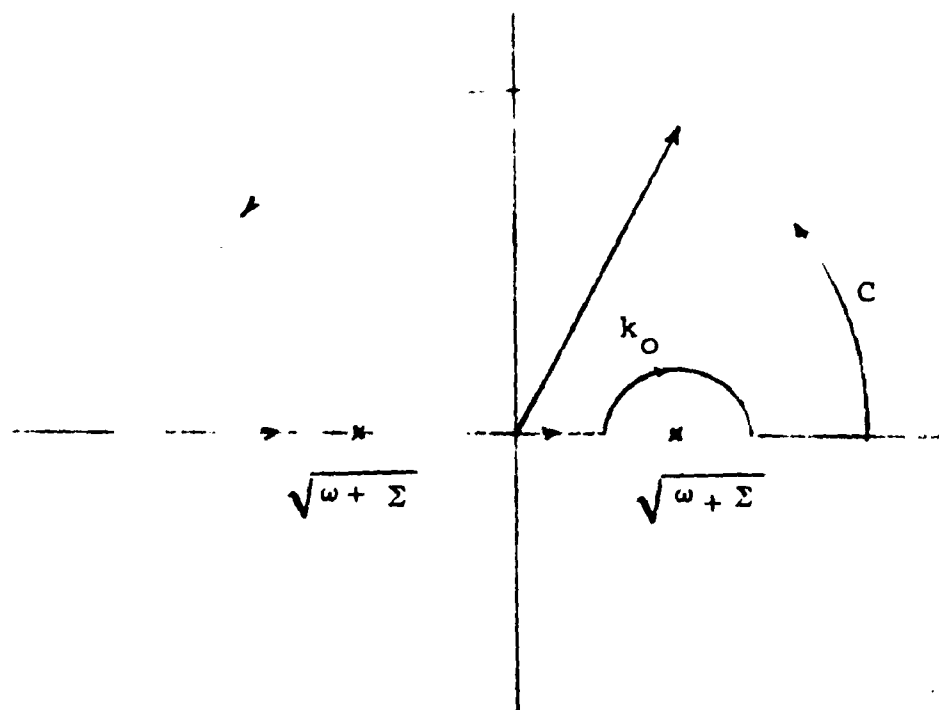


Figure 46

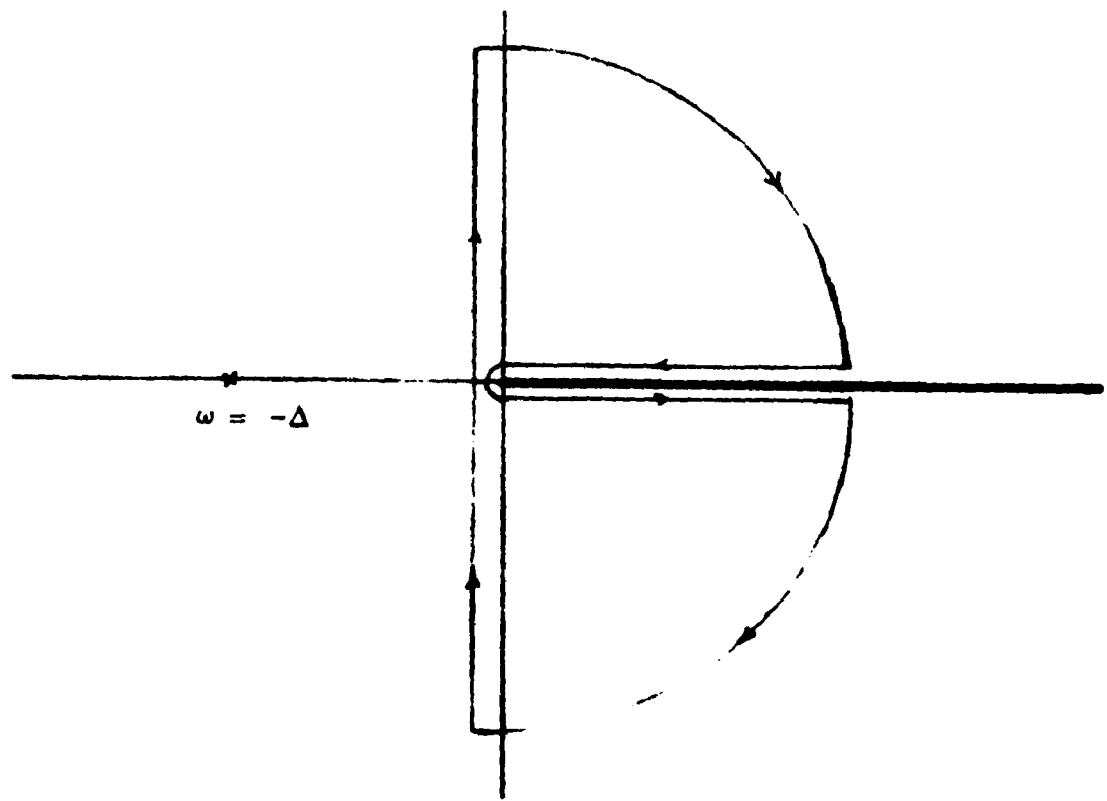
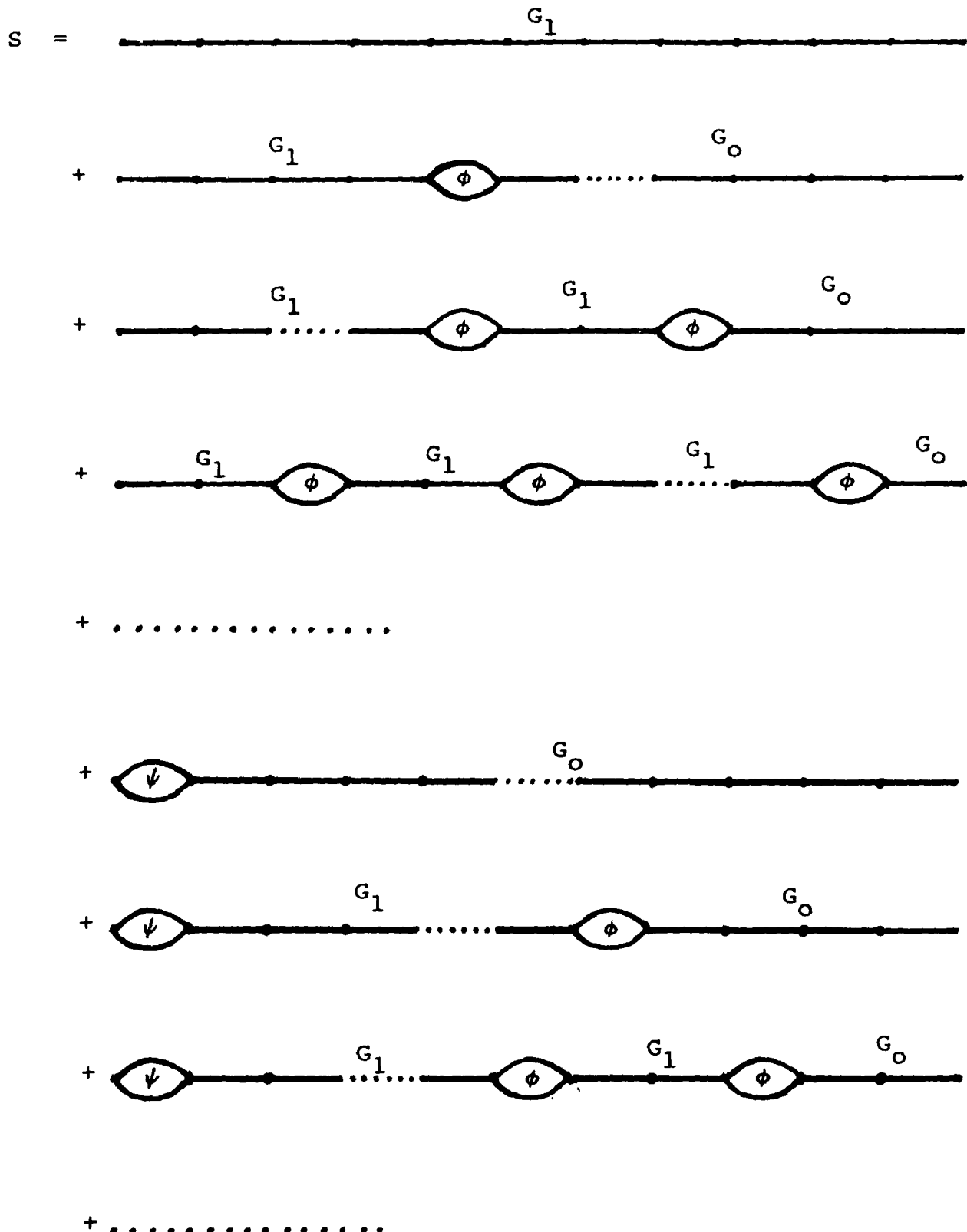
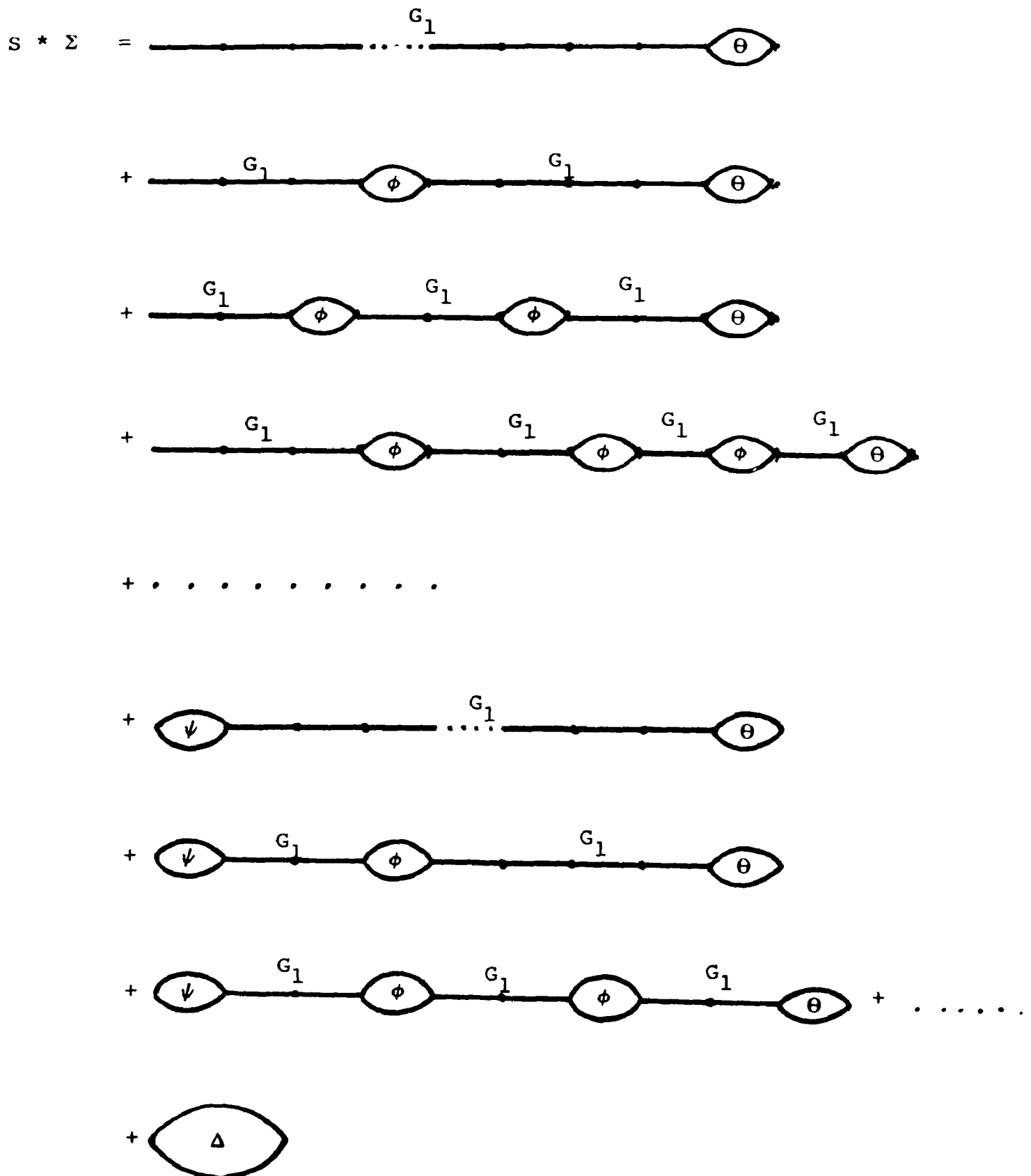


Figure 47



Each step represents a two-line bubble contains a factor $z^2 u$.

Figure 48



Each step represents a two-line bubble which contains a factor z^2 .

Figure 49

$$\Theta = 2 \left(\text{Diagram} + \text{Diagram} + \text{Diagram} + \dots + \right.$$

$$+ \text{Diagram} + \text{Diagram} + \text{Diagram} + \dots + \text{Diagram} + \dots + \dots$$

$$+ \text{Diagram} + \text{Diagram} + \dots + \text{Diagram} + \dots + \dots$$

$$+ \text{Diagram} + \text{Diagram} + \dots + \text{Diagram} + \dots + \dots$$

$$+ \text{Diagram} + \dots + \dots \left. \right)$$

The factor of two is due to connecting a G_1 -line with Θ .

Figure 50

$$\mathcal{L} = \text{---} \overset{G_1}{\cdot \cdot \cdot} \text{---} \delta$$

$$+ \text{---} \overset{G_1}{\cdot \cdot \cdot} \text{---} \phi \overset{G_1}{\cdot \cdot \cdot} \text{---} \delta$$

$$+ \psi \text{---} \overset{G_1}{\cdot \cdot \cdot} \text{---} \phi \overset{G_1}{\cdot \cdot \cdot} \text{---} \delta$$

$$+ \text{---} \overset{G_1}{\cdot \cdot \cdot} \text{---} \phi \overset{G_1}{\cdot \cdot \cdot} \text{---} \delta$$

$$+ \psi \text{---} \overset{G_1}{\cdot \cdot \cdot} \text{---} \phi \overset{G_1}{\cdot \cdot \cdot} \phi \overset{G_1}{\cdot \cdot \cdot} \delta$$

$$+ \text{---} \overset{G_1}{\cdot \cdot \cdot} \text{---} \phi \overset{G_1}{\cdot \cdot \cdot} \phi \overset{G_1}{\cdot \cdot \cdot} \phi \overset{G_1}{\cdot \cdot \cdot} \delta$$

$$+ \psi \text{---} \overset{G_1}{\cdot \cdot \cdot} \text{---} \phi \overset{G_1}{\cdot \cdot \cdot} \phi \overset{G_1}{\cdot \cdot \cdot} \phi \overset{G_1}{\cdot \cdot \cdot} \delta$$

+

$$+ \delta'$$

$$\delta = 2 \left(1 + 3 \text{ } \begin{array}{c} 4 \\ \diagup \quad \diagdown \\ \text{---} \end{array} + 3 \text{ } \begin{array}{c} 4 \\ \diagup \quad \diagdown \\ \text{---} \end{array} \begin{array}{c} 4 \\ \diagup \quad \diagdown \\ \text{---} \end{array} + 3 \text{ } \begin{array}{c} 4 \\ \diagup \quad \diagdown \\ \text{---} \end{array} \begin{array}{c} 4 \\ \diagup \quad \diagdown \\ \text{---} \end{array} \begin{array}{c} 4 \\ \diagup \quad \diagdown \\ \text{---} \end{array} \right.$$

$$\sum = \text{Diagram 1} + \text{Diagram 2} + \text{Diagram 3} + \dots$$

$$\mathcal{L} \Sigma \mathcal{L} = \text{Diagram showing } \mathcal{L} \text{ in ovals connected by } \Sigma$$

Each step in denotes as a two-line bubble containing a factor of $z^2 u$. The factor of two in the diagrams of δ due to connecting with a G_1 -line and the factor of three in front of (4) si due to connecting (4) with (—) in Σ .

Figure 51

